UNIVERSITA' VITA-SALUTE SAN RAFFAELE

CORSO DI DOTTORATO DI RICERCA INTERNAZIONALE IN MEDICINA MOLECOLARE

CURRICULUM IN TERAPIA GENICA E CELLULARE

IMPROVING THE EFFICIENCY OF *IN VIVO* LENTIVIRAL GENE THERAPY TO HEPATOCYTES AND APPLICATION TO FAMILIAL HYPERCHOLESTEROLEMIA

DoS: Prof. Alessio Cantore

Second Supervisor: Prof. Thierry VandenDriessche

Tesi di DOTTORATO di RICERCA di Cesare Canepari

matr. 015481

Ciclo di dottorato XXXV

SSD BIO/11 BIO/17

Anno Accademico 2021/2022

CONSULTAZIONE TESI DI DOTTORATO DI RICERCA

Il/la sottoscritto/a	Cesare Canepari
Matricola / *registration number*	015481
nato a/ *born at*	Voghera
il/*on*	21/04/1994

autore della tesi di Dottorato di ricerca dal titolo / *author of the PhD Thesis titled*

Improving the Efficiency of *in Vivo* Lentiviral Gene Therapy to Hepatocytes and Application to Familial Hypercholesterolemia

☐ AUTORIZZA la Consultazione della tesi / AUTHORIZES *the public release of the thesis*

☒ NON AUTORIZZA la Consultazione della tesi per 12 mesi /DOES NOT AUTHORIZE *the public release of the thesis for* 12 *months*

a partire dalla data di conseguimento del titolo e precisamente */ from the PhD thesis date, specifically*

Dal / *from* 27/02/2023 Al / *to* 27/02/2024

Poiché /*because*:

☒ l'intera ricerca o parti di essa sono potenzialmente soggette a brevettabilità/ *The whole project or part of it might be subject to patentability;*

☒ ci sono parti di tesi che sono già state sottoposte a un editore o sono in attesa di pubblicazione/ *Parts of the thesis have been or are being submitted to a publisher or are in press;*

□ la tesi è finanziata da enti esterni che vantano dei diritti su di esse e sulla loro pubblicazione/ *the thesis project is financed by external bodies that have rights over it and on its publication.*

E' fatto divieto di riprodurre, in tutto o in parte, quanto in essa contenuto / *Copyright the contents of the thesis in whole or in part is forbidden*

Data /Date 26/01/2023 Firma /Signature 

DECLARATION

This thesis has been:

- composed by myself and has not been used in any previous application for a degree. Throughout the text I use both 'I' and 'We' interchangeably.
- has been written according to the editing guidelines approved by the University.

Permission to use images and other material covered by copyright has been sought and obtained.

All the results presented here were obtained by myself, except for:

1) *Electron microscopy experiments (Results, chapter 3.1.1, fig. 1D) were performed in collaboration with Dr. A Raimondi, ALEMBIC facility, IRCCS San Raffaele Scientific Institute, Milan, Italy, who performed staining and acquired images.*

2) *Immune fluorescence staining (Results, chapter 3.1.3, 3.2.4, 3.5.2; fig. 3G, 9D, G, H, 20C) was performed with the help of Francesco Starinieri, SR-TIGET, Milan, Italy and Eugenia Cammarata, ALEMBIC facility, IRCCS San Raffaele Scientific Institute, Milan, Italy, who created the program, using Matlab, to analyze the images.*

3) *Cholesterol, LDL, ALT serum concentrations were evaluated by Micol Rava in "mouse clinic" Results, chapter 3.3.1-3.3.4; fig. 4B, C, 5B, C, 6B, C, 7B-I, 10B, C, 11D, E, 12B, 13C, 14C, 15C, 16C)*

4) *Liver and aorta (Results, chapter3.2.4, 3.2.5; fig. 8A-C, 9A, 10G) were embedded in formalin and cut by Rossana Norata and Martina Rocchi, GLP test facility, IRCCS San Raffaele Scientific Institute, Milan, Italy; the images were then analyzed by Francesca Sanvito, who wrote the corresponding histopathology reports.*

5) *Mass spectrometry assay for caffeine metabolism was performed by ProMeFa facility, IRCCS San Raffaele Scientific Institute, Milan, Italy.. In particular, by Denise Drago and Annapaola Andolfo. (Results, chapter 3.3.3; fig. 14E-G, 15E-G)*

6) *Large-scale LV preparations for use* in vivo *in mice were performed with the help of Mauro Biffi or Lucia Sergi Sergi, SR-TIGET, Milan, Italy.*

All sources of information are acknowledged by means of reference.

ACKNOWLEDGEMENTS

I would like to thank Dr. Alessio Cantore for giving me the opportunity to work on this inspiring project, and for the guidance and support. Thank you for sharing with me your expertise on the field, for insisting on taking part in congresses, since the work of a scientist is not just benchwork and literature reading. You were the proof that a good mentor can be authoritative and friendly at the same time. Thank you for always listening to my eccentric scientific ideas, and for, most of the times, encouraging me to verify their values (I still think that the solution for type I diabetes could be synthetic-PCSK9-promoter-driven insulin gene transfer to hepatocytes).

My sincere gratitude goes to Professor Luigi Naldini, for being always updated on each scientific project, for always trying to make speculations, for your overall view of the Tiget institution direction. Not less important, for your diplomacy and infinite patience, when approaching pharmaceutical companies. You are an example for all of us, young scientists still sometimes guided by impetuosity.

I would like to thank my Second Supervisor, Professor Thierry VandenDriessche. Despite never being able to see you in person thanks to Covid pandemic, the two private online meetings that we had were very useful.

My gratitude goes also to Daniela Talarico for holding her Tutor position earnestly, and for keeping me updated with the latest cinema masterpieces released in a particular festival.

Thank you, Michela, for being always supportive, for our day-to-day discussions during coffee breaks and last-minute dinners, talking about science, cinema, music, scuba-diving, trekking, ambitions. Thank you for the energies that you spent at the beginning of my laboratory staying.

I would like to thank Elena, Fabio, Mauro, Anna, Camilla, Sofia, Andrea for being by my side every day physically, in the same laboratory bench, and metaphorically, by participating with me in the hypes and falls of this mesmerizing project.

Chiara and Francesco, thank you for the laughs and jokes, for your smart suggestions and precious friendship. Your company has been crucial through this journey.

Dr. Francesca Sanvito, a special thank goes to you, for being always curious about my project and never bored by my unexpected visits asking for microscope slides histopathology evaluations. I am grateful for the scientific discussions that we had throughout these years.

Finally, a few words deserve some people out of this laboratory.

Eugenio, Carlo, Niccolò, Francesco, Eleonora, Micol, Camilla, thank you all for being a safe harbor each time we all come back home.

Mom and Dad, thank you for providing me with the tools to compete in the world, for all the passions that you passed to me and for pushing me to keep following the ones that I nurtured by my own.

Carolina, thank you for always being my disinterested counselor and assistant in the hardest times.

Giulia, the biggest thanks go to you, for always being by my side, for giving me advice without stepping on my freedom of choice, for amusing me every day.

Abstract

Mutations in genes expressed by hepatocytes cause a plethora of monogenic diseases, which may be treated by liver directed *in vivo* gene therapy. Adeno-associated viral (AAV) vectors represent the most advanced platform to reach this goal. However, the mostly episomal conformation of AAV vectors in target cells causes their dilution during liver growth, challenging treatment of pediatric patients. In contrast, lentiviral vectors (LV) integrate in the genome and are maintained upon cell proliferation. We previously showed stable LV-mediated liver gene transfer in neonatal and adult mice, dogs and non-human primates. Here we applied for the first time this strategy to a cell autonomous disease, familial hypercholesterolemia (FH), which is due to mutations in the low-density lipoprotein receptor (LDLR) gene. Despite LDLR is reported as the main receptor of VSV.G, used to pseudotype LV, we observed efficient gene transfer in *Ldlr*$^{-/-}$ mice by VSV.G LV, with even higher transgene output compared to normal mice. We obtained instead very low infectious titers when producing LDLR encoding VSV.G LV, due to LDLR-VSV.G interaction and possible re-infection of producer cells. We solved the issue by changing pseudotype, or by avoiding LDLR expression during LV production. With these upgraded LV, we treated juvenile *Ldlr*$^{-/-}$ mice and obtained long term LDL-C normalization, maintained even following a challenge with a high cholesterol diet. Moving to adult mice, we did not show phenotypic correction because of reduced transduction efficiency. Enhancing gene transfer efficiency is crucial for facing new diseases where most of the liver mass must be corrected, but also for reducing doses when approaching non-cell autonomous diseases like hemophilia, a disease due to lack of coagulation factors. With this in mind, we tested strategies to increase corrected liver mass *a posteriori* (inducing a selective advantage of corrected towards non-corrected hepatocytes) or *a priori*. To increase potency *a priori*, we identified several procedures (fasting, inhibition of interferon or proteasome pathways) to implement before LV administration, that allowed increase LV-mediated in vivo gene transfer to hepatocytes. When fasting and proteasome inhibition were used in combination, we achieved >11-fold higher gene transfer and transgene output. These findings corroborate the rational of using LV for the treatment of diseases that are life-threatening in childhood and shed light on molecular pathways that could be targeted to enhance the potency of LV-mediated in vivo gene transfer to hepatocytes.

TABLE OF CONTENTS

ACRONYMS AND ABBREVIATIONS....6

LIST OF TABLES AND FIGURES....11

1. INTRODUCTION....13

1.1 Gene therapy general concepts....13

1.1.1. The liver: ideal target for in vivo GT....17

1.2 AAV GT *in vivo* to the liver....19

1.2.1 AAV wild type viruses turned into GT vectors....19

1.2.2 In vivo AAV GT achievements....20

1.2.2.1 HA and HB state of the art....20

1.2.3 AAV vectors current limitations....23

1.3 LV GT *in vivo* to the liver....24

1.3.1 LV wild type viruses turned into GT vectors....24

1.3.2 In vivo LV GT achievements....27

1.3.3 LV current limitations....29

1.3.4 Comparing LV and AAV vectors for liver GT....30

1.3.5 Potency, manufacturing, cell autonomous diseases....30

1.4 Familial hypercholesterolemia....31

1.4.1 Lipoproteins metabolism....33

1.4.1.1 Dietary lipids and cholesterol absorption....33

1.4.1.2 Distribution of TG to peripheral tissues by CM....36

1.4.1.3 CM remnant uptake by hepatocytes....37

1.4.1.4 VLDL formation and secretion by hepatocytes....38

1.4.2 LDL-driven atherosclerosis....39

1.4.3 Reverse cholesterol transport....40

1.4.4 Available treatments 41
1.4.4.1 Liver transplantation 41
1.4.4.2 LDL apheresis 41
1.4.4.3 Statins 42
1.4.4.4 Bile acids sequestrants 43
1.4.4.5 NPC1L1 as a target 43
1.4.4.6 PCSK9 as a target 44
1.4.4.7 APOB100 as a target ..... **Error! Bookmark not defined.**
1.4.4.8 Angptl3 as a target 46
1.4.4.9 CETP as a target 47
1.4.5 Gene therapies for FH 48
1.4.5.1 Genetic inactivation of PCSK9 and ANGPTL3 48
1.4.5.2 LDLR gene transfer 49
1.5 Improving efficacy of liver directed LV GT 52
1.5.1 IFN mediated mechanism of defense against lentiviral vectors 53
1.5.2 Proteasome involvement in defense against LV 53
1.5.3 Fasting induced improvement in AAV mediated GT 54
1.5.4 Positive selection of hepatocytes corrected through GT 54
2. AIM OF THE WORK 56
3. RESULTS 57
3.1 Challenges of LV *in vivo* GT for FH 57
3.1.1 Reduced productivity of LDLR-encoding LV 57
3.1.2 Rescue of productivity of LDLR-encoding LV and validation in vitro ... 59
3.1.3 Higher transgene output in $Ldlr^{-/-}$ than in control mice, by in vivo LV GT 61
3.2 *LDLR* gene transfer in FH mice 64
3.2.1 hLDLR gene transfer in adult $Ldlr^{-/-}$ mice fails to reduce LDL-C 64

3.2.2 mLdlr gene transfer in adult Ldlr$^{-/-}$ mice fails to reduce LDL, independently on the immune system 65

3.2.3 mLdlr gene transfer in young Ldlr$^{-/-}$ mice stably reduces LDL-C 67

3.2.4 mLdlr gene transfer in young Ldlr$^{-/-}$ mice fully normalizes LDL-C and protects from ATH, even after a diet challenge 68

3.2.5 Long term efficacy and safety following Ldlr LV GT in young Ldlr$^{-/-}$ mice 75

3.2.6 Expression of LDLR inhibitor rescues productivity of sense-oriented LV, which fully normalize LDL-C in Ldlr$^{-/-}$ mice 76

3.3 Endowing transduced hepatocytes with a selective advantage 79

3.3.1 Selectable LV GT is feasible for HB 79

3.3.2 Selectable LV GT is feasible for HA 82

3.3.3 Selectable LV GT is feasible at different ages but stably impairs CYP450 activity 84

3.3.4 Selectable LV GT allows for >50-fold increase in transgene output, when starting from very low transgene amounts 88

3.4 Transduction enhancers: targeting anti-viral pathways 90

3.4.1 MarI and Bortezomib as single treatments increase LV gene transfer potency 90

3.4.2 Lack of additive/synergistic effect in enhancing LV gene transfer of MarI and Bortezomib 93

3.5 Transduction enhancers: fasting 94

3.5.1 Fasting increases LV gene transfer to hepatocytes in vivo 94

3.5.2 Fasting impacts on LDLR pathway 98

3.6 Transduction enhancers in combination, in C57 and *Ldlr*$^{-/-}$ mice 99

4. DISCUSSION 102

4.1 LV mediated liver GT for FH 102

4.2 The risk of insertional-mutagenesis in LV-mediated liver GT 103

4.3 Rescue in productivity of sense-oriented LDLR encoding LV 105
4.4 Future directions of HoFH treatment by *in vivo* liver-directed LV GT 106
4.5 Selection of corrected hepatocytes mediated by paracetamol 108
4.6 Inhibition of proteasome activity and IFN signaling before LV enhance hepatocyte gene transfer.....110
4.7 Fasting before LV enhance gene transfer and induces additive effect if combined with proteasome inhibition.....111
4.8 Conclusions.....114
5. MATERIAL AND METHODS 117
5.1 Plasmid generation 117
5.2 Plasmid DNA purification 118
5.3 Cell line cultures 118
5.4 LV production 118
5.5 LV titration.....119
5.6 ddPCR and VCN determination.....120
5.7 Gene expression assays 120
5.8 Flow cytometry 122
5.9 Mice experiments 122
5.10 Paracetamol preparation and selection protocol 123
5.11 Sorting of liver sub-populations.....124
5.12 Total cholesterol and LDL-C measurements 125
5.13 Aorta and liver collection for histopathology analysis.....126
5.14 In vitro transduction experiments.....126
5.15 Dietary regimens 127
5.16 Mass spectrometry on caffeine and on its metabolites.....127
5.17 Electron microscopy.....128
5.18 ELISA assays 129

5.19 Immunofluorescence imaging.....130

6. REFERENCES 132

ACRONYMS AND ABBREVIATIONS

AAV	Adeno associated viruses
AAV 2, 5, 8	AAV serotype 2, 5, 8
AAVS1	Adeno associated virus integration site 1
AAV vectors	Adeno-associated viral vectors
Ab	Antibody
Abs	Antibodies
ABCA1	ATP binding cassette protein A1
ABCG1, 5, 8	ATP binding cassette subfamily G member1, 5, 8
ABE	Adenine base editor
ADA	Adenosine deaminase
ALT	Alanine aminotransferases
ANGPTL3	Angiopoietin like-3
ANGPTL4	Angiopoietin like-4
ANGPTL8	Angiopoietin like-8
APAP	Acetaminophen, paracetamol
ApoAI	Apolipoprotein AI
ApoAV	Apolipoprotein AV
ApoB	Apolipoprotein B
APOBEC	ApolipoproteinB mRNA editing catalytic polypeptide-like
ApoCII	Apolipoprotein CII
ApoCIII	apolipoprotein CIII
ApoE	Apolipoprotein E
ARSA	Arylsulfatase A
ASGPR	Asialoglycoprotein receptor
ASO	Antisense oligonucleotide
ATH	Atherosclerosis

BCMA	B-cell maturation antigen
BDD	B domain deleted
Bort	Bortezomib
BSEP	Bile salts export pump
CAR	Chimeric antigen receptor
Cas9	CRISPR-associated protein 9
CBE	Cytidine base editor
CCL4	Carbon tetrachloride
CD19	Cluster of differentiation 19
CE	Cholesterol esters
CETP	Cholesterol ester transfer protein
CHD	Coronary heart disease
CM	Chylomicrons
CMR	CM remnant
CMV	Cytomegalovirus
c.o.	Codon optimized
cPPT	Central polypurine tract
CRISPR	Clustered regulatory interspaced short palindromic repeats
CTS	Central termination site
CVD	Cardiovascular disease
CYP450	Cytochrome P450
DLBCM	Diffuse large B-cell lymphoma
EC	Endothelial cells
EMA	European Medical Agency
ER	Endoplasmic reticulum
ET	Enhanced transthyretin
FAH	Fumarylacetoacetate hydrolase
FDA	Food and Drug Administration
FFA	Free fatty acids
FH	Familial hypercholesterolemia

FIX	Coagulation factor IX
FL	Follicular lymphoma
FL3B	Follicular lymphoma grade 3B
FRG	$Fah^{-/-}Rag2^{-/-}IL2rg^{-/-}$
FVIII	Coagulation factor FVIII
GAlNac	N-Acetyl-Galactosamine
GFP	Green fluorescent protein
GOF	Gain of function
GPIHBP1	Glycosylphosphatidylinositol anchored HDL binding protein 1
GSH	Glutathione
gRNA	Guide RNA
GT	GT
HCC	Hepatocellular carcinoma
HDR	Homology direct repair
HEK	Human embryonic kidney
HDL	High density lipoproteins
He	Heterozygous
HIV	Human immune-deficiency virus
HL	Hepatic lipases
hLDLR	Human LDLR
HMG-CoA reductase	3-hydroxy-3methylglutaryl coenzyme A reductase
Ho	Homozygous
HSPC	Hematopoietic stem and progenitor cells
HSPG	Heparan sulfate proteoglycans
IDL	Intermediate density lipoprotein
IFNARI	Interferon alpha/beta receptor subunit 1
IRES	Internal ribosome entry site
ITR	Inverted terminal repeats
IU	International units
Kb	Kilobases

KC	Kupffer cells
KO	Knock out
LDL	Low density lipoproteins
LDLR FM	LDLR family members
LDLR	Low density lipoproteins receptor
LDLRAP	Low density lipoprotein receptor adaptor protein 1
LILP	Endothelial lipases
LMF1	Lipase maturation factor 1
LNP	Lipid nanoparticles
LOF	Loss of function
Lp(a)	Lipoprotein(a)
LPL	Lipoprotein lipase
LRP1	Low-density lipoprotein receptor related protein 1
LSEC	Liver sinusoidal endothelial cells
LTR	Long terminal repeats
LV	Lentiviral vectors
MAG	Monoacyl glycerol
MHC-I	Major histocompatibility complex class I
MM	Multiple myeloma
mIFNAR1	Mouse interferon alpha/beta receptor subunit 1
mLDLR	Murine LDLR
mRNA	Messenger RNA
MTTP	Microsomal triglycerides transfer protein
NAPQI	N-acetyl-p-benzoquinone imine
NHEJ	Non-homologous end joining
NHP	Non-human primates
nPC	Non-parenchymal cells
NPC1L1	Niemann-Pick C1-Like 1
NTBC	Nitisinone
oxLDL	Oxidized LDL

PAM	Protospacer adjacent motif
PCSK9	Proprotein convertase subtilisin/kexin type 9
pDC	Plasmacytoid dendritic cells
PL	Phospholipids
PLA2	Phospholipase A2
PMBCL	Primary mediastinal B-cell lymphoma
Ψ	LV packaging signal
RPE65	Retinal pigment epithelium-specific 65 KDa protein
RRE	Rev responsive element
SA	Splice acceptor
SD	Splice donor
SIN	Self inactivating
SMA	Spinal muscular atrophy
SMN1	Survival motor neuron 1
SRB1	Scavenger receptor B1
SREBP2	Sterol regulatory element binding protein 2
ssDNA	Single strand DNA
TALEN	Transcription activator-like effector nuclease
TG	Triglycerides
VCN	Vector copy number
VLDL	Very low density lipoproteins
VSV.G	Vesicular stomatitis glycoprotein
WHHR	Watanabe heritable hyperlipidemic rabbits
WD	Western diet
WHP	Woodchuck hepatitis virus
WPRE*	Woodchuck hepatitis virus posttranscriptional regulatory element mutated
ZFN	Zinc-fingers nucleases

LIST OF TABLES AND FIGURES

Table 1…….14

Figure I……18
Figure II……...25
Figure III……..32
Figure IV……..35
Figure V……...55

Figure 1……58
Figure 2……60
Figure 3……62
Figure 4……64
Figure 5……66
Figure 6……67
Figure 7……69
Figure 8……71
Figure 9……73
Figure 10……..75
Figure 11……..78
Figure 12……..80
Figure 13……..83
Figure 14……..85
Figure 15……..87
Figure 16……..89
Figure 17……..91
Figure 18……..93
Figure 19……..95
Figure 20……..96

Figure 21……..98
Table 2……...100
Figure 22……100

1. INTRODUCTION

1.1 Gene therapy general concepts

The idea of gene therapy (GT) blossomed more than 50 years ago. In 1972, the paper "GT for human genetic disease?", written by Theodore Friedman and Richard Roblin, was published on Science (Friedmann & Roblin, 1972). They strongly believed the answer was yes, since "good DNA" could have been used to replace defective DNA in people affected by genetic diseases. The work is now considered among the milestones on which the field was built, together with Asilomar Conference on ethics of recombinant DNA/genetic modification, arranged three years later (Berg & Mertz, 2010). In monogenic diseases, GT aims to treat the disease through delivery of correct sequence of the mutated gene (gene replacement). Alternatively, GT can provide new functions to the target cell (gene addition). Targeting immune cells to instruct them to fight cancer or infections is an example of this (Dunbar *et al*, 2018). The most used vehicles for gene transfer are viruses, efficient in infecting cells. They can be deprived of their pathological features, which are replaced with the therapeutic sequence of interest. They are turned in carriers, which allow the therapeutic genetic sequence to be safely unexposed during the journey up to the nucleus of the target cells. They are referred to as viral vectors, and the process of delivering a functional copy of the gene of interest is called gene transfer.

GT can be accomplished *ex vivo* or *in vivo*.

In *ex vivo* GT, the cells are harvested from the body and genetically modified, before being re-infused back into the patient. This strategy is especially effective in diseases related to the hematopoietic system: hematopoietic stem cells are mobilized from bone marrow, collected from circulation, modified through introduction of the gene sequence that was lacking and re-infused. Cells derived from differentiation of the cells corrected *ex vivo* will contain the gene sequence of interest, and the patient will be cured potentially forever.

In vivo GT: the therapy is delivered to the patient, either *in situ*, in defined anatomical compartments (example: administration in retinal pigment epithelium of Luxturna, Table 1) or systemically, with the aim of reaching organs such as the liver (example of Hemgenix, Table 1).

Most of the GT drugs now approved relies on *ex vivo* genetic modification of hematopoietic stem and progenitor cells (HSPC). Particularly, most of them aims to gene

replacement for immune deficiencies or chimeric antigen receptors (CAR) gene addition, to instruct immune cells to recognize and destroy malignant cells. *In vivo* GT, at a less advanced stage of development, is counting 6 approved drugs in a total of 16.

Table 1: approved GT drugs as of March 2023

Drug name	**Application**	**Mechanism**	**Year of approval**	***Ex vivo*/ *in vivo***
Imlygic	Recurrent melanoma	Oncolitic vector, gene addition	2015	*in vivo*
Strimvelis	Adenosine deaminase deficiency	Gene replacement: ADA cDNA	2016	*ex vivo*
Kymriah	Relapsed or refractory follicular lymphoma	CAR-T vs CD19	2017	*ex vivo*
Luxturna	Inherited retinal dystrophy	Gene replacement: Rpe65 cDNA	2017	*in vivo*
Yeskarta	DLBCL, PMBCL, FL	CAR-T vs CD19	2017	*ex vivo*
Libmeldy	Metachromatic leukodystrophy	Gene replacement: ARSA cDNA	2020	*ex vivo*
Tecartus	Mantle cell lymphoma	CAR-T vs CD19	2021	*ex vivo*
Abecma	Multiple myeloma	CAR-T vs B cell maturation antigen	2021	*ex vivo*

Breyanzi	DLBCL, PMBCL, FL3B	CAR-T vs CD19	2022	*ex vivo*
Carvykti	Relapsed and refractory MM	CAR-T vs BCMA	2022	*ex vivo*
Skysona	Early cerebral adreno-leukodystrophy	Gene replacement: ABCD1 cDNA	2022	*ex vivo*
Zynteglo	β-thalassemia	Gene replacement: β-globin cDNA	2022	*ex vivo*
Zolgensma	Spinal Muscular Atrophy (SMA)	Gene replacement: SMN-1 cDNA	2022	*in vivo*
Upstaza	severe aromatic L-amino acid decarboxylase deficiency	Gene replacement: AADC cDNA	2022	*in vivo*
Hemgenix	Hemophilia B	Gene replacement: FIX cDNA	2022	*in vivo*
Roctavian	Hemophilia A	Gene replacement: FVIII cDNA	2023	*in vivo*

Despite the simplicity of the concept of GT, a plethora of complexities are required for its efficient fulfilment: i) the amount of genetically corrected target cells required to see a phenotypic correction (efficacy) may vary among different diseases, ii) transgene expression should last overtime, potentially forever (durability), iii) host immune responses against the vector and/or the transgene product could compromise efficacy and safety of the therapy (immune tolerability), iv) in case of particular diseases, transgene expression should be controlled spatially or temporally (selectivity), v) in case of transgene expression cassettes which integrate in the host cell genome, perturbation of gene expression of genomic loci localized near the integration site may lead to cellular

toxicity or cell transformation (insertional mutagenesis), ultimately leading to cancer (safety) (Cavazzana *et al*, 2019). Efficacy, durability, immune tolerability toward transgene product, and safety are thus the pillars that hold up a successful GT.

Concerning selectivity, it can be accomplished through genome editing, an innovative branch of gene therapy. The concept of genome editing defines strategies to target precisely and exclusively desired *loci* in the genome. This can be achieved using an editing machinery able to specifically recognize the DNA target sequence and cut it; consequently, the target cell either repairs the DNA break through non-homologous end joining (NHEJ, error prone, if the aim is gene disruption), or through homology-directed repair (HDR, if the aim is gene correction). In the latter case, the template sequence to be used for HDR is part of the editing machinery to be delivered (donor DNA). Concerning recognition and cut of the target DNA sequence, different tools have been developed: zinc finger nucleases (ZFN), transcription activator-like effector nucleases (TALENs) and clustered regulatory interspaced short palindromic repeats (CRISPR)/CRISPR-associated (Cas) nuclease. CRISPR/Cas is a dual system, composed of Cas protein and guide RNA (gRNA). Cas9 performs a DNA double strand break following gRNA binding to the target DNA site. It is currently the most widely used tool to edit the genome and earned the Nobel Prize to the scientists first describing it, Jennifer Doudna and Emilie Charpentier (Doudna, 2020). No matter which is the technology used, once the break is introduced, the cell will fix it. Repair can occur through i) NHEJ or ii) HDR. NHEJ is an excellent way for creating knockout of genes since the outcome are frameshift mutations (indels) leading to loss of gene expression in most cases. HDR is less efficient but accurate DNA repair pathway. The cell conventionally uses the sister chromatid to perform this process. In genome editing, the template used in place of the sister chromatid is called donor DNA. If the aim is gene correction through HDR, efficiency is usually quite low and an important percentage of cut will anyway be fixed through NHEJ (Musunuru, 2022).

In case of gene correction, two are the main advantages, compared to gene transfer: i) virtual absence of safety concerns previously mentioned (no genomic perturbation should be present, since the integration of the cassette should be in the locus of the gene), ii) transgene expression should be controlled temporally, being subjected to physiological regulation (selectivity).

While the success rate for gene disruption is quite high, the main limitation of gene correction is currently the low rate of homologous recombination. Recently, a new

technology made headlines: base editing. This approach involves the use of two components fused together: a Cas9 bound to gRNA, which identifies the target sequence in the genome, and a base converting enzyme, which induces the desired edit in a specific base. The process is achievable through the following steps: i) gRNA-Cas9 complex searches for a docking sequence, ii) it unwinds DNA adjacent to the target DNA position and, iii) searches for a perfect match between gRNA and target DNA, iv) if docking and match sequences are present, Cas9 makes a nick, and the base converting enzyme makes the base exchange, a few bases distant, on the opposite strand, v) the cell repairs the base change, leading to a permanent modification in the genome. These new technologies are referred to as adenine base editors (ABE) or cytidine base editors (CBE) in case conversion is from A•T-to-G•C or C•G to T•A base pairs respectively (Huang *et al*, 2021). With this technology, it is now possible to turn a coding codon in a stop codon, and obtain gene disruption at high rates. The other application of base editors is the correction of specific codons, particularly relevant in diseases where a single mutation is particularly diffuse (sickle cell anemia, for example).

1.1.1. The liver: ideal target for in vivo *GT*

The liver is the human second biggest organ (behind skin). Hepatocytes are the parenchymal cells contributing for >70% of this organ. 15% of the liver is made by liver sinusoidal endothelial cells, LSEC. LSEC form a monolayer with specific features: presence of fenestrations and lack of basement membrane. This configuration confers to LSEC their sieve function. 6% are Kupffer cells (KC), the liver resident macrophages. They localize in perisinusoidal space. Remaining 9% are hepatic stellate cells, bile duct cells (cholangiocytes) and other cell types (Racanelli & Rehermann, 2006). Structural and functional unit of the liver is the lobule, which appears in hexagonal shape when looked at in histological cross sections (Fig. I).

Among liver functions: detoxification of various metabolites (drugs included), synthesis of plasma proteins (among which coagulation factors), carbohydrate and lipid metabolism, production of bile acids. The liver is supplied with blood coming from the portal vein (75%) and from the hepatic artery (25%). The two vessels merge in the sinusoids, the thin hepatic capillaries displaying features of slow blood flow, low perfusion pressure, low oxygen tension. Flow reaches the central veins and leaves the liver through hepatic veins. The central vein represents the center of the lobule, while the

hexagon is shaped through portal triads (each "corner" corresponds to a triad). Portal triad is composed by portal vein, hepatic artery and bile duct. While blood flows from periphery towards central vein, bile flows through bile canaliculus in opposite direction, towards bile duct and converges in the gallbladder.

In accordance with their distance from the portal vein or central vein, hepatocytes are conventionally divided in zones. Hepatocytes in each zone slightly differ in their transcriptome, in accordance with different functions they must perform. Zone 1 is called peri-portal and comprises hepatocytes lying in the perimeter of a lobule. These hepatocytes are the first touched by high oxygen high nutrients containing blood, entering the liver. They are involved in liver metabolic functions, among which lipid metabolism, gluconeogenesis, ureagenesis, protein and glycogen synthesis.

Zone 2 are currently considered the ones mostly contributing to homeostasis repopulation and regeneration (He *et al*, 2021).

Zone 3 hepatocytes surround central veins, so they are called pericentral hepatocytes. Xenobiotic metabolism, glutamine synthesis, glycolysis, and are among the functions of these hepatocytes. More specifically, the vast majority of cytochrome P450 (CYP450) are expressed in this zone. Recently, hepatic zones have been further divided in 9, with each zone comprising hepatocytes expressing hepatic genes differentially (Halpern *et al*, 2017).

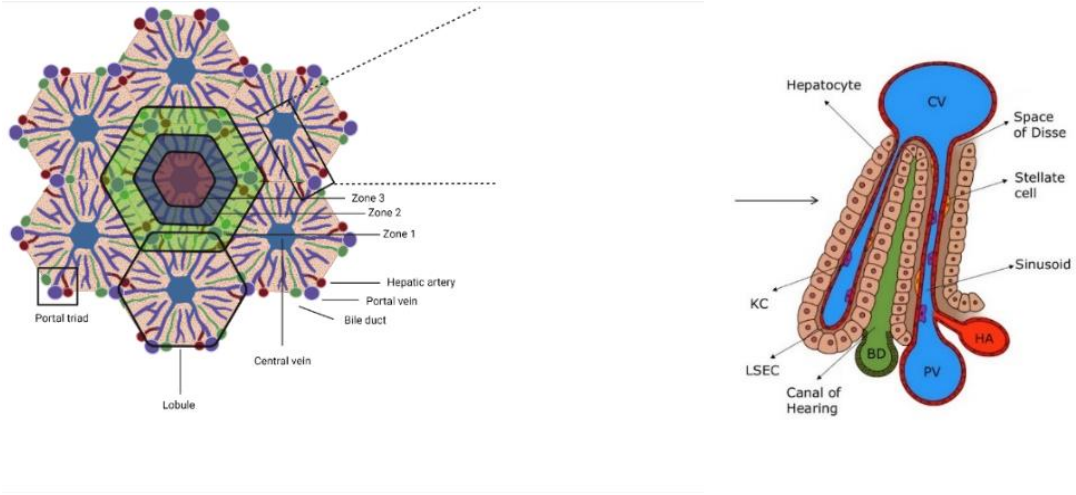


Figure I. Liver structure. *The liver is organized in hexagonally shaped lobules. In the center of each lobule is the central vein, while at each corner of the lobule stands a portal triad. Portal triads comprise branches of the portal vein, hepatic artery and bile duct. Blood enters the liver through portal vein and hepatic artery, flowing towards the central vein. Vessels connecting portal and central veins are called sinusoids and are made of LSEC. Lines of hepatocytes laying*

between portal and central vein are called cordons. Hepatocytes are separated from LSEC by space of Disse, where stellate cells reside. Hepatocytes are polarized cells: one side is in contact with the space of Disse, the other with the canal of Hearing, where bile acids are secreted, to then converge in the bile duct. Abbreviations: KC = Kupffer cells; BD = bile duct; PV = portal vein; HA = hepatic artery; CV = central vein. Created with BioRender.com.

The liver is provided with efficient secreting capabilities; moreover, it is the metabolic hub of our body. As such, and considering the number of monogenic diseases whose genetic impairment resides in hepato-specific genes, hepatocytes are intriguing candidates for *in vivo* directed GT of both intracellular and secreted proteins. Throughout the years numerous viral vectors were used for GT. Currently, the most widely used for *in vivo* GT are adeno-associated viral vectors, derived from adeno-associated viruses.

1.2 AAV GT *in vivo* to the liver

1.2.1 AAV wild type viruses turned into GT vectors

Adeno associated viruses (AAV) are non-enveloped, 25 nm, icosahedral shaped, single stranded DNA (ssDNA) viruses, belonging to the Parvoviridae family. AAV require contemporary presence of other viruses (conventionally adenoviruses) to replicate. AAV genome encodes 4 non-structural proteins, called REP, 3 capsid proteins, called V1, V2, V3, and an assembly activating protein (Wang *et al*, 2019). Genome is flanked by so called inverted terminal repeats (ITR), 145 bases long, necessary to package the genome into the capsid. Different natural serotypes have been described. Each of them exhibits specific tropism. AAV accesses target cells through receptor-mediated endocytosis, escaping endosome and uncoating itself in proximity to the nucleus. Then, it converts its genome in double stranded and integrates mainly in a 2 kb region located on chromosome 19, named AAVS1 locus. There, it is maintained in latency state until adenovirus infects the same cell. At that point, it will exploit adenovirus genes to replicate itself.

Moving to recombinant AAV vectors, used as viral vectors for GT, it is necessary to transfect HEK293 cells with 3 plasmids, to generate them: i) transgene-containing plasmid, flanked by ITR, to be packaged into the capsid, ii) plasmid encoding rep and cap genes, required for capsid formation and replication, iii) plasmid encoding adenovirus helper genes. Capsid modification has been proposed throughout years, to induce change in tropism. Moreover, other modifications are now performed: trans-capsidation, adsorption of foreign peptides and mosaic capsids. Trans-capsidation: the process of packaging the ITR of one serotype into the capsid of another serotype. Adsorption of

receptor ligands: addition of foreign peptides on the surface of the recombinant AAV capsid. Mosaic capsid: recombinant AAV transgene is packaged in a capsid comprising a mixture of unmodified proteins from capsids of different serotypes. Chimeric capsids: capsids comprising foreign protein sequences inserted in open reading frame with a capsid gene.

In the last two decades, adeno-associated viral vectors (AAV vectors) have become the most used vectors for *in vivo* liver GT. AAV vectors display low immunogenicity and nearly negligible inflammatory responses, at least up to certain doses. Recombinant AAV vectors no longer show preferential integration at AAVS1 locus, since they lack rep proteins. Instead, they (mostly) remain episomal. Since hepatocytes are long living cells, AAV vectors can be used to correct them, in case of patients treated as adults.

1.2.2 In vivo *AAV GT achievements*

AAV vectors are showing promising results in a series of clinical trials. Moreover, as mentioned before, 6 are the commercial *in vivo* GT. All of them are AAV vectors GT. Five of them are gene replacement GT. Luxturna delivers a transgene encoding a functional enzyme into the retinal pigment epithelium and is restoring vision in people affected by Laber congenital amaurosis. It is administered in subretinal space. Zolgensma encodes for regulatory protein survival of motor neuron and is indicated for the treatment of spinal muscular atrophy (SMA), an otherwise lethal disease. It is delivered systemically. Imlygic, an oncolytic vector, is designed for the treatment of melanoma. Upstaza delivers a functional copy of AADC gene to the brain of children affected by severe aromatic L-amino acid decarboxylase deficiency (Keam, 2022). Finally, Hemgenix and Roctavian have been approved for the treatment of HB and HA, respectively (Blair, 2022). Despite these were the latest AAV vector drug to be approved, hemophilias was among the first diseases faced by *in vivo* GT.

1.2.2.1 HA and HB state of the art

Hemophilia A (HA) and hemophilia B (HB) are X linked coagulation disorders due to mutations in coagulation factor VIII (*FVIII*) and coagulation factor IX (*FIX*) respectively. HA has a frequency of 1/5000 males, hemophilia B of 1/25 000. Hemophilia is a suitable candidate for GT for different reasons: it is a monogenic disease, the genes mutated are

conventionally expressed by the liver, and it is sufficient a minimal expression of the lacking protein to get major improvements in bleeding phenotype. Coagulation factors have short half-life, and require >2-3 administration weekly. Synthetic modifications (PEGylation, inclusion of XTEN peptide) have increased their stability and half-life, making possible to reduce frequency of administration, but the impact of these conditions on the quality of life remains severe.

First AAV vectors mediated GT for hemophilia tried to tackle hemophilia B. *FIX* transgene is shorter than human *FVIII* and easier to be packaged in AAV vectors. In the first clinical trial, designed around 20 years ago, human *FIX* (*hFIX*) AAV vectors were injected intra-muscular. FIX expression was below 1% and lasted 3 years. From that time on, every following clinical trial chose hepatocytes as target cells for FIX expression, since FIX is normally produced by them. In 2006, AAV2 *FIX* vectors were injected directly into the hepatic artery. Despite FIX expression lasting 3 months, this trial was crucial for two main aspects. Firstly, it was shown that hepatocytes could be transduced with AAV vectors, ensuring expression of the desired transgene. Secondly, the issue of pre-existing immunity was faced for the first time: the reason behind the loss of efficacy was attributed to pre-existing memory T cells against the viral capsid used, which cleared away the transduced cells while still presenting AAV-derived capsid antigens (Ronzitti *et al*, 2020).

The first *FIX* successful clinical trial was performed at St. Jude/UCL in 2011 (Nathwani, 2019). AAV2 serotype was replaced with AAV8, based on i) the lower seroprevalence of this serotype (~25%) compared to AAV2 (>70%) and on ii) the liver specific remarkable tropism of AAV8. Ten patients without AAV8 pre-existing immunity were treated at three doses: 2 patients at $2x10^{11}$ viral genomes/kg, vg/kg, 2 patients at $6x10^{11}$ vg/kg, 6 patients at $2x10^{12}$ vg/kg. All of them had detectable hFIX circulating amounts, spanning between 1 and 8%. Elevation in liver alanine aminotransferases (ALT), detected in 4 patients treated at the highest dose, was the alarm bell indicating an ongoing immune response against capsid components, confirmed by reduction in FIX amounts. A short regimen of corticosteroid prednisolone restored ALT values to normal. FIX circulating amounts were stable from then on (follow up >8 years).

In 2009, a point mutation in FIX sequence was identified as the cause of thrombophilia in an Italian family: substitution of leucine with arginine at position 338. FIX level was normal, but the activity of FIX was 5-8-fold higher. The mutation was annotated as

"Padua", from the name of the city where it was identified (Simioni *et al*, 2009). In order to increase efficacy of GT, Padua FIX sequence started to be used in GT and almost all the current ~50 clinical trials ongoing (Leebeek & Miesbach, 2021) for the treatment of HB are exploiting this mutation. One of these candidates just reached the marketing authorization: Hemgenix. The key clinical trial for its approval was Hope-B, supervised by Dr. Stephen Pipe. Hemgenix is an AAV5 vector carrying *FIX* Padua. The important exception of this trial, compared to the past, was the choice to enroll even patients with pre-existing antibodies (Ab) against AAV5, 54 patients in total. Among them, just in two patients the therapy was not effective. The first patient had pre-existing immunity against AAV, and experienced strong increase in neutralizing Ab, responsible for inefficacy of the therapy. The second patient experienced an adverse reaction during the infusion, ending with just 10% of the volume injected and lack of therapeutic effect. 11/54 patients experienced elevation in ALT; they were subjected to 80 days of prednisolone regimen, which solved the issue. Six months post GT, the average hFIX circulating amounts were 39%; 24 months post GT, they were 36.7% (https://abstracts.isth.org/abstract/52-week-efficacy-and-safety-of-etranacogene-dezaparvovec-in-adults-with-severe-or-moderate-severe-hemophilia-b-data-from-the-phase-3-hope-b-gene-therapy-trial/) (von Drygalski *et al*, 2022).

Concerning HA, *FVIII* transgene is considerably longer than *FIX*, impossible to fit in an AAV vector. However, since FVIII B domain is not required for its activity, it has been removed (McIntosh *et al*, 2013). FVIII B domain deleted, FVIII-BDD, is the version commonly used for GT purposes. The first clinical trial of AAV vectors encoding FVIII was reported in 2017. It showed promising results: a median of 77 IU (international units)/dL (normal plasma FVIII levels average approximately 100 IU/dL). However, overtime, FVIII progressively declined. Among the possible explanations, it has been proposed that ectopic FVIII expression in hepatocytes may lead to toxicity and progressive loss of the highest expressing cells. Indeed, LSEC are the physiologic source of FVIII, not hepatocytes. Forcing FVIII expression by hepatocytes, together with codon optimizations may be the reason behind progressive endoplasmic reticulum (ER) stress and loss of transduced hepatocytes (Poothong *et al*, 2020). Codon optimization (c.o.) is a process which improves gene expression increasing translation efficiency of a transgene, based on the accommodation of codon bias of the host organism. Despite being a fascinating explanation for the outcome, the jury is still out.

Different clinical trials were initiated in the next years, but the trend of decline was shared among most of them. This unexpected outcome compelled FDA to wait for approval of the AAV5 vector GT candidate at the most advanced stage of development, voloctocogene roxaparvovec (Biomarin). After two more years of follow up, this GT has finally been approved under the name of Roctavian (Blair, 2022).

1.2.3 AAV vectors current limitations

Despite the highlighted advantages of AAV vectors, a few substantial drawbacks should be noted.

i) AAV are widely spread throughout human population. Therefore, around 30% of people are pre-immunized and has to be excluded from GT where AAV are used as vectors and administered i.v. Indeed, as said above, immunological memory against viral components would be responsible for clearance of target cells, exposing epitopes derived from viral components in the days/weeks following GT (Aronson *et al*, 2019). The only exception is by now represented by AAV5. AAV5 vectors were indeed applied, as mentioned above, to patients with pre-existing AAV5 immunity, with partial success.

ii) AAV have limited cargo capacity (~4.7 Kb). Thus, in case of long transgenes, this platform is not optimal. Certain genes might be shortened, like *FVIII* for HA, which can be deprived of its B domain (thus generating FVIII-BDD, as said before) or dystrophin for Duchenne muscular dystrophy, DMD, thus generating micro-dystrophin, to turn DMD in the milder Becker syndrome (Duan, 2018). Despite strategies to split long transgenes in different AAV vectors cassettes, to generate the final product following joining of the two parts of the protein, are under investigation, this is still at early stage of development (Esposito *et al*, 2022).

iii) AAV vectors mediated GT gives rise to mostly episomal transgene forms, progressively lost by dividing cells. Thus, patients must be treated as adults or late juvenile, once the liver is not growing anymore. Indeed, if pediatric patients would be dosed, they would dilute transgene product overtime, ultimately leading to non-therapeutic transgene amounts. Strategies to re-dose GT are under investigation, but the concept of GT as "single one-and-done administration" would be lost (Leborgne *et al*, 2020).

iv) AAV vectors have always been considered non-integrating viral vectors. However, recently, different studies are reporting integrations of AAV vectors into the genome of

target cells. Concerning primary hepatocytes, it has been reported between 1 and 3% of integrations following AAV vectors mediated gene transfer both *ex vivo* and *in vivo*. Particularly, most of integrated retrieved forms were genomic rearrangements of AAV genome. Moreover, at the site of insertion, deletions of genomic sequences were found (Dalwadi *et al*, 2021). Insertions and clonal expansion were even reported in livers from dogs treated with *FVIII* AAV (Nguyen *et al*, 2021). This aspect poses safety concerns on an aspect which in the past was not considered.

1.3 LV GT *in vivo* to the liver

1.3.1 LV wild type viruses turned into GT vectors

Lentiviruses are a subtype of retroviruses. The most famous lentivirus is human immunodeficiency virus (HIV). They are enveloped viruses, with 2 copies of a 9.7 kb single strand RNA genome. Diameter of LV is 120 nm, and the genome is organized in three different reading frames. LV efficiently access nucleus of dividing and non-dividing cells since they can pass through nuclear pore complexes. LV are intriguing vehicles for liver directed GT, since they stably integrate in the genome of target cells, ensuring their maintenance during liver growth, in case GT is performed during childhood. They are replicant defective. Currently, the most used ones are third generation LV. For safety purposes, to reduce the likelihood that a replication-competent LV is formed, LV production requires LV genome to be split in different plasmids (Fig. II). The transgene cassette is part of a plasmid which conserves LV sequences required for efficient packaging of LV and sequences required for genetic transfer in target cells (particularly, retro-transcription and integration). This plasmid is referred to as “transfer plasmid” and is flanked by long terminal repeats (LTR), necessary for vector integration. LTR comprise 3 elements: U3, R and U5. U3 acts as a promoter/enhancer of HIV genome. Thus, for safety reasons, to generate self-inactivating LV (SIN-LV), with no TATA box or residual transcriptional activity, 400 bp were deleted from U3, turning it in ΔU3 (Zufferey *et al*, 1998). Since HIV promoter is removed, transgene expression is driven by an internal promoter, which can be selected based on the desired potency of transcription and the cell type in which the transgene should be expressed. Moreover, removal of HIV promoter reduces the risk of genotoxicity. Genotoxicity, in GT, is referred to as a dangerous perturbation of genomic landscape resulting in up-regulation of cellular proto-oncogenes, ultimately leading to cancer. This perturbation is due to insertion of the GT cassette inside

or near to these genes, inducing promoter activation or truncation of regulatory domains or trans-activation of nearby genes through enhancer mediated mechanisms (David & Doherty, 2017).

The minimal set of capsid proteins required are instead provided *in trans*, conventionally split in 3 additional plasmids. These additional plasmids are expressed by the cells during vector production but not incorporated into the virions. First additional plasmid is encoding gag and pol genes. Gag genes: capsid proteins p24, nucleoprotein and matrix. Pol genes: protease, reverse transcriptase, integrase. Gag is translated as single polypeptide and protease cleaves it, generating the functional proteins. Second additional plasmid encodes Rev (regulator of expression of virion proteins). Rev binds to rev responsive elements (RRE) which are conventionally present on HIV, to mask splicing sites and allow for transcription of the entire genome of the virus. Full RNA transcription in producer cells is feasible thanks to the presence of cytomegalovirus (CMV) promoter upstream the LTR. Finally, a third plasmid encodes the surface protein of LV. It is typically derived from vesicular stomatitis virus glycoprotein (VSV.G), thus making LV vectors hybrid enveloped. VSV.G, generally, ensures high titers and broad tropism. VSV.G efficiently transduces hepatocytes *in vivo* following systemic administration of LV, so does baculovirus derived glycoprotein 64 (gp64). Baculovirus conventionally infect butterflies, and gp64 is supposed to interact with heparan sulfate proteoglycans (HSPG) (Duisit *et al*, 1999).

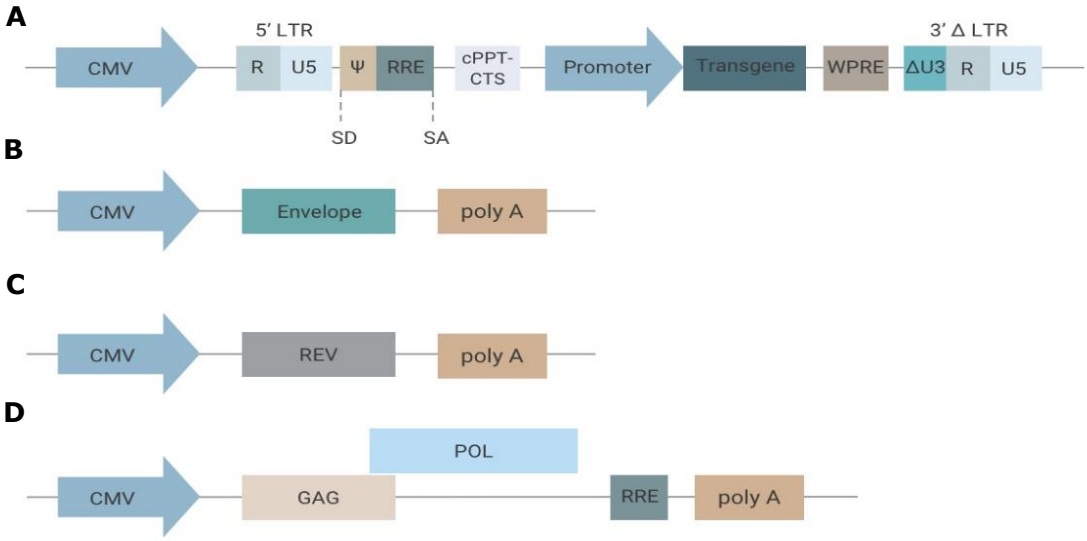


Figure II. Plasmids needed for assembly of third generation LV

A) *Transfer plasmid, containing transgene cassette. Cytomegalovirus promoter (CMV) drives the transcription of the plasmid from R at 5' to U5 at 3'. The corresponding RNA molecule is packaged in the LV particle and transferred to the target cells genome. LTR, long terminal repeats, comprise U3, R, U5 in the wild type HIV virus. Just like in HIV, transfer LV RNA and transfer plasmid lack U3; U3 will indeed be copied at 5' during the jumping step of LV during reverse transcription process. U3 is indeed present at the 3' of LV (and HIV) genome. In LV, however, it is turned into ΔU3: 400 bases of U3 genomic sequences, i.e. the ones providing promoter activity to LTR, are removed, to make LV self-inactivated (SIN) once integrated into target cells. SD, SA: splice donor, splice acceptor: these sequences are maintained in third generation LV since between them is the packaging signal (Ψ). Ψ ensures the RNA molecule to be packaged into the particle. RRE: rev responsive element, bases recognized by REV, which will bind to them, masking the splicing sequences and ensuring that the entire genomic sequence, from R at 5' to U5 at 3' is transcribed in a full genome RNA molecule. cPPT and CTS (central polypurine tract and central termination site): they ameliorate reverse transcription and import of LV genome into the nucleus of target cells. Promoter: an internal promoter drives the expression of the transgene of interest; different transgenes require different promoters. More specifically, the choice of a specific promoter occurs according to the specific cell type where the transgene has to be expressed and according to the transgene amounts that each target cell has to produce. Wpre: it stabilizes transgene transcript and gives advantage in transgene expression, since it increases nuclear export. It gives an advantage even during vector production, since even full genomes are increased in their nuclear export.* ***B)*** *Viral envelope plasmid usually encodes VSV.G and is separated from GAG POL PRO for safety reasons.* ***C)*** *Packaging plasmid, expressing Rev protein.* ***D)*** *Packaging plasmid required for expression of HIV proteins necessary in trans: gag genes (matrix, capsid, nucleoprotein), pol genes (protease, reverse transcriptase, integrase). Created with BioRender com.*

Together with already mentioned CMV, R, U5, SD, ψ and SA, additional sequences are included in the transfer plasmid, being essential for generating highly infective LV.

Central poly-purine tract and central termination site (cPPT and CTS, respectively) ameliorate the efficiency of reverse transcription and import by LV into the target cells genome (Follenzi *et al*, 2000). After the transgene of interest, woodchuck hepatitis virus

post transcriptional regulatory element (wpre) has been added. This sequence increase the stability of transgene transcript and facilitate the nuclear export (Zufferey *et al*, 1999). However, this sequence contains the open reading frame which results in the expression of part of the woodchuck hepatitis X protein, which is potentially oncogenic. Thus, to overcome this risk, mutations were made that eliminate the start codon and reduce promoter activity (wpre feature in LV is now referred to as mutated wpre, wpre* (Kingsman *et al*, 2005) (Zanta-Boussif *et al*, 2009)

All HIV accessory genes (*Vpr, Nef, Vpu, Vif*), which are associated with immune system escape and increased infectivity, potentially useful in a GT setting, were removed for safety reasons. To sum up, split of the viral components in these 4 different plasmids reduces the risk of recombination, rendering the chances of creating replication-competent viruses almost negligible (Dull *et al*, 1998).

1.3.2 In vivo LV GT achievements

Throughout the years, our group has contributed to advancing lentiviral vectors for usage in *in vivo* GT application. Early attempts to use LV *in vivo* failed to show stable gene transfer to the liver (Follenzi *et al*, 2004). Hepatocyte transduction is indeed challenged by rapid inflammatory responses induced by LV delivery, with innate immune cells responsible for enhancement of adaptive immune responses against transduced hepatocytes. More specifically, plasmacytoid dendritic cells (pDC) are activated by LV-contained nucleic acids, which are sensed by toll like receptors. pDC, in response, secrete type I interferon (IFN), which in turn induces in hepatocytes an anti-viral state. Permissiveness is thus reduced (Brown *et al*, 2007). Together with IFN, antigen presenting cells (APC) secrete other pro-inflammatory cytokines (i.e. interleukin 1, IL1, tumor necrosis factor α, TNFA). APC undesired transduction and subsequent transgene expression are responsible for antigen presentation to T cells, which once activated clear transduced hepatocytes.

For this reason, engineering of a hepatocyte specific cassette had to be optimized. Different hepatocyte specific promoters have been tested (Brown *et al*, 2006; Follenzi *et al.*, 2004; Vigna & Naldini, 2000). The best performing promoter in terms of strength and specificity was a chimeric promoter based on the proximal transthyretin promoter and a synthetic enhancer made by fusion of hepatocyte-specific transcription factors binding

sites (Enhanced Transthyretin, ET). However, presence of residual off target transgene expression induced immune responses in *FIX* LV treated *F9*$^{-/-}$ mice, with loss of *FIX* expression due to clearance of transduced cells. LV were further engineered through addition of microRNA 142 target sequences, in the 3' untranslated region (UTR) of LV, to switch off, post transcriptionally, transgene expression in cells of hematopoietic lineages (Brown *et al.*, 2006). As a result of this *escamotage*, FIX was stably expressed by hepatocytes, for more than one year after GT. Following correction of the mouse model, LV *FIX* GT was applied to larger animal models, hemophilic dogs. Adult and juvenile *F9*$^{-/-}$ dogs showed long term (>10 years follow up) stable FIX expression (1% of normal in adults, 5-10% of normal in juvenile, treated at a higher dose), following intra-venous administration of LV *FIX*. Transient signs of inflammation were observed, but were reduced through administration of anti-inflammatory drugs. Importantly, long term toxicity was not observed, neither was the presence of Ab against FIX.

In the past, we showed that cell-derived polymorphic class-I major histocompatibility complexes (MHCI) are included in the LV particle. This is due to the fact that, during budding from producer cells, enveloped vectors bring along proteins exposed on the membrane of producer cells. Because of the presence of MHC-I, LV may trigger allo-antigen T-cell responses. However, if beta-2 microglobulin gene is disrupted in producer HEK293T cells, LV particle are deprived of MHC and display marked reduction in immunogenicity (Milani *et al*, 2017).

Incorporation of proteins exposed on the membrane of producer cells into the LV particle can represent an issue, like in the example just seen, which could be solved by genetically inactivating the detrimental component, but it can even be an advantage. Particularly, producer cells could be forced to over-express proteins known or supposed to give an advantage to the LV particle, once injected *in vivo*. As mentioned before, 6% of the liver is composed of KC, liver resident macrophages. Once administered *in vivo*, most of LV end up in KC, reducing the number of LV particles entering hepatocytes. Phagocytosis is achieved through combination of positive and negative signals sensed by phagocytes. Among the negative ones, CD47 has been described as one of the strongest (Oldenborg *et al*, 2001). It inhibits phagocytosis by interacting with SIRP alpha receptor, exposed on the surface of macrophages. While CD47 is normally expressed at low level in HEK293T cells, we increased its amounts on cell surface, ending up with LV with high content of CD47. When administered *in vivo*, these vectors showed to be protected from

phagocytosis in small and large animal models (Milani *et al*, 2019). Following these promising results, our group applied LV GT to HA. We achieved stable liver gene transfer in HA mice and NHP, and phenotypic correction of HA mice. This was obtained using c.o.*FVIII* LV, but the best outcome was achieved when XTEN peptide, known to increase half-life of the payload protein was incorporated into the cassette (Milani *et al*, 2022). All these results pave the way for a clinical translation of LV-mediated liver GT in the near future.

1.3.3 LV current limitations

Despite the highlighted advantages of LV, a few substantial drawbacks should be noted.

i) Manufacturing. As highlighted above (see 1.3.1), LV production is currently obtained through transient plasmid transfection. In the future, inducible cell lines capable of expressing LV components *on demand*, following delivery of small molecules, might reduce the costs and time required currently. Up to now, the yields are too low to make it possible (Milani *et al.*, 2017).

ii) Enrichment of infectious LV particles is currently unfeasible. Especially for LV with low infectivity, this represents an issue, since the number of particles to be injected may be particularly high.

iii) LV are integrating vectors. So are gamma-retroviral vectors, employed in the past, which, after showing promising results in pre-clinical models and in clinical trials, turned out to be genotoxic (Poletti & Mavilio, 2021). However, not all the vectors' backbones behave the same, and genotoxicity can be influenced by viral type and target cell type. LV have been shown to preferentially integrate inside gene bodies, thus displaying a safer profile, compared to their ancestor gamma-retroviral vectors. Concerning the liver, our group focused on the safety of LV in mice in the past. The animals were treated as neonates with high doses of LV, challenged with repeated injections of toxic carbon tetrachloride, and followed for one year. The compound induces waves of hepatocyte death and regeneration. Compared to a known genotoxic LV, where the enhanced transthyretin enhancer promoter is placed inside the LTR, showing 40% of hepato-carcinomas HCC, "therapeutic" LV did not induce any HCC, thus overall reassuring on their usage as cargo for GT (Cantore *et al*, 2015).

1.3.4 Comparing LV and AAV vectors for liver GT

While around 30% of people are pre-immunized against AAV viral components, seroprevalence anti-HIV or anti-VSV.G Ab in the population in low. Despite of this, cross-reacting Ab against VSV.G have been described (DePolo *et al*, 2000).

LV cargo capacity is 9 Kb, compared to 4.7 Kb of AAV vectors. Thus, most of transgenes can be efficiently packaged into LV, giving rise to high infectious titers. Despite this, for very long transgenes like *FVIII*, LV preparations are more challenging, giving rise to LV titers lower than those obtained with shorter transgene encoding LV.

The integrating feature of LV, in the context of *in vivo* liver GT, broadens their potential application to pediatric patients, where the liver is still growing. LV would indeed be maintained during hepatocytes divisions, allowing for the treatment of diseases which are severely debilitating or lethal early in childhood.

1.3.5 Potency, manufacturing, cell autonomous diseases

The above-mentioned (see 1.3.2) promising results of LV-mediated liver gene therapy were obtained using, as transgenes, coagulation factors. The difference between non-cell-autonomous and cell-autonomous liver diseases deserves a few words. In non-cell autonomous liver diseases, it is not required to correct most of the liver mass. Especially in the context of secreted transgenes, it may be sufficient to correct a small percentage of hepatocytes, pushing them to produce more than each hepatocyte of a healthy person. This is particularly true for FIX, while the overproduction of very high amounts of FVIII by few hepatocytes might even engulf the transduced hepatocytes (Kapelanski-Lamoureux *et al*, 2022).

Cell autonomous diseases, instead, usually require weaker expression *per* cell, but considerably higher percentage of corrected liver mass. In certain cases, a selective advantage is responsible for a natural expansion of healthy transduced hepatocytes at the expense of non-corrected ones. An example of this is disease Tyrosinemia type I, inborn error of metabolism due to defective activity of fumaryl-acetoacetate hydrolase, $Fah^{-/-}$. The enzyme is essential for survival of hepatocytes, since accumulation of fumaryl-acetoacetate is toxic. Thus, corrected hepatocytes can replace the damaged ones, ultimately representing almost all the liver of the animal. LV gene therapy has been successfully applied to this disorder, in a porcine model (Nicolas *et al*, 2022). However, not all cell autonomous diseases have this positive peculiarity. Indeed, a special mention

goes to the challenging familial hypercholesterolemia (FH) disease (see 1.4 below). In that case, the non-corrected hepatocytes are totally healthy, because they can synthetize the cholesterol they need. Thus, no selective advantage is present. Expanding LV application to challenging conditions like FH would be crucial to validate their applicability.

1.4 Familial hypercholesterolemia

FH is an autosomal dominant disease, due to mutations in mainly four genes: i) *LDLR* LOF mutations, accounting for >90% of patients, ii) *APOB100* LOF mutations (Innerarity *et al*, 1987), iii) *PCSK9* gain-of-function mutations (GOF) (Abifadel *et al*, 2003), iv) low density lipoprotein receptor adaptor protein 1, *LDLRAP1*, LOF mutations, the only ones leading to a recessive form (Tada *et al*, 2011). LDLR, if mutated, causes FH due to massive accumulation of LDL in circulation, which are not able to access hepatocytes and extra-hepatic tissues. Excluding deletions and mutations affecting regulatory regions, more than 1300 missense/nonsense mutations have been reported to occur throughout the gene (https://www.hgmd.cf.ac.uk/ac/gene.php?gene=LDLR). Particularly, among its 860 codons, 550 are reported to cause, if mutated, hypercholesterolemia. Mutations, spread throughout the protein, can lead to a receptor i) defective in ligand-binding, ii) incapable of transporting its ligand, iii) internalization defective, iv) unable to be recycled, v) null, where the protein is undetectable (Hobbs *et al*, 1990). APOB100, instead, is the ligand required for LDL to enter through the LDLR. Thus, if APOB is mutated, the interaction with its receptor is less efficient and LDL accumulate in circulation, causing FH as well. PCSK9 is the modulator of LDLR levels. Indeed, it causes LDLR degradation instead of its recycling on cell membrane. Mutations in PCSK9 causing FH are thus GOF mutations: in patients carrying these mutations, LDLR degradation is enhanced, and its amounts on cell membrane become insufficient to clear LDL from circulation. PCSK9 expression is activated during cholesterol synthesis by sterol regulatory element binding protein 2 (SREBP2), just like LDLR (Horton *et al*, 2002). It can interact with LDLR both intracellularly, mediating its degradation prior to its expression on the membrane, and extracellularly, since it is released into the bloodstream (Poirier *et al*, 2008). The portion of LDLR interacting with PCSK9 is different from the one interacting with APOB contained in LDL (Wang *et al*, 2021). While, conventionally, LDLR-LDL complex is

internalized and the receptor recycled back multiple times, in case of PCSK9 binding to LDLR, the entire complex is brought to the lysosome to be degraded. Finally, the role of LDLRAP1 is to mediate the internalization of LDLR (Figure III).

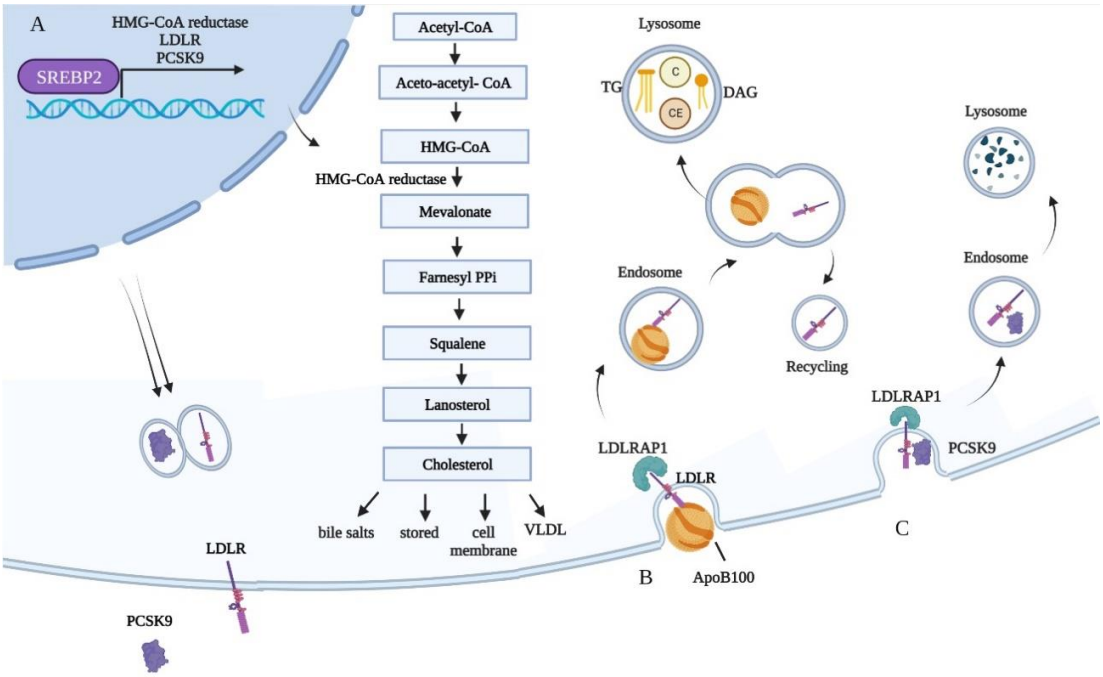


Figure III. Genes involved in familial hypercholesterolemia and their function in standard conditions

*(**A**) Transcription factor SREBP-2 is responsible for expression of HMG-CoA reductase, LDLR and its modulator PCSK9. Once translated, LDLR is exposed on hepatocytes cell membrane, while PCSK9 is secreted in the circulation. HMG-CoA reductase converts HMG-CoA in mevalonate. This is the rate-limiting step during cholesterol synthesis, and the enzyme is inhibited by statins. Newly synthetized cholesterol is then i) stored as cholesterol ester, ii) used for cell membranes, iii) used for generating bile salts, iv) packaged into VLDL. (**B**) LDL is internalized into hepatocytes (and extra-hepatic tissues) following interaction between ApoB100, structural component of LDL, and LDL-R. LDLRAP1 mediates internalization of LDL-R, which occurs through clathrin-mediated endocytosis. The early endosome acidic environment induces disassociation between LDLR and LDL, with the former being recycled back on cell membrane. As LDL-containing endosomes mature in lysosomes, LDL are subjected to the action of lysosomal enzyme, and their components are released. (**C**) PCSK9 binds to LDLR exposed on cell membrane. Because of the tight interaction between the two, in this case the whole complex is targeted to lysosome for degradation. C = cholesterol; CE = cholesterol esters; DAG = diacylglycerol. Created with BioRender.com.*

From the clinical point of view, HeFH is more manageable, while HoFH requires multiple combined treatments, as discussed below. The frequency of FH is 1:250 individuals for the former, 1:250,000 – 300,000 in case of the latter. Ideally, circulating total cholesterol and LDL-C should be <200 mg/dL (<5 mmol/L) and <100 mg/dL (<2.5 mmol/L), respectively. In heterozygous patients, they range between 350-550 mg/dL (9 – 14 mmol/L) and >200 mg/dL (>5 mmol/L), respectively (Pejic, 2014). Heterozygous untreated patients have 50% increase in risk of CVD by age 50 (men), or 30% increased risk by age 60 (women) compared to normal individuals. In homozygous patients circulating total cholesterol and LDL-C range between 650 - 1000 mg/dL (17- 26 mmol/L) and >400 mg/dL (10 mmol/L), respectively, i.e. 4 times more than healthy subjects. HoFH patients display atherosclerosis in childhood, CVD within the first two decades of life, myocardial infarction, and death before 30 years of age, if left untreated. Besides CVD, other typical manifestation of the ongoing cholesterol accumulation in the wrong body compartments is the presence of xanthomas and xanthelasma. Both terms refer to cutaneous manifestation of lipidosis, the first due to foam cells within the skin, the second at the level of the medial portion of the eye (Cuchel *et al*, 2014; Nordestgaard *et al*, 2013; Tromp *et al*, 2022).

For a clear overview on the pathological condition, we consider crucial a precise description of lipoprotein metabolism in a physiological condition, which will be tackled in the next paragraph.

1.4.1 Lipoproteins metabolism

1.4.1.1 Dietary lipids and cholesterol absorption

The digestion of lipids – triglycerides (TG) cholesterol esters (CE) and phospholipids (PL) - assumed through diet, starts in the oral cavity, mediated by lipases produced by salivary glands. It continues in the stomach, mediated by the action of gastric lipases. Lipids are then subjected to hydrolysis and micellization in the duodenum. Pancreatic lipases break down TG generating 2-monoacyl-glycerol (MAG) and two molecules of free fatty acids (FFA) (Xiao *et al*, 2019). Phospholipase A2 and CE hydrolase act on PL, generating FFA and lysophospholipids, and on CE, generating cholesterol and FFA, respectively. These are the forms required to access enterocytes. FFA and PL are

supposed to be absorbed mainly through passive diffusion. In contrast, cholesterol requires active transport, which is mediated by Niemann-Pick C1 like protein 1 (NPC1L1) (Altmann *et al*, 2004) (Figure IVA). NPC1L1 is a target for lowering cholesterol levels (Ezetimibe, discussed below). In addition to NPC1L1, ATP binding sub-family G members 5 (ABCG5) and 8 (ABCG8) are involved in cholesterol transport. They function as a heterodimer, and are responsible for the opposite function, compared to NPC1L1: the transport of sterols from the enterocytes back in the intestinal lumen. They are highly specific for plant-derived sterols. ABCG5 and ABCG8 transport, together with plant sterols, even cholesterol, in case it is in excess. However, compared to 45-55% of cholesterol, less than 5% of dietary plant sterols is absorbed (Yu *et al*, 2002a). In the enterocytes, TG and CE are re-synthesized in the smooth endoplasmic reticulum (ER). Since cholesterol and TG are hydrophobic molecules, each time they travel in the circulation, they must be assembled into a particle, called lipoprotein. Lipoproteins are made of CE and TG, surrounded by free cholesterol, PL and apolipoproteins (Xiao *et al.*, 2019). All lipoproteins except high density lipoproteins (HDL) rely on Apolipoprotein B (APOB) as structural component. Particularly, the ones generated in enterocytes are called chylomicrons (CM). Their assembly occurs through the action of chaperone microsomal TG transfer protein (MTTP). As expected, MTTP expression is enriched at the level of the villus, the highest absorbing region, while is almost absent at the level of the crypt, under standard diet (Swift *et al*, 2005). MTTP, located in the lumen of mammalian intestinal and hepatic microsomes is able, during ApoB translation, to make the protein coil around TG and CE, incorporating them into a particle. Just one molecule of ApoB is required *per* lipoprotein (Sniderman *et al*, 2019). ApoB contains 4536 residues in its complete form: ApoB 100. However, since its transcript is subjected to the action of RNA editing enzyme complex, which in humans is active in the intestine, the structural component of CM is ApoB48, comprising the first 2152 residues, where 48 stands for 48% of the ApoB 100 form (Chen *et al*, 1987; Powell *et al*, 1987). The molecular mechanism responsible for production of ApoB48 is a site-specific RNA modification, C-U RNA editing, mediated by ApoB mRNA editing enzyme catalytic polypeptide 1 (APOBEC 1 (Swift *et al.*, 2005)). CM are secreted by enterocytes at the basolateral membrane, entering lamina propria. After travelling through lymphatic ducts, they access circulation at the level of left subclavian vein. There, several apolipoproteins dissociate from the lipoproteins they are associated with, and bind to CM.

The apolipoproteins which are transferred to CM, once in the blood, are indeed exchangeable apolipoproteins. Indeed, they are transferred among lipoproteins overtime. Among others, ApoCII, ApoAV, ApoE. They derive from HDL (discussed more in detail below) and will be essential for the rest of CM journey (Mehta & Shapiro, 2022).

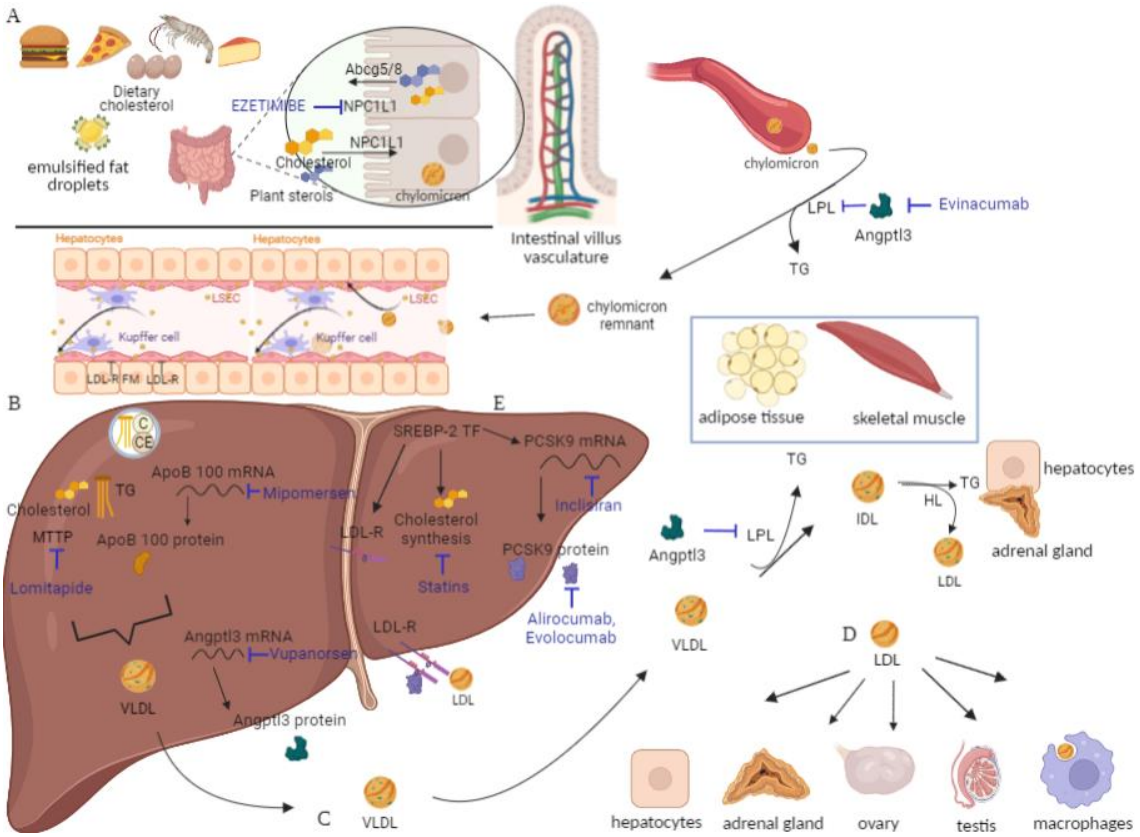


Figure IV. Lipoproteins metabolism

*(**A**)Cholesterol assumed through diet is transferred into enterocytes through NPC1L1. There, chylomicrons are assembled. Once in circulation, chylomicrons are deprived of most of their triglycerides (TG), which are delivered to adipose tissue and skeletal muscle through action of lipoprotein lipases (LPL). Chylomicrons turn into chylomicron remnants, which access hepatocytes through LDLR and LDLR FM. (**B**) Cholesterol contained in chylomicron remnants can be used by hepatocytes or packaged in VLDL and secreted into circulation. (**C**) VLDL are deprived of most triglycerides (TG), delivered to adipose tissue and skeletal muscle through action of lipoprotein lipases (LPL) and turn into IDL. IDL can either access hepatocytes through LDLR and LDLR FM or be converted in LDL by hepatic lipases (HL). (**D**) LDL can be internalized by hepatocytes or move to districts particularly dependent on cholesterol for hormonal synthesis, like adrenal gland and gonads. LDL can either be phagocytosed by macrophages which, in case of LDL overload, appear as foam cells. **E)** SREBP2 transcription*

factor is responsible for synthesis of i) cholesterol, ii) LDLR, iii) PCSK9. Cholesterol-lowering drugs, inhibiting different targets, have been developed (written in blue). Particularly: Ezetimibe inhibits NPC1L1, Evinacumab inhibits Angptl3, Mipomersen inhibits APOB100 (at RNA level), Lomitapide inhibits MTTP, Vupanorsen inhibits Angptl3 (at RNA level), Inslisiran inhibits PCSK9 (at RNA level), Alirobumab-Evolocumab inhibit PCSK9, and statins inhibit cholesterol synthesis. Created with BioRender.com.

1.4.1.2 Distribution of TG to peripheral tissues by CM

Once in circulation, CM first travel to peripheral capillary beds of adipose tissues and skeletal muscles. Those two are indeed the tissues in the greatest need for TG – to be used for energy or lipogenesis – which CM are carrying. This process is mediated by lipoprotein lipases (LPL), exposed on the lumen of these vessels. TG lipases consist of a family comprising LPL, endothelial lipases (LIPG) and hepatic lipases (HL) (Mehta & Shapiro, 2022). Lipases are responsible for the hydrolysis of TG present in a lipoprotein to FFA and glycerol, and their subsequent uptake by tissues.

The three lipases display with a different substrate preference: for TG: LPL>>HL>>EL; for phospholipid: EL>>HL>>LPL.

As said before, once in circulation, CM are decorated with several apolipoproteins, whose function is defined as follows:

i) ApoAV is involved in the docking of CM on the endothelial wall, by interacting with heparan sulfate proteoglycans (HSPG) present there (Nilsson *et al*, 2011).

ii) ApoCII is LPL cofactor (Wolska *et al*, 2017). People bearing mutations in one of these genes (LPL, ApoAV, ApoCII) are affected by hypertriglyceridemia: since they are not able to efficiently distribute TG to tissues, TG accumulate into the bloodstream (Carrasquilla *et al*, 2021).

iii) ApoE, used by lipoproteins to access target cells, will be discussed in the next paragraph.

The last players involved in TG release process are angiopoietin like proteins (ANGPTL), 3, 4 and 8. They are expressed differentially according to fasting or fed state, and function as inhibitors of LPL activity (Zhang, 2016). Loss-of-function (LOF) mutations of *ANGPTL3* in humans is characterized by low TG (due to enhanced LPL activity), low HDL-C (due to enhanced EL activity) and low LDL-C. The mechanism responsible for LDL lowering is not well understood, but increased EL activity may be a

contributing factor (Adam *et al*, 2020; Kathiresan *et al*, 2008; Musunuru *et al*, 2010; Wu *et al*, 2020). ANGPTL3 will be described later, as a possible target for lipid lowering drugs (see Figure IV A).

1.4.1.3 CM remnant uptake by hepatocytes

Deprived of most of TG, CM turn into CM remnants (75nm) (Cooper, 1997). APOCII is given back to HDL (Wolska *et al.*, 2017). The reduced size of CM remnants, compared to CM, allows them to be "sleeved" through endothelial hepatic *fenestrae* and to reach the space of Disse in the liver (see Figure IVA). There, CM remnants are rapidly internalized by hepatocytes, based on the interaction between APOE and LDL receptor (LDLR) and LDLR family members (LDLR FM, among which, the most expressed by hepatocytes is LDLR related protein 1, LRP1) (van de Sluis *et al*, 2017). APOE is responsible for the clearance of CM remnant, through receptor-mediated endocytosis (Mehta & Shapiro, 2022). CM remnant components are used by hepatocytes. Particularly, PL can be used for cellular membranes, proteins for amino acids and leftover TG can be stored. Finally, cholesterol can be i) converted into bile salts, essential for emulsification of fats assumed with diet, ii) stored as CE, iii) used for cellular membranes, iv) re-packaged into very low-density lipoproteins (VLDL) (Trapani *et al*, 2012). Concerning bile salts, their classic synthesis starts with 7alpha-hydroxylation of cholesterol and converges in secretion of bile salts into the bile canaliculus through bile salts export pump (Trapani *et al.*, 2012). However, not all cholesterol ends up in the bile canaliculus in the form of bile salts, since the already mentioned ABCG5 and ABCG8 are expressed even by hepatocytes (Yu *et al*, 2002b). The two mediate the transport of free cholesterol into the canaliculus, representing a relevant route for excretion. Transgenic mice overexpressing human ABCG5 and ABCG8 display reduced cholesterol absorption (50%) - contribution of the enterocytes to the outcome – and bile cholesterol levels increased >5-fold – contribution of the hepatocytes to the outcome. In a compensatory fashion, these mice increase cholesterol synthesis by hepatocytes (Yu *et al.*, 2002b). In contrast, mice lacking ABCG5 and ABCG8 display lower biliary cholesterol amounts, and 2-3-fold increase in absorption of dietary plant sterols, resembling the condition of people bearing mutations in these two genes (Yu *et al.*, 2002a). Cholesterol in hepatocytes derives from the CE present in lipoproteins and from *de novo* synthesis. Particularly, the expression of LDL-R, responsible for lipoproteins internalization, is synchronized with

the synthesis of cholesterol: the less LDL-R is produced, the less cholesterol is synthesized (Horton *et al.*, 2002). A third gene is tied hand in glove to LDL-R: its negative modulator, proprotein convertase subtilisin kexin type 9 (PCSK9) (Abifadel *et al.*, 2003). PCSK9 will be described later, for its implication in FH and as a possible target for lipid lowering drugs. As mentioned above, excess cholesterol present in hepatocytes is packaged in VLDL and secreted into the bloodstream (Figure III B).

1.4.1.4 VLDL formation and secretion by hepatocytes

Steps required for VLDL assembly resemble those mentioned for CM formation, with one main difference: the structural component of VLDL is ApoB100 instead of ApoB48 (Chen *et al.*, 1987; Powell *et al.*, 1987). In the human liver, the RNA editing enzyme APOBEC1 is not expressed, thus ApoB gene is translated in its complete form. Assembly of VLDL requires the already mentioned MTTP (Swift *et al*, 2003). Again, just one molecule of ApoB is required *per* VLDL (Elovson *et al*, 1988; Sniderman *et al.*, 2019; Sundaram & Yao, 2010), which contains PL, free cholesterol, CE and TG. ApoB expression is constitutive. What determines the rate of VLDL production are TG themselves, since ApoB is degraded when TG are not abundant to justify generation of VLDL (Nakajima *et al*, 2011) (see Figure IVB). Once in circulation, VLDL can either be internalized by VLDL receptor (VLDLR), expressed in heart, muscle and adipose tissues (Huang & Lee, 2022), or be subjected to same destiny of CM. In the latter case, the following events occur i) APOCII and APOE, derived from HDL, bind to VLDL, ii) LPL-APOCII in adipose tissue and skeletal muscle capillaries mediate TG hydrolysis, iii) APOCII moves back to HDL, iv) VLDL turn into intermediate density lipoproteins (IDL) (Huang & Lee, 2022). The newly formed IDL can be i) internalized by hepatocytes just like CM remnants or ii) move to adrenal cortex, which express LDLR and LDLR FM (Hoekstra *et al*, 2010; Hu *et al*, 2010; Schneider *et al*, 1982). There, the cholesterol just internalized can be used to generate different steroid hormones, or it can be stored. IDL can also be iii) deprived of leftover TG through the action of HL in the liver and adrenal cortex (Choi *et al*, 1994). When this happens, APOE moves back to HDL, and IDL turn into LDL, which contains very low amount of TG and is mostly composed of cholesterol and CE (Figure IV C). The newly formed LDL, being smaller than the other lipoproteins (Islam *et al*, 2022), circulate and move to anatomical districts, such as gonads, which express LDLR. There, once again the cholesterol contained can be used to make

hormones, in this case sexual hormones (Choi *et al.*, 1994). Despite the contribution of adrenal cortex and gonads to the uptake of LDL, the vast majority of LDL (around 75-80%) (Ishigaki *et al*, 2019), move back to the liver, where they interact with LDL-R and get internalized (Figure IV D). APOB100, structural component of LDL, can interact exclusively with LDLR and with none of LDLR FM. This is one of the main reasons why in FH, if the receptor is mutated, the main lipoprotein massively accumulating into the bloodstream is LDL. Once inside hepatocytes, LDL components undergo the same destiny described for CM remnant. In healthy individuals, the system works as described up to now, and LDL cholesterol is kept within the normal range. However, in individuals displaying high LDL amounts, atherosclerosis may develop.

1.4.2 LDL-driven atherosclerosis

Atherosclerosis is defined as a disease of the arteries, characterized by deposition of fatty material within the tunica intima of the arterial wall, called atherosclerotic plaque. (Libby, 2021a; Libby *et al*, 2019). Hypercholesterolemia may induce damage in cells of endothelial wall, however, the mechanisms by which LDL triggers the lesion remains unclear (Libby, 2021b). The endothelial damage increases permeability of endothelial lining, allowing LDL to access the vessel wall. LDL accumulate in tunica intima, where the absence of plasma antioxidants results in an increase in oxidized LDL (oxLDL). Moreover, dysfunctional endothelial cells expose adhesion molecules on the vessel surface, which recruit inflammatory cells, particularly monocytes, which access sub-endothelial layer through diapedesis. There, monocytes turn into macrophages and start phagocytosing oxLDL. Macrophages, filled with oxLDL, are called “foam cells”, as their appearance become foamy. Smooth muscle cells, localized in the tunica media, are involved as well in the formation of the plaque. Particularly, they migrate from the media to the intima. Once there, they start proliferating and synthesizing extra-cellular matrix, which constitute the fibrous cap overlying the lipid core. This plaque is covered by endothelial cells. Since cells proliferate and perish during this process, the inflammatory state is increased. As the plaque progresses, the vessel lumen is reduced thus causing tissue damage as a consequence of the decreased or absent blood flow, such as in myocardial infarction. Moreover, the plaques often develop calcification. Calcified atheromas may have a higher tendency to rupture. If left untreated, this series of events may lead to the disruption of the plaque and thrombosis (Libby, 2021b). Despite the threat

represented by foam cells, human beings still bear a protection mechanism in healthy conditions: HDL. HDL is the last piece of the puzzle, capable of counteracting the development of atherosclerosis by inducing cholesterol efflux from foam cells.

1.4.3 Reverse cholesterol transport

The initial component of HDL particle is apolipoprotein A1 (APOA1), expressed mainly in enterocytes and hepatocytes. ApoA1 circulates into the bloodstream and interacts with receptors ATP binding cassette protein A1 (ABCA1) and ATP binding cassette protein G1 (ABCG1), expressed on tissues and macrophages (Rader & Tall, 2012). Upon interaction with ABCA1, cholesterol is released in the nascent HDL, which then moves to ABCG1, incorporating additional cholesterol. LCAT esterifies free cholesterol (effluxed from the cells via ABCA1 or ABCG1) to cholesteryl ester (CE), allowing the maturation of HDL, from nascent to mature HDL.

Mature HDL moves back to the liver, interacts with SRB1, present on the hepatocytes' membrane, and release the carried cholesterol (Heinecke, 2012). Now reduced in size, HDL recommences its journey into the bloodstream, while cholesterol internalized into hepatocytes can be excreted into the bile. The capability of HDL to incorporate excess cholesterol from tissues and macrophages, transporting it to the liver where it can be eliminated, has been named "reverse cholesterol transport". It is supposed to play a major role in counteracting the atherosclerosis process. Indeed, mice and rabbits lacking a functional APOA1 showed increased atherosclerosis, while *ldlr*$^{-/-}$ mice overexpressing human APOA1 showed >50% reduction in atherosclerosis progression after 6 months of high cholesterol diet, compared to controls (Belalcazar *et al*, 2003). Increasing HDL levels has been pursued as a strategy to reduce the risk of CVD (HDL cholesterol hypothesis). However, throughout the years, the causal relationship between higher HDL amounts and reduced risk of CVD has been challenged (Voight *et al*, 2012). It has more recently been proposed that the most relevant parameter should be to define the functionality of HDL, i.e. its cholesterol efflux capacity, rather than their absolute amounts (Hovingh *et al*, 2015; Rader & Hovingh, 2014). As said before, HDL contain multiple apolipoproteins in addition to ApoA1, like the already mentioned ApoCII and ApoE. HDL donate them to CM, VLDL and IDL, together with part of the CE. This is carried out as a barter: CE are given; TG are earned in exchange. And the mediator of this swap is cholesterol ester transfer protein (CETP), which will be discussed later, since it

was selected as lipid lowering target in the past without success and was recently resuscitated as target (Nicholls *et al*, 2022).

1.4.4 Available treatments

1.4.4.1 Liver transplantation

The only available option when FH was discovered was liver transplantation. Despite being a life-saving alternative for children affected by FH, it was not sufficient to reach circulating LDL-C comparable to those of healthy people (Starzl *et al*, 1984). This is because around 75-80% of LDL are captured by hepatocytes through LDLR, as mentioned before. Since the rest of the body remains devoid of LDLR, the contribution of extrahepatic tissues remains absent. Notwithstanding this aspect, LDL-C amounts are decreased almost by 80% following liver transplantation. All the consequences of a transplant, however, persist: i.e. surgical complications, requirement of life-long immune suppression. Moreover, liver transplantation remains a high-risk procedure, despite the outcomes are generally favorable. Whatever the treatment of a patient affected by HoFH, the sooner the treatment is delivered, the better it is. Notably, of >40 liver transplants performed from 1984 in HoFH patients, 10 of them were of liver and heart concurrent transplantation, since the development of heart disease was already exaggerated. Given the paucity of available donors for liver transplantation, an alternative deserving mention is the liver transplantation of homozygous patients using their heterozygous parents as donors, recently successfully reported in Japan (Ishigaki *et al.*, 2019). This kind of procedure, attempted for the cure of HoFH, has been the first case of liver transplant from a living donor.

1.4.4.2 LDL apheresis

Despite being a valuable option to reduce LDL, which in this case would be cleared away from the body, this extracorporeal technique is not devoid of issues, including high costs and life-long maintenance of blood access. The duration of each session of LDL apheresis is ~140 minutes. The process must be repeated every 2 weeks. Despite what the name suggests, other plasma components are removed from the blood of patients. Among others: PCSK9, oxLDL, inflammatory cytokines and this may be a beneficial aspect.

Once again, the sooner the better, and homozygous patients starting the procedure in adulthood have poor prognosis (Makino *et al*, 2019).

1.4.4.3 Statins

Statins inhibit the enzyme HMG-CoA reductase (see Figure IV), which catalyzes the oxidoreduction of HMG-CoA to mevalonate, during cholesterol synthesis. They are divided in high intense and moderate intense. Statins are most often administered orally, on a daily basis. Their capability to reduce LDL content is due to i) reduced intra-cellular synthesis of cholesterol and ii) increased expression, and exposure of LDLR on the membrane of hepatocytes, which in turn interacts with LDL mediating their internalization.

This happens because once the hepatocyte senses the cholesterol inside the cell is not enough, it increases its synthesis, as feedback mechanism.

The transcription factor mediating cholesterol synthesis, SREBP-2, however, also mediates expression of the LDLR (Horton *et al.*, 2002). Thus, cholesterol levels are kept down, despite increased activation of cholesterol biosynthetic pathway, because HMG-CoA reductase is inhibited, while the amounts of LDLR are increasing overtime. This, in turn, mediates the internalization of more LDL and release of cholesterol in the cell (Wang *et al.*, 2021). The first statin to be approved was Lovastatin in 1989. Following that, others came (pravastatin, simvastatin, 1991). The Scandinavian Simvastatin Survival Study (4S), showed that statins were effective even as strategy for secondary preventions: participants had experienced heart attack or angina, and deaths were reduced in the treated group, compared to controls (8% deaths vs. 12% deaths) (Pedersen *et al*, 2004). What came out overtime was that i) statins caused benefit, both in primary (Shepherd *et al*, 1995) and secondary CVD prevention, ii) more intensive statins were better than less intensive dosing (Cannon *et al*, 2004) (Nissen *et al*, 2006), iii) the greater the reduction in LDL cholesterol, the greater the reduction in cardiovascular events, iv) not all statins were equally safe: in 2001 cerivastatin was withdrawn, after 52 deaths, caused by kidney failure following drug-related rhabdomyolysis (Furberg & Pitt, 2001). Statins have revolutionized the management of hypercholesterolemia patients. However, while the reduction in HeFH was up to 60%, in HoFH it could barely reach 20%. Indeed, since the vast majority of HoFH patients lacks a functional LDLR, circulating LDL will remain unable to access liver and extra-hepatic tissues. The most common side effect of statins

is skeletal muscle pain, observed in 10-15% of patients (Adhyaru & Jacobson, 2018). However, this is a controversial topic (Cholesterol Treatment Trialists, 2022).

1.4.4.4 Bile acids sequestrants

Bile acids sequestrants inhibit the re-absorption of bile salts by enterocytes. Cholesterol is part of bile salts. If bile salts are eliminated from the body, hepatocytes will induce a feedback loop to restore bile salts amounts. By doing this, more cholesterol will be pushed out of the hepatocyte in the canaliculus (Feng *et al*, 2021). Among the ones available there are Colesevelam (15% reduction), Colestipol (16% reduction), Cholestiramine (10% reduction). As said before, HoFH patients in most cases lack a functional LDLR. Thus, the cholesterol which access hepatocytes is considerably reduced. Indeed, hepatocytes of HoFH patients synthetize more cholesterol than hepatocytes of healthy individuals. If the amount of cholesterol excreted by hepatocytes is further increased, because of the usage of bile acids sequestrants, the response by them will be a further increase in cholesterol synthesis. This is the reason why the option of bile acids sequestrants is not effective on HoFH (Sniderman *et al*, 2013).

1.4.4.5 NPC1L1 as a target

NPC1L1 is responsible for cholesterol transport from intestinal lumen inside enterocytes and cholesterol re-uptake from the bile canaliculus. Mice knock out for *npc1l1* are resistant to atherosclerosis even when fed with high-fat high cholesterol diet (referred to as Western Diet), despite $ldlr^{-/-}$ or $apoE^{-/-}$ genetic background (Davis *et al*, 2007) (Yamamoto *et al*, 2019). Humans carrying homozygous LOF mutations in NPC1L1 have not been described to date. However, heterozygous individuals display mean LDL-C reduction of 12 mg/dL (0.3 mmol/L), reported to reduce the risk of CVD by >50% (Myocardial Infarction Genetics Consortium *et al*, 2014). This is because, despite the reduction is minimal, it is life-long. This evidence elects NPC1L1 as a good target for lipid lowering purposes. Ezetimibe (Zetia) is a selective and highly potent inhibitor of cholesterol absorption, since it acts by inhibiting NPC1L1 (Van Heek *et al*, 1997) (Bays *et al*, 2001). NPC1L1 is expressed by both enterocytes and hepatocytes, in humans. Ezetimibe acts on both cell types, leading to both reduced cholesterol absorption

and decreased re-uptake from the bile canaliculus, thus lowering plasma cholesterol. Its efficacy is limited in HoFH patients.

1.4.4.6 PCSK9 as a target

PCSK9 has been selected as a target, to be therapeutically inhibited, in hypercholesterolemia, throughout recent years. PCSK9 GOF mutations were discovered to be associated with high cholesterol in 2003 (Abifadel *et al.*, 2003), when a French proband, aged 49, died from myocardial infarction. His LDL-C was 356 mg/dL (9 mmol/L), but LDLR and ApoB were not carrying mutations. The GOF mutation F216L in PCSK9 was associated with the cause of death. Following this evidence, other groups looked deeply in their hypercholesterolemic cohorts and PCSK9 was confirmed as mutated and causing GOF of the protein in some of these people. PCSK9 overexpression in wild type mice, through adenoviral (AdV) vector-mediated delivery of PCSK9 cDNA, made the mice hypercholesterolemic (Maxwell & Breslow, 2004), while the generation and characterization of PCSK9 knock-out mice showed that they were hypocholesterolemic (Rashid *et al*, 2005). An experiment of parabiosis between wild type mice and mice overexpressing PCSK9 showed decreased LDLR in the livers of wild type mice, making clear that the secreted form could induce hypercholesterolemia by inhibition of the LDLR (Lagace *et al*, 2006). In the same period, healthy people carrying LOF mutations of PCSK9 were identified. They displayed hypocholesterolemia, around 30% lower circulating LDL-C amounts (Cohen *et al*, 2005; Cohen *et al*, 2006) and up to 88% reduction in the risk of developing CVD. Taken together, all this knowledge about the positive correlation between high PCSK9 and high LDL-C levels, opened the way to targeting PCSK9 for reducing LDL. The first strategy to be developed was based on a neutralizing monoclonal antibody (mAb) (Chan *et al*, 2009). At that point, it seemed that this strategy could be applied just to patients with still one functional copy of LDLR (HeFH), since the mAb was not effective in LDLR KO mice (Chan *et al.*, 2009). The first anti-PCSK9 mAb tested in humans made clear that i) LDL-C levels could be reduced significantly in both healthy individuals, hypercholesterolemic and genetically confirmed HeFH patients, ii) the effect was significant even in patients concomitantly taking statins, iii) the effect, in combination with statins, was additive. The reason of additive effect is the following: statins, by inducing activity of SREBP-2, enhance the production of LDLR, while PCSK9 mAb decrease its degradation (Stein *et al*, 2012). These positive

results led to the approval of the first mAb targeting PCSK9, Alirocumab (Praluent, Sanofi-Regeneron), in 2015, followed by Evolocumab (Repatha, Amgen) in the same year (Sabatine *et al*, 2017). To date, Alirocumab is taken subcutaneously every two weeks (Robinson *et al*, 2015). Evolocumab administration is subcutaneous every two weeks or once monthly at a higher dose (Sabatine *et al.*, 2017). Outcome on LDL-C is comparable between the two: reduction of around 60%, in HeFH patients (Raal *et al*, 2014). When Alirocumab was tested in HoFH patients (once every two weeks), surprisingly, a decrease in LDL-C levels was obtained, 26.9% (Blom *et al*, 2020). Similar results have been obtained using Evolocumab for HoFH, with a follow up of over one year. Injections every 4 weeks showed stable LDL-C reduction of 54.9% in HeFH and 21.2% in HoFH (Santos *et al*, 2020). The partial efficacy is probably due to residual activity of the LDLR. Based on these promising results, inhibiting this target directly at the RNA level seemed an attractive alternative. PCSK9 was efficiently silenced in mice, rats and cynomolgus monkeys (Frank-Kamenetsky *et al*, 2008) following injection of a lipid nanoparticle (LNP), carrying a small interfering RNA (siRNA). LDL-C reduction was 50-60% and the effect lasted 3 weeks. The drug was then optimized, with a series of *escamotage* which turned it into Inclisiran. Firstly, its structural component was switched from LNP to N-Acetyl-Galactosamine (GalNac)-enriched LNP. This trick made it subcutaneously injectable and with a high hepatocyte targeting efficiency, since GalNac exploits asialoglyoprotein receptor (ASGPR), abundantly expressed on their membrane. Then, chemical modification to the siRNA improved its molecular stability and activity (Fitzgerald *et al*, 2014). Efficacy was confirmed in phase I (Fitzgerald *et al*, 2017) and phase II (Ray *et al*, 2017) clinical trials. Inclisiran is now approved, and is currently the most promising tool available, concerning efficacy, safety and convenience for the treatment of HeFH. Patients receive the first dose, followed by the next dose three months later. Subsequently, the administration is every 6 months. The drug is provided in a pre-filled syringe, containing Inclisiran, commercial name Levquio.

1.4.4.7 VLDLR synthesis as a target

FH occurs when mutations in this gene are downstream the first 48% of the protein (Innerarity *et al.*, 1987). Mutations in the upstream portion of ApoB would not result into reduced internalization of LDL in hepatocytes, giving rise to FH; rather they would result

into inefficient synthesis of CM in the intestine. Since ApoB48 is CM structural component, mutations in this portion would result in apobetalipoproteinemia, a disorder due to intestinal malabsorption (Lee & Hegele, 2014). When FH is due to ApoB100, the amino-acidic residues interacting with LDLR are the ones mutated. ApoB has been selected as a possible target to lower cholesterol in FH patients, with the idea to inhibit VLDL formation in the liver, thus allowing reduction of circulating cholesterol. Mipomersen is a second-generation anti-sense oligonucleotide (ASO) targeting the ApoB gene RNA. Studies in mice have been done using ISIS-1467764, which targets the murine counterpart. It showed to reduce circulating ApoB, and thus LDL, following injections in both healthy mice and *ldlr*$^{-/-}$mice (Mullick *et al*, 2011). Preclinical studies in animal models provided evidence of reduction of ApoB, total cholesterol and LDL-C in a dose-dependent manner. During clinical development, the phase III clinical trial showed an additive effect of mipomersen, in HoFH, when combined with statins, with an LDL-C reduction of 27% (Raal *et al*, 2010). However, several side effects have been reported, among which the most concerning is liver steatosis, due to accumulation of TG and cholesterol inside hepatocytes, since formation of VLDL is impeded. Steatosis is resolved once the treatment is discontinued. In the end, the drug was approved exclusively in the United States, where the Food and Drug Agency (FDA) authorized its use for HoFH patients, in combination with other therapies. The delivery is subcutaneous, once a week. Lomitapide is a different drug which is targeting the same pathway. It is an inhibitor of MTTP (Cuchel *et al*, 2013). Since it is impairing the formation of both VLDL and CM, unlike mipomersen, which was active just on ApoB100 and not ApoB48 mRNA, gastrointestinal adverse events have been reported. Steatosis is also among the risks of lomitapide, but at a lower extent, probably because, since the uptake of CM remnants by hepatocytes is reduced, the liver is less stressed, while enterocytes are more. Notwithstanding the side effects, it appeared safer than mipomersen and was approved by both FDA and the European Medicine Agency (EMA). It is orally assumed, under the name of Lojuxta (Alonso *et al*, 2019; Raper *et al*, 2015).

1.4.4.8 Angptl3 as a target

Angptl3 was hypothesized as a possible cholesterol and TG lowering target in 2002 in a strain of mice displaying hypolipidemia (Koishi *et al*, 2002). Adenoviral gene transfer

of Angptl3 and recombinant Angptl3 injections, both inducing a rise in plasma lipid levels, confirmed this conjecture. It acts by inhibiting the action of LPL and endothelial lipases, thus enriching the pool of TG in the bloodstream (Shimizugawa *et al*, 2002). Angptl3 was considered a good target, since people carrying mutations in this gene are hypocholesterolemic and healthy, display lower TG, lower HDL and LDL than normal, and have reduced risk of CVD (Musunuru *et al.*, 2010; Pisciotta *et al*, 2012). Heterozygous individuals display Angptl3 circulating levels around 50% of normal (Dewey *et al*, 2017). This target has been selected for treatment of hypercholesterolemia. As for PCSK9, first to be tested and approved has been a mAb, followed by siRNA. The mAb was shown to decrease TG and LDL-C even in mice lacking a functional LDLR, thus suggesting its action was independent from LDLR pathway (Wang *et al*, 2015). The mAb Evinacumab (Evkeeza, Regeneron) was approved as add-on treatment for patients affected by HoFH, 12 years old or older. Evinacumab is a fully human mAb administered intravenously, once monthly. The reason of LDL reduction is still to be determined. Just like for PCSK9, attempts to target Angptl3 also at the RNA level were made. As for PCSK9, even Angptl3 targeting ASO exploits ASGPR present on hepatocytes, by virtue of being conjugated to GAlNac. It has been developed by Ionis Pharmaceuticals, under the name of Vupanorsen. Studies on several mouse models, including the *ldlr*$^{-/-}$, showed the efficacy of this strategy, as well as the first clinical trial on healthy individuals and patients with elevated cholesterol and TG (Graham *et al*, 2017). Subsequently, a phase II clinical trial was carried out in HoFH patients and people affected by other types of dyslipidemia. Results of this trial confirmed reduction of Angptl3, up to 95% at the highest dose tested. TG were reduced, as expected, of around 50%. LDL-C reduction, however, was mild, reaching not more than 15%. Moreover, dramatic increase in hepatic steatosis, led to the discontinuation of the program (Bergmark *et al*, 2022). Thus, currently, only anti-Angptl3 mAb, Evinacumab, is commercially available.

1.4.4.9 CETP as a target

As mentioned above, CETP is responsible for transfer of cholesterol and TG among lipoproteins. Particularly, it transfers cholesterol from HDL to VLDL and LDL and it transfers TG from VLDL and LDL to the HDL. Throughout the years, according to the "HDL hypothesis", CETP inhibition was supposed to reduce LDL cholesterol. Indeed, if cholesterol transport from HDL to LDL was impeded, cholesterol could have been

cleared more easily, without needing LDLR. Moreover, mice naturally lack CETP gene, and their LDL-C amounts in a *ldlr*$^{-/-}$ genetic background, are considerably lower than LDL amounts of HoFH patients. CETP is produced by the liver and secreted into the bloodstream where it exerts its activity. CETP is supposed to perform these steps: i) it bridges between smaller HDL and larger LDL (or VLDL, or CM), ii) the two distal CETP domains twist, opening a tunnel for lipid exchange, iii) transport of CE from HDL to LDL and TG from LDL to HDL occur (Zhang *et al*, 2012). Four CETP inhibitors candidates were selected in the last three decades. A summary of the results obtained follows. Torcetrapib testing was discontinued in 2006: the trial was blocked prematurely following numerous deaths and increased CVD in the CETP inhibitor group (Barter *et al*, 2007). Dalcetrapib development was halted once phase III failed to show clinical benefit, same for evacetrapib, discontinued in 2015 (Tall & Rader, 2018). Anacetrapib was the only one showing modest efficacy. Compared to its forerunners, anacetrapib was safer than torcetrapib, more potent than dalcetrapib, and the study was designed with a sufficiently long duration to render the benefit of the therapy manifest (in contrast with Evacetrapib). However, the benefit was too modest, and the sponsor Merk discontinued the program. Recently, CETP has come back as a possible target for lowering LDL-C: obicetrapib, designed to inhibit it and with primary objective of reducing LDL, proved to be effective in a phase IIb trial, with a 51% reduction of LDL-C in patients already under statin regimen (Nicholls et al., 2022). In principle, however, possible side effect could be the accumulation of TG in LDL and VLDL.

1.4.5 Gene therapies for FH

1.4.5.1 Genetic inactivation of PCSK9 and ANGPTL3

Towards a "one-and-done" inactivation of *PCSK9*, genome editing, base editing and epigenome editing have been exploited (Kaiser, 2022; Musunuru *et al*, 2021; Rothgangl *et al*, 2021; Wang *et al*, 2018), with the most advanced being base editing at the moment. Particularly, ABE were used to treat 4 NHP (Musunuru *et al.*, 2021). mRNA encoding for ABE and guide RNA (gRNA) targeting *PCSK9* were packaged in a LNP and injected systemically by a one-time treatment. Over 60% of the liver was edited. Reduction of circulating PCSK9 and LDL-C were 90% and 60%, respectively, and were stable for 8 months. The follow up study showed that the treated NHP maintained the reduction in PCSK9 and LDL-C until sacrifice at 476 days, and that their offspring did not inherit the

modification (Lee *et al*, 2022). In July 2022, Verve Therapeutics, the company sponsoring these studies, administered the first base editor *in vivo* in humans. The single dose, dose escalating trial, based in New Zealand and UK aims to deliver a definitive cure for HeFH. While interim results are expected in 2023 (ClinicalTrials.gov Identifier: NCT05398029), up to now, 3 patients have been treated. Attempts to genetically inactivate *ANGPTL3* are also undertaken by Verve Therapeutics. The strategy to permanently inactivate *ANGPTL3* in hepatocytes is aimed to treat HoFH. However, the inefficient entry of LNP in hepatocytes lacking LDLR brought to the development of LNP exploiting the already mentioned GAlNac-ASGPR axis (Kasiewicz *et al*, 2021). This modification allowed editing efficiencies comparable to the ones achieved with wild type mice treated with standard LNP. With this configuration they obtained almost 90% reduction in circulating Angptl3 but reduction of circulating LDL-C was not reported (Khera *et al*, 2022). Verve selected this BE as their leading candidate for HoFH. As said previously, *PCSK9* targeting, in HoFH, can induce partial reduction in LDL-C levels. Verve Therapeutics showed that LNP can be administered subsequently in the same NHP. The aim was to genetically inactivate *PCSK9* and *ANGPTL3* using the same LNP core. Eleven monkeys were injected with *PCSK9*-targeting BE followed by *ANGPTL3*-targeting BE 1 month later. Fifteen days after the second injection, 69% editing of *PCSK9* and 52% *ANGPTL3* were achieved in the liver. Their strategy could imply, in the future, the administration of both LNP with the hope to have an additive reduction in LDL-C levels, not shown yet (Bellinger *et al*, 2022).

1.4.5.2 LDLR gene transfer

As already mentioned, in case of mutations in *LDLR*, LDL accumulate in the bloodstream. The other lipoproteins are approximately under control since they can interact with LDLR FM in addition to LDLR. As mentioned before, the peculiarity of LDL is the exclusive presence of APOB100 as ligand for LDL internalization. APOB100, being able to interact exclusively with LDLR, is not able to access hepatocytes anymore once the receptor is not exposed on the membrane. Even in HeFH patients, the amount of LDLR is not sufficient to ensure normal LDL and cholesterol levels, and pharmacological intervention is required (gene dosage effect). *LDLR* gene transfer, as a strategy, could be applied to *LDLR* LOF mutations, *PCSK9* GOF mutations, and to the portion of mutations in *APOB* responsible for a reduced interaction between LDL and LDLR, since higher

amounts of receptor on hepatocytes membrane could ameliorate the pathological outcome. In the 1990s, *LDLR* gene transfer was attempted into hepatocytes collected from hypercholesterolemic Watanabe heritable hyperlipidemic rabbits (WHHR). Twelve WHHR were subjected to 30% hepatectomy. Isolated hepatocytes were transduced *in vitro* with vectors derived from retroviruses (the only available at that time) and then transplanted back into the rabbits. This treatment provided stable reduction, between 20 and 40%, of circulating cholesterol, despite the low number of transplanted cells (Chowdhury *et al*, 1991). Rabbits were followed for 4.5 months. In non-human primates (NHP), the hepatocytes were confirmed to engraft following injection through the inferior mesenteric vein (Grossman *et al*, 1992). Following these results, a clinical trial started. Five hypercholesterolemic patients were subjected to partial hepatectomy. The procedure was the same: their hepatocytes were transduced with a retroviral vector expressing human *LDLR* and re-infused. High variability was observed among patients, with one patient where LDL-C levels were unchanged following transplant and the best responder patient showing 20% LDL-C reduction (Grossman *et al*, 1995). This is among the first reports of human GT where, in a portion of subjects, the therapeutic endpoint was achieved. However, this strategy was not further pursued as it became clear, in the next years, that *in vivo* delivery to hepatocytes of genetic information encoding *LDLR* would have been preferable, especially because it would have not required hepatectomy and would have been relatively easier to deploy. Toward this goal, AAV vectors have been considered for *in vivo* liver-directed GT of FH. Efficacy and safety were shown in different mouse models followed long term, including both the canonical HoFH mice (*Ldlr*$^{-/-}$) and the double knockout mouse model *Ldlr*$^{-/-}$ and *Apobec*$^{-/-}$. Indeed, compared to humans, mice express *Apobec* even in hepatocytes, thus a considerable fraction of LDL carries APOB48 as structural component, thus can be cleared even by LDLR FM. As a result, the double knock out model better recapitulates the high LDL-C of human HoFH patients, indeed these mice display higher LDL-C than *Ldlr*$^{-/-}$ mice thanks to the presence of exclusively APOB100 in LDL (and CM), compared to *Ldlr*$^{-/-}$ (and wild type mice) (Greig *et al*, 2017b). Safety of the vector was then assessed in NHP, both wild type and heterozygous for the spontaneous truncating *LDLR* mutation W284stop (NHP homozygous for this *LDLR* mutation are not vital). They were sacrificed either 28 days or 1 year after gene transfer. While safety profile was positive, the authors found AAV vector DNA in the liver at the end of experiment, and *LDLR* RNA, which was reduced

over the time course of the experiment (Greig *et al*, 2017a). LDL-C was not reported. Following this study, a clinical trial of AAV-mediated gene transfer of a functional copy of human *LDLR* to the liver started in 2016 sponsored by Regenxbio (ClinicalTrials.gov Identifier: NCT04080050). Nine adult patients with HoFH were treated in 3 cohorts of increasing vector doses. Efficacy data are still to be reported, however the sponsor informed about discontinuation of the clinical development (http://ir.regenxbio.com/news-releases/news-release-details/regenxbio-reports-second-quarter-2020-financial-results-and/). In the meanwhile, a "second-generation" AAV vector expressing *LDLR* has been generated. These the main modifications: i) inclusion of Kozak sequence, ii) codon optimization, iii) addition of part of the human beta globin gene intron, iv) incorporation of the WPRE* (woodchuck hepatitis virus post-transcriptional regulatory element) at the 3' end of the cassette, v) modifications of *LDLR* sequence with three GOF point mutations (L318D, K809R, C818A), reported to reduce PCSK9 and consequently receptor degradation (Gu *et al*, 2013). All these modifications allowed the treatment of mice at significantly lower doses of AAV than before (Wang *et al.*, 2021).

As said before, cholesterol biodistribution is different between mice and humans and this may represent a limitation in the transability of results obtained in the formers. As a matter of fact, it is now possible to perform experiments in mice with a liver carrying human hepatocytes, known as "humanized mouse". These mice are immune deficient and lack fumarylacetoacetate fumarase, $Fah^{-/-}$ (FRG mice). The enzyme is essential for survival of hepatocytes; thus these mice die if left untreated, however they can be compensated by providing Nitisinone (NTBC). Slightly after discontinuation of the drug, human hepatocytes are transplanted. Given the selective advantage that they have towards the murine $Fah^{-/-}$ hepatocytes, they can replace them with a percentage of chimerism up to 90 (Lisowski *et al*, 2014). The technology was successfully applied to hypercholesterolemia (Bissig-Choisat *et al*, 2015). Briefly, hepatocytes from a HoFH female child, undergoing liver transplantation, were transplanted into FRG mice. Once fed with WD, they became hypercholesterolemic. The condition was reverted by delivery of an AAV vector encoding human *LDLR*, even though gene transfer was more efficient in residual murine hepatocytes. Despite all the advantages of this approach, the remaining major limitation is that human hepatocytes are placed in a non-physiological environment, where blood composition and signals may be markedly different. Particularly, in the context of FH, unless challenged with WD, the mice were not

hypercholesterolemic, probably because of the residual uptake of cholesterol by extra-hepatic tissues, together with uptake by residual murine hepatocytes, carrying functional *Ldlr*.

AAV vectors remain mostly episomal in transduced cells, thus they are diluted upon cell proliferation such as during liver growth, leading to a progressive decrease in the therapeutic transgene. Effective re-dosing is currently difficult to achieve, due to immune responses to the vector elicited by the first administration and research efforts are underway to make it possible (Leborgne *et al.*, 2020; Meliani *et al*, 2018). This limitation currently challenges application of AAV vector mediated gene transfer to pediatric patients. Yet, young kids would be the ideal target population for GT of FH, since they would most benefit from an early intervention. Indeed, high LDL-C since birth causes progressively increasing ATH. In contrast, HIV-derived lentiviral vectors (LV) integrate their genetic cargo into the host cell genome, thus are maintained upon cell replication. LDLR have been reported to be the entry route of vesicular stomatitis protein G (VSV.G) pseudotyped LV (Finkelshtein *et al*, 2013). Interaction of LDLR and VSV.G during LV production has been shown to cause a substantial decrease in LV production and viral titers (Al-Allaf *et al*, 2019b). Despite this problem, LV were used to treat WHHR, achieving partial reduction in circulating cholesterol (around 25%). Recently, a novel hypercholesterolemic mouse model was generated, carrying the truncating *Ldlr E208stop* mutation, then it was tempted to treat it using AAV vector-based delivery of CRISPR-Cas9 and a corrective donor DNA. Genetic correction occurred in a subset of hepatocytes, total cholesterol and TG were reduced even if not normalized and atherosclerotic plaque were smaller but still present, compared to untreated mice (Zhao *et al*, 2020). More recently, intravenous delivery of exosome based *LDLR* mRNA proved to be effective in decreasing cholesterol in *Ldlr*$^{-/-}$ mice (Li *et al*, 2021). A clinical trial using this strategy has started (ClinicalTrials.gov Identifier: NCT05043181) and results are still undisclosed. However, this approach would result in transient efficacy and repeated administration of the mRNA would be required.

1.5 Improving efficacy of liver directed LV GT

Non-specific cross-reacting antibodies against VSV.G have been reported in humans. These antibodies could reduce the efficacy of GT by fixing the complement (DePolo *et*

al., 2000). Moreover, our group showed that the complement-mediated inactivation of LV is dose-dependent, and tends to be rapidly saturated at LV concentrations similar to the ones expected to be found, in the circulation, immediately following the infusion (Annoni *et al*, 2019).

High quantity highly purified LV are required to treat large animals and potentially human beings. Thus, it would be essential to improve the efficiency of LV gene transfer, to make possible reducing the doses required to achieve the therapeutic outcome. This is true for both non cell autonomous diseases but even more for cell autonomous, where the therapeutic outcome may be particularly challenging to achieve. Different pathways and drugs have been described to induce an increase in gene transfer, when associated with GT. Here will follow a description of the ones showing the best outcomes, together with a strategy recently published aiming to increase the percentage of corrected hepatocytes *a posteriori*, if the therapeutic outcome is not achieved because of inter-subject variability issue (Vonada *et al*, 2021).

1.5.1 IFN mediated mechanism of defense against lentiviral vectors

Mice lacking a functional IFN alpha/beta receptor (IFNAR) display higher gene transfer than wild type mice (Brown *et al.*, 2007). The induction of IFN response occurs within the first 4 hours following GT, it is unrelated to the envelope used and it is dependent on the entry of LV in the cells. A transient blockage of IFNARI may be a strategy to improve liver directed LV mediated GT. IFNARI inhibition is a safe strategy: Anifrolumab is an anti-interferon-α-receptor monoclonal antibody, used in cases of moderate-to-severe systemic lupus erythematosus (Loncharich & Anderson, 2022).

1.5.2 Proteasome involvement in defense against LV

Proteasome inhibition has been described as a strategy to improve LV mediated gene transfer *ex vivo* (Santoni de Sio *et al*, 2006). This may be due to a i) direct binding of proteasome to the uncoating vector core or ii) indirectly, by targeting factors required by the vector to efficiently perform the early steps of transduction. A transient blockage of proteasome activity may be a strategy to improve liver directed LV mediated GT. Proteasome inhibition may be a clinically viable strategy, since Bortezomib (Velcade) is a proteasome inhibitor used in cases of multiple myeloma (Raedler, 2015).

1.5.3 Fasting induced improvement in AAV mediated GT

Improving efficiency of gene transfer is a hot topic even in AAV GT. One of the most effective ways to achieve it has been through fasting mice or NHP (Hosel *et al*, 2017). Mechanism of improved gene transfer was explained by linking fasting to induction of autophagy, which positively impacts on efficient AAV transduction. TorinI and Rapamycin, known to trigger autophagy, were used to confirm the involvement of autophagy in increase gene transfer.

As said, LV are reported to access cells through LDLR and LDLR FM. While autophagy may induce an increase in gene transfer even when using LV, fasting may also be impacting on LDLR pathway. Fasting reduces the activity of SREBP2 in both mice and humans (Horton *et al.*, 2002) (Browning & Horton, 2010). SREBP2, as already mentioned (see 1.4.2.3), drives the expression of cholesterol synthesis, *PCSK9* and *LDLR* expression. Thus, the beneficial effect of autophagy in increasing efficiency of gene transfer may be masked by the detrimental effect of reduction of LDLR.

1.5.4 Positive selection of hepatocytes corrected through GT

The strategy has been proposed in a paper recently published (Vonada *et al.*, 2021). Paracetamol (APAP, acetaminophen) is a non-opioid analgesic and antipyretic conventionally used in case of pain and fever. Once performed its action, it is then metabolized in the liver, through different pathways (Figure V). 90% through glucuronidation and sulfation reactions, generating glucuronides sulfates (non-toxic metabolites). However, 5-10% of APAP is funneled into cytochrome P450 (CYP450) oxidation reactions (Yoon *et al*, 2016), which give rise to N-acetyl-para-benzoquinone-imine (NAPQI). This toxic metabolite covalently binds macromolecules in the hepatocyte, ultimately leading to cell necrosis. This is not an issue, since glutathione (GSH) immediately reduces NAPQI, generating cysteine conjugates and mercapturic acids (non-toxic metabolites). However, glutathione levels are limited, and storages are easily depleted. In case of APAP overdose, liver toxicity occurs. Since CYP450 expression is enriched in the pericentral area, APAP mediated liver toxicity is mostly limited to that zone. This pathway was exploited to select, *a posteriori* (i.e. post GT), the number of genetically corrected hepatocytes. The therapeutic transgene was coupled with

a siRNA targeting NADPH-cytochrome P450 oxidoreductase (CYPOR), indispensable redox partner for all microsomal CYP450 enzymes to be functional. Then, toxic doses of paracetamol were injected in the mice. Pericentral hepatocytes damage and subsequent necrosis was induced exclusively in the non-corrected hepatocytes, where CYPOR activity was functional. Corrected, healthy hepatocytes replaced the damaged ones, ultimately leading to increase in transgene output and phenotypic correction (Vonada *et al.*, 2021).

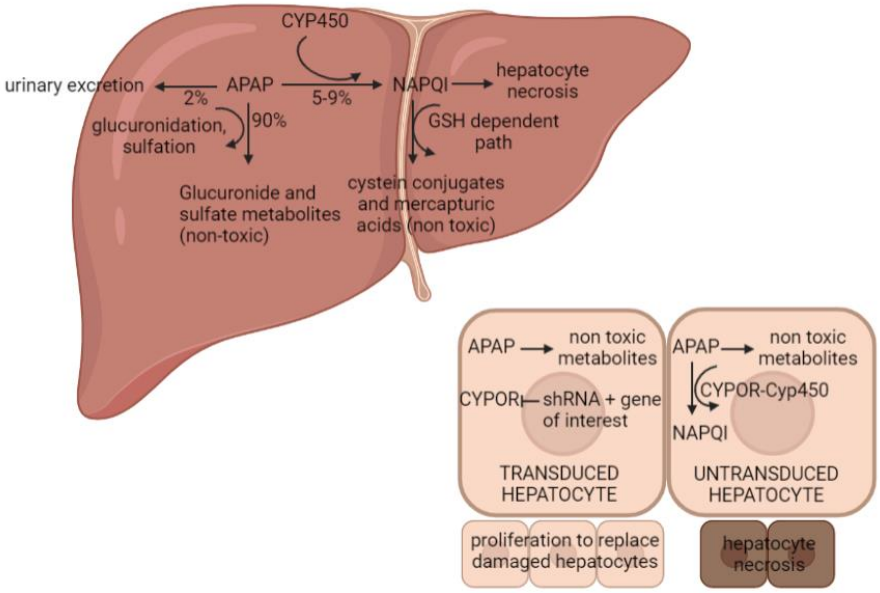


Figure V. Paracetamol metabolism and GT-mediated selection of corrected hepatocytes. *In case of APAP overdose, NAPQI is generated. When GSH storages are depleted, NAPQI interacts with macromolecules in the cell, ultimately leading to hepatocyte necrosis. If LV cassette encodes, together with the transgene, a shRNA for Cypor, NAPQI is not generated following overdose of APAP. In contrast, non-transduced hepatocytes are still subjected to APAP induced damage. Following APAP overdose, non-transduced hepatocytes will die, and transduced hepatocytes will replace them, increasing the transduced liver mass. Created with BioRender.com.*

This could be a fancy strategy to guarantee to each person entering a LV GT clinical trial to reach the therapeutic amount of transgene, by expansion of the corrected cells up to the desired threshold. However, this strategy will just guarantee an expansion of corrected hepatocytes in pericentral zone, without any enrichment in the periportal. Moreover, by definition, clonal expansion would be induced.

2. AIM OF THE WORK

The overall objective of this work was to improve the efficiency of LV-mediated gene transfer to hepatocytes *in vivo* and to evaluate its applicability to the treatment of the cell autonomous metabolic disease FH. Toward this objective, we identified the following specific aims:

- To evaluate the efficacy, durability and safety of *in vivo* liver directed LV GT for FH in a mouse model of the disease.
- To evaluate the feasibility and safety of a paracetamol-based strategy to endow LV transduced hepatocytes with selective advantage.
- To identify and exploit enhancers of LV gene transfer into hepatocytes, based on viral infection pathways.

3. RESULTS

3.1 Challenges of LV *in vivo* GT for FH

3.1.1 Reduced productivity of LDLR-encoding LV

We first set out to apply our LV-mediated liver directed *in vivo* GT to the more challenging setting of a cell-autonomous metabolic disease: FH. LDLR has been reported to be a receptor for VSV.G pseudotyped LV. As a result, high yield of VSV.G LV encoding LDLR may be difficult to obtain, because of a possible interaction between LDLR and VSV.G, impeding the correct packaging of viral particles. We produced VSV.G LV encoding human LDLR (hLDLR), codon optimized (c.o.) hLDLR or GFP, used as control. Infectious titer of each LV preparation was measured by transducing 293T cells. We observed a considerable >10-fold drop in infectious titer, physical particles and infectivity (fig. 1A) of LV encoding LDLR, both standard and c.o., compared to LV encoding GFP. These data suggest a detrimental interaction between the receptor and VSV.G, or a re-infection of the producer cells, due to the overexpression of the LDLR on the membrane of the cells, resulting in the accumulation of LV inside the cell at the expense of the amount in the supernatant. The drop was occurring despite the presence of a hepatocyte specific promoter upstream *LDLR*. Since 293T cells cannot read this promoter, this implies the expression of *LDLR* was resulting from CMV promoter upstream the long terminal repeats (LTR) of the lentiviral plasmid (fig. 1B).

To better clarify if overexpression of LDLR resulted in particles with reduced amounts of VSV.G, due to intracellular interaction prior to LV budding, VSV.G content was visualized on LV particles through immune staining and electron microscopy. Comparison between VSV.G content *per* virion in LV encoding LDLR or LV encoding human FIX (hFIX used as control) did not show a decrease in VSV.G amounts in LDLR-encoding LV (fig. 1C), suggesting the drop in infectious titer was, at least partially, due to reinfection of the producer cells by LV; in line with the reduced physical particles retrieved in the supernatant. Compared to historical data comprising a pool of LV encoding different transgenes, VSV.G content *per* virion was generally lower in this experiment.

The dramatic decrease in particle content of LDLR-encoding LV was appreciable even by looking by eye at the electron microscopy images (fig. 1D).

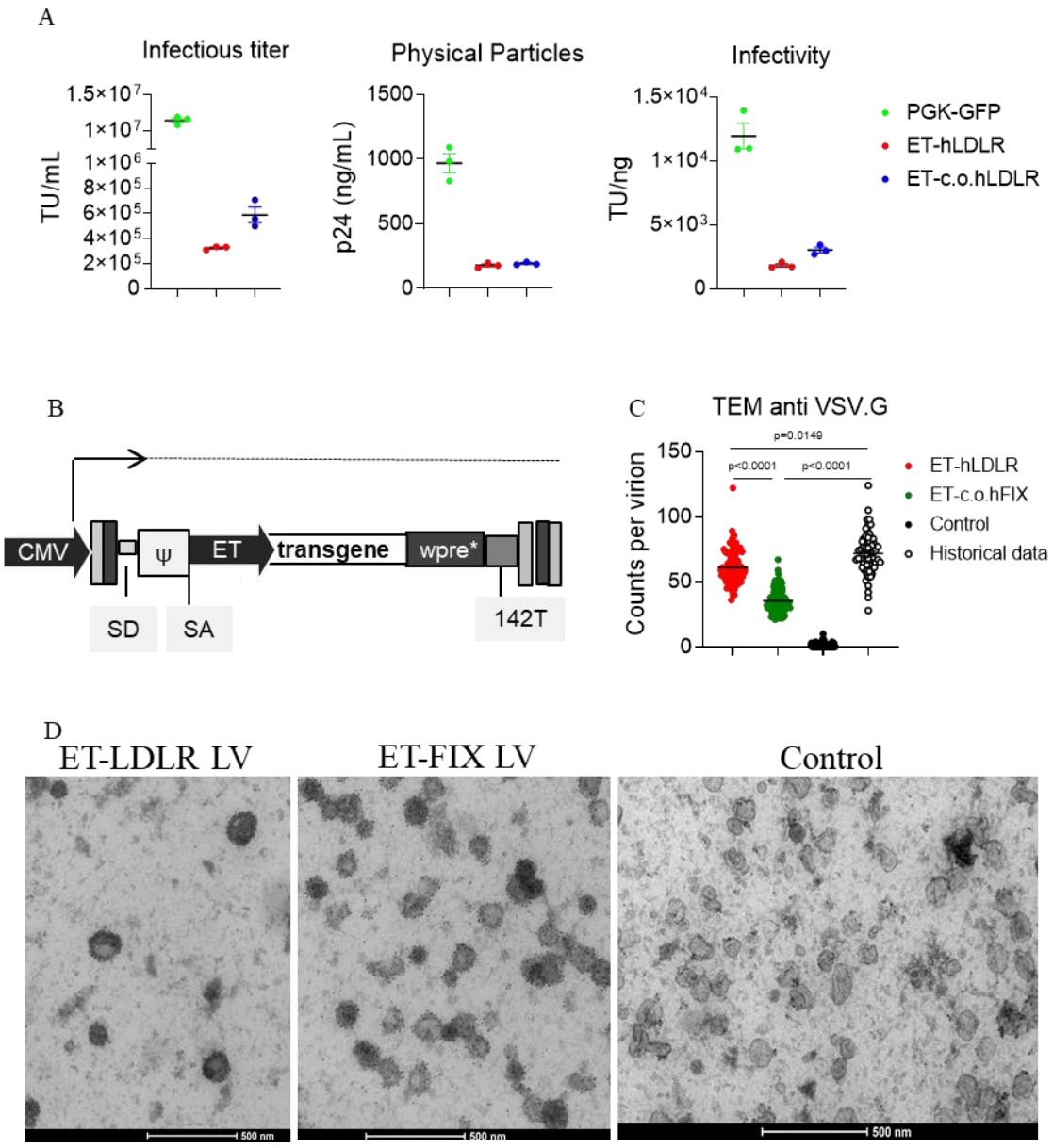


Fig. 1: Reduced productivity of LDLR-encoding LV. *(**A**)Single values and mean with standard error of the mean (SEM) of infectious titer (left panel), LV particles (ng HIV Gag p24/mL, middle panel) and specific infectivity (TU/ng p24, right panel) of non-concentrated LV encoding hLDLR (red dots) or c.o.hLDLR (blue dots), compared to LV encoding GFP (green dots), produced through transient transfection. (**B**) Schematic representation of the third-generation Self Inactivating (SIN) lentiviral vectors (proviral form) used in these experiments. SD: splicing donor site; SA: splicing acceptor site; ψ: packaging signal; Wpre*: mutated woodchuck hepatitis virus post-transcriptional regulatory element; 142T: miR-142 target sequence made of 4 tandem copies*

*of a sequence perfectly complementary to miR-142; Hepatocyte-specific Enhanced Transthyretin (ET) promoter composed of synthetic hepatocyte-specific enhancers and transthyretin promoter. **(C)** Transmission electron microscopy (TEM) mediated VSV.G counts per virion. Kruskal-Wallis test with Dunn's multiple comparisons test. (**D)** representative electron microscopy images of LV encoding LDLR (left panel, stained for VSV-G), of LV encoding hFIX (middle panel, stained for VSV.G), or of LV encoding FIX unstained (right panel).*

3.1.2 Rescue of productivity of LDLR-encoding LV and validation in vitro

Since LDLR-encoding LV displayed infectious titer so low to be not compatible with *in vivo* LV injections in mice, we tried different strategies to solve the issue. Firstly, we changed the pseudotype. We produced LV encoding hLDLR, c.o.hLDLR or hFIX (used as control), pseudotyped with VSV.G or GP64 (described in 1.3.1), known to target hepatocytes in vivo quite efficiently (Kang *et al*, 2005). We determined titer, physical particles and infectivity. Infectious titer of each LV preparation was measured by transducing 293T cells. While we confirmed the drop in infectious titer for VSV.G-pseudotyped LDLR-encoding LV, we observed a rescue when GP64 was used to pseudotype LDLR-encoding LV, which were as infectious as FIX-encoding LV produced using GP64 (fig. 2A). 293T are transduced by GP64 LV less efficiently than by VSV.G LV (compare hFIX LV VSV.G pseudotyped and hFIX LV GP64 pseudotyped in figure 2A), possibly because they lack the main GP64 receptor. Indeed, we observed >30-fold lower infectious titer of GP64-LV compared to VSV.G-LV, in line with a previous report (Schauber *et al*, 2004).

In parallel, to confirm the issue was due to overexpression of LDLR during LV production, we flipped the cassette, to have the transgene in antisense (a.s.) orientation. Using this kind of construct, the expression of the transgene product should be avoided during LV production but guaranteed once the LV is integrated into the target cells which, being hepatocytes, will be able to read the hepato-specific promoter sequence. Even in this case, we observed a rescue in infectious titer: LDLR-encoding VSV.G LV were comparable to FIX-encoding VSV.G LV (fig. 2B). As expected, infectious titer of a.s. oriented LDLR encoding LV pseudotyped with GP64 were comparable to control FIX-encoding LV pseudotyped with GP64 (fig. 2B).

The vast majority of the data that our group collected throughout the years were obtained using VSV.G as pseudotype. Moreover, we recently performed a comparison

between VSV.G and GP64, finding out that VSV.G LV transduce hepatocytes at higher efficiency than GP64-LV both *in vivo* and *ex vivo* (Milani et al, in preparation).

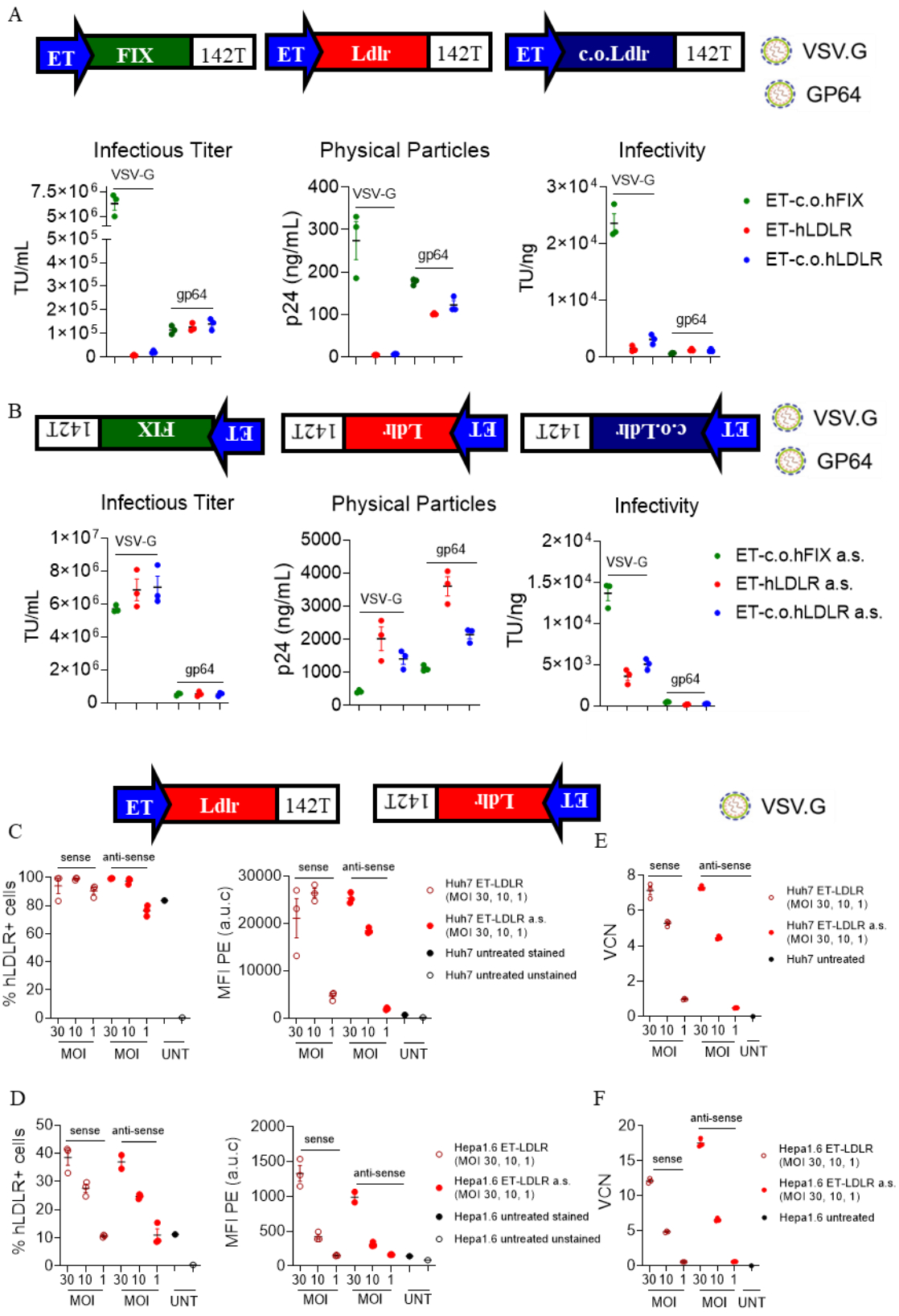


Fig. 2: Rescue of productivity of LDLR-encoding LV and validation* in vitro.** ***(A) *Single values and mean with SEM of infectious titer (left panel), LV particles (ng HIV Gag p24/mL, middle panel) and specific infectivity (TU/ng p24, right panel) of non-concentrated. LV encoding hLDLR (red schematic representation and red dot plots) or c.o.hLDLR (blue schematic representation and red dot plots), compared to LV encoding hFIX (green schematic representation and green dot plots), pseudotyped with VSV.G, left part of each panel, or gp64, right part of each panel.* ***(B)*** *Single values and mean with SEM of infectious titer, LV particles (ng HIV Gag p24/mL) and specific infectivity (TU/ng p24) of non-concentrated. antisense-oriented LV encoding hLDLR (red schematic representation and red dot plots) or c.o.hLDLR (blue schematic representation and red dot plots), compared to anti-sense-oriented LV encoding hFIX (green schematic representation and green dot plots), pseudotyped with VSV.G, left part of each panel, or gp64, right part of each panel.* ***(C)*** *Single values and mean with SEM of percentage of hLDLR positive Huh7 cells (left part of the panel) and mean fluorescence intensity (MFI) (right part of the panel) transduced in triplicate with indicated LV at indicated multiplicity of infection (MOI). (**D**) Same as (**C**) but concerning Hepa1.6 cells. Single values and mean with SEM of VCN of Huh7 cells (**E**) and Hepa1.6 cells (**F**).*

For these reasons, we selected VSV.G LV a.s. oriented cassette as the leading candidate to treat FH mice. We then validated the feasibility of using an a.s. oriented construct in hepatoma cell lines. We transduced human Huh7 (fig. 2C) and murine Hepa1.6 (fig. 2 D) hepatoma cell lines at different (30, 10, 1) multiplicity of infection (MOI). We looked by flow cytometry at % of LDLR positive cells, mean fluorescence intensity (MFI) and at VCN (fig. 2 E, F) of transduced cells. Huh7 normally express hLDLR, but overexpression can be appreciated looking at MFI. Sense and a.s cassettes were quite comparable in transgene expression (fig. 2C, D), confirming that placing the transgene in a.s. orientation may be an intriguing strategy to produce high titers of LV when transgene overexpression in producer cells negatively affects LV productivity (Poletti & Mavilio, 2021).

3.1.3 Higher transgene output in Ldlr$^{-/-}$ *than in control mice, by* in vivo *LV GT*

Once selected the best performing construct for *LDLR* gene transfer, we faced another possible issue related to the animal model: reduced efficiency of gene transfer in mice lacking LDLR, one of the receptors used by VSV.G LV.

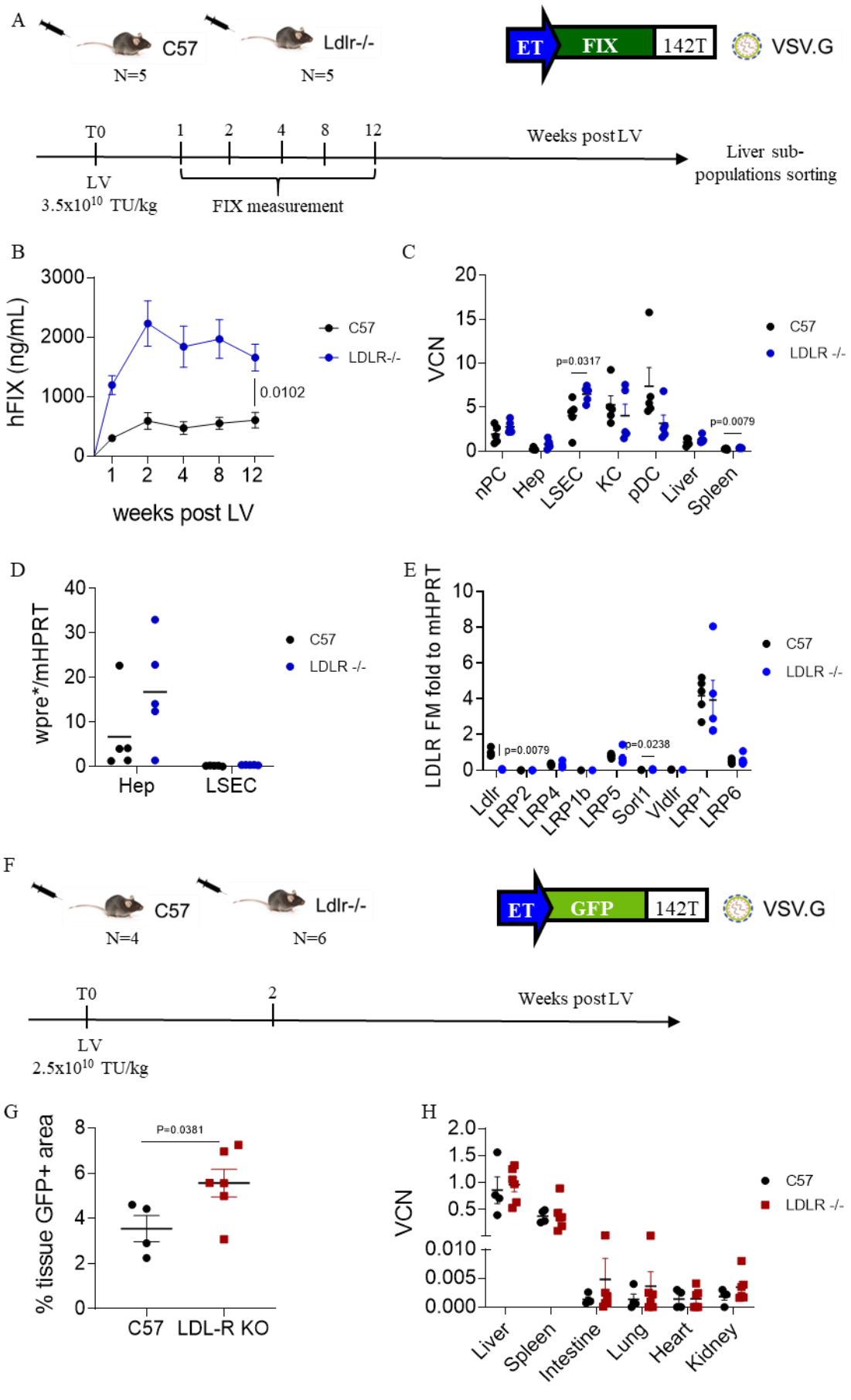

A
C57
N=5
Ldlr-/-
N=5
ET
FIX
142T
VSV.G
T0
1
2
4
8
12
Weeks post LV
LV
3.5x10^10 TU/kg
FIX measurement
Liver sub-populations sorting
B
hFIX (ng/mL)
3000
2000
1000
0
0.0102
C57
LDLR-/-
1
2
4
8
12
weeks post LV
C
VCN
20
15
10
5
0
p=0.0317
p=0.0079
C57
LDLR -/-
nPC
Hep
LSEC
KC
pDC
Liver
Spleen
D
wpre*/mHPRT
40
30
20
10
0
C57
LDLR -/-
Hep
LSEC
E
LDLR FM fold to mHPRT
10
8
6
4
2
0
p=0.0079
p=0.0238
C57
LDLR -/-
Ldlr
LRP2
LRP4
LRP1b
LRP5
Sorl1
Vldlr
LRP1
LRP6
F
C57
N=4
Ldlr-/-
N=6
ET
GFP
142T
VSV.G
T0
2
Weeks post LV
LV
2.5x10^10 TU/kg
G
% tissue GFP+ area
8
6
4
2
0
P=0.0381
C57
LDL-R KO
H
VCN
2.0
1.5
1.0
0.5
0.010
0.005
0.000
C57
LDLR -/-
Liver
Spleen
Intestine
Lung
Heart
Kidney

Fig. 3: Higher transgene output in Ldlr$^{-/-}$ than in control mice, by in vivo LV GT. *(**A**) Experimental design: 8-week-old mice, C57 or* Ldlr$^{-/-}$*, are injected i.v. with LV (dose 3.5x10^{10} TU/kg), pseudotyped with VSV.G, encoding hFIX reporter transgene, to compare transgene output overtime and transduction efficiency at end of experiment (**B**) Mean with SEM of hFIX antigen measured in the plasma of LV treated* Ldlr$^{-/-}$ *or C57 mice overtime (n=5 for C57 mice, n=5 for* Ldlr$^{-/-}$ *mice). Two-way ANOVA with Sidak's multiple comparisons test. (C) Single values and mean with SEM of VCN measured in nPC, fractionated and FACS-sorted liver subpopulations (hepatocytes, LSEC, KC, pDC), total liver and spleen of treated mice, 3 months after LV administration. (**D**) Single values and mean with SEM of expression analysis by quantitative PCR of WPRE* normalized on the endogenous hprt gene on RNA extracted from the livers of treated mice. (**E**) Single values and mean with SEM of expression analysis by quantitative PCR of* Ldlr *and* Ldlr FM*, normalized on the endogenous hprt gene on RNA extracted from the livers of C57 or* Ldlr$^{-/-}$ *mice. Mann-Whitney test. (**F**) 8 weeks old mice, C57 or* Ldlr$^{-/-}$*, are injected i.v. with LV (dose 2.5x10^{10} TU/kg), pseudotyped with VSV.G, encoding GFP reporter transgene (**G**) Single values and mean with SEM of percentage of liver area expressing GFP by immunofluorescence analysis 14 days after LV administration, Mann-Whitney test. (**H**) Single values and mean with SEM of VCN measured in the total liver, spleen, intestine, lung, heart, and kidney.*

We thus compared liver GT efficiency between *Ldlr$^{-/-}$* and C57 mice. We treated the two strains with VSV.G pseudotyped LV, encoding hFIX as reporter, to longitudinally monitor the transgene output in these mice (fig. 3A). Surprisingly, mice lacking LDLR showed >2.5-fold higher circulating hFIX amounts, compared to mice with functional LDLR. The difference was maintained throughout the experiment, until 3 months post GT (fig. 3B). At the end of experiment, mice were perfused, and liver subpopulations sorted. VCN detected in KC, pDC and total liver were comparable between the two strains, while in LSEC and spleen it was higher in *Ldlr$^{-/-}$* mice (fig. 3C). Despite the increase in VCN of sorted hepatocytes was not statistically significant (fig. 3C), RNA analysis showed transgene expression to be higher in *Ldlr$^{-/-}$* mice and to derive exclusively from hepatocytes (fig. 3 D). Since VSV.G LV is known to enter target cells with LDLR and its FM, we checked if the other FM were upregulated, in a compensatory fashion, in response of lack of LDLR, in mice *Ldlr$^{-/-}$*. However, by looking at RNA of mice *Ldlr$^{-/-}$* and C57, we did not observe any difference in levels of expression of hepatic *Ldlr FM* (fig. 3E).

To confirm the result observed with reporter hFIX and to visualize the transduced cells in liver sections, we treated C57 and *Ldlr*$^{-/-}$ with LV encoding GFP (fig 3F). Two weeks later, we euthanized the mice and collected organs for VCN and immunofluorescence. We observed an increase in % of tissue positive area of the liver of mice *Ldlr*$^{-/-}$ compared to C57, confirming the higher transgene output observed before (fig. 3G). VCN was evaluated in the liver and in other organs (fig. 3H), to assess if *Ldlr*$^{-/-}$ had different pattern of LV biodistribution. No difference in VCN was observed between the two strains.

3.2 *LDLR* gene transfer in FH mice

3.2.1 hLDLR *gene transfer in adult* Ldlr$^{-/-}$ *mice fails to reduce LDL-C*

Once defined the cassette to be used (a.s. oriented) and assessed that GT with VSV.G LV was feasible in this mouse model, we moved to the therapeutic experiment.

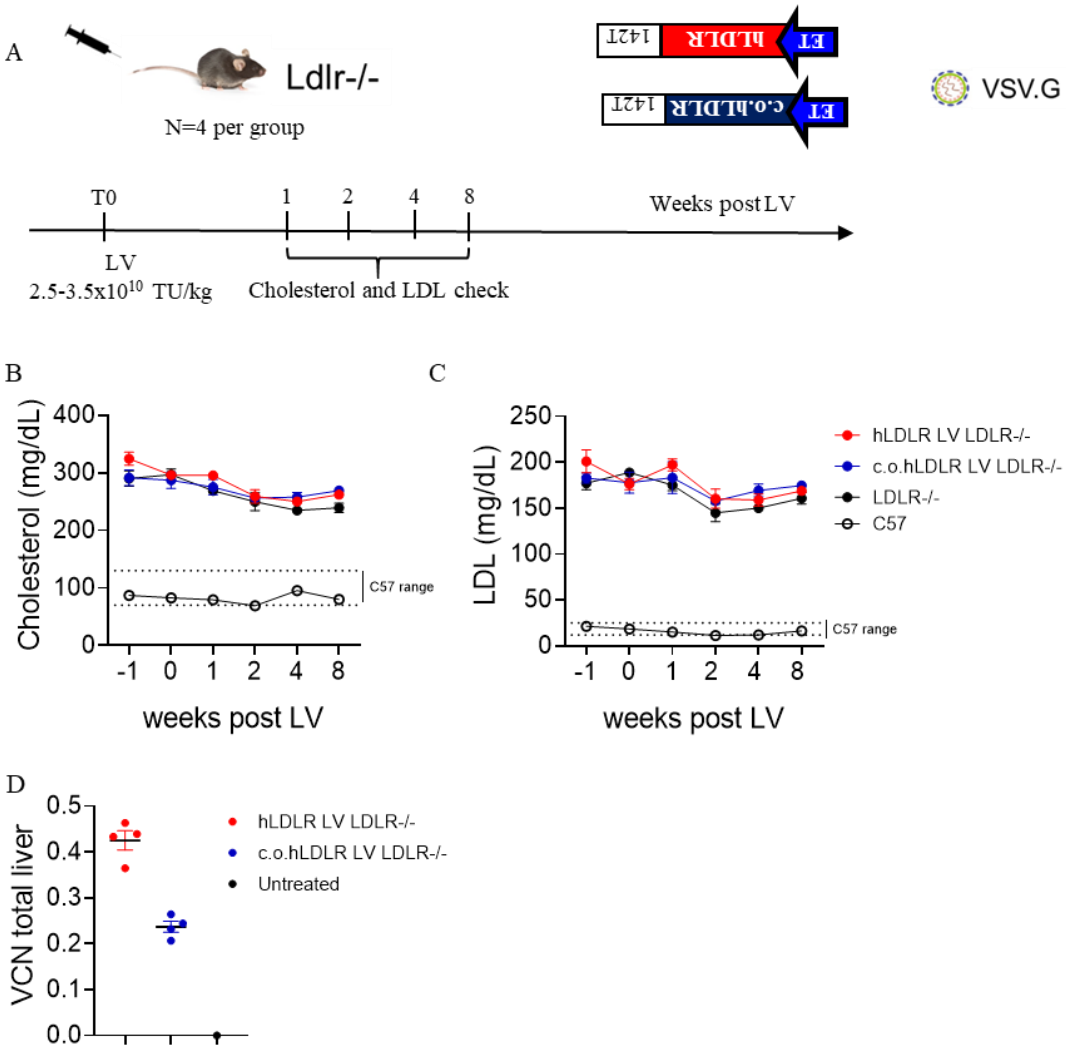


Fig. 4:* hLDLR *gene transfer in adult* Ldlr$^{-/-}$ *mice fails to reduce LDL-C. *(**A**) Experimental design: 8-week-old mice,* Ldlr$^{-/-}$*, are treated with LV, pseudotyped with VSV.G, encoding hLDLR or c.o.hLDLR therapeutic transgene. Mean with SEM of total (**B**) and LDL (**C**) circulating cholesterol measured in the serum of experimental mice overtime (**D**) Single values and mean with SEM of VCN measured in the total liver.*

We treated adult *Ldlr*$^{-/-}$ mice with LV carrying the *hLDLR* or c.o.*hLDLR*. Blood samples were collected overtime, to assess possible cholesterol reduction (fig. 4A). However, no reduction in total cholesterol or LDL-C was observed in treated mice, independently on the constructs used (fig. 4B, C). Mice were euthanized 8 weeks after GT. VCN on total liver was detectable (fig. 4D), even if lower than expected based on previous results with other transgenes like hFIX or GFP.

3.2.2 mLdlr gene transfer in adult Ldlr$^{-/-}$ *mice fails to reduce LDL, independently on the immune system*

The homology between human LDLR and murine LDLR is 78% at the amino acid sequence level. In the context of AAV-mediated *LDLR* liver gene transfer, it was shown that the dose required to achieve phenotypic correction of the *Ldlr*$^{-/-}$ mouse model was higher using the human sequence, compared to the murine. This is due to the less efficient interaction between human, transgene derived, LDLR with circulating murine LDL-C (Kassim *et al*, 2013). Thus, for *in vivo* experiments in mice, we moved to the murine *Ldlr* (*mLDLR*) sequence. Moreover, since these mice lack LDLR, an immune response could be induced against the transgene product, following GT, possibly leading to a cytotoxic T cell mediated clearance of corrected hepatocytes. For this reason, we generated immune deficient *Ldlr*$^{-/-}$ mice by crossing *Ldlr*$^{-/-}$ mice and *Rag1*$^{-/-}$ mice. We thus injected i.v. adult *Ldlr*$^{-/-}$ and *Ldlr*$^{-/-}$ - *Rag1*$^{-/-}$, with *mLdlr* LV or c.o.*mLdlr* LV. Blood samples were collected overtime, to assess possible cholesterol reduction (fig. 5A), however even in this case we did not see a reduction in total cholesterol (fig. 5B) or LDL-C (fig. 5C) of treated mice compared to untreated controls. Interestingly, *Rag1*$^{-/-}$ - *Ldlr*$^{-/-}$ showed lower total and LDL cholesterol throughout experiment, in line with previously reported reduction in those parameters in immune deficient mice (Reardon *et al*, 2001). The only trend of reduction that we observed was in the c.o.*Ldlr* LV group, possibly suggesting higher expression of that transgene due to the codon optimization.

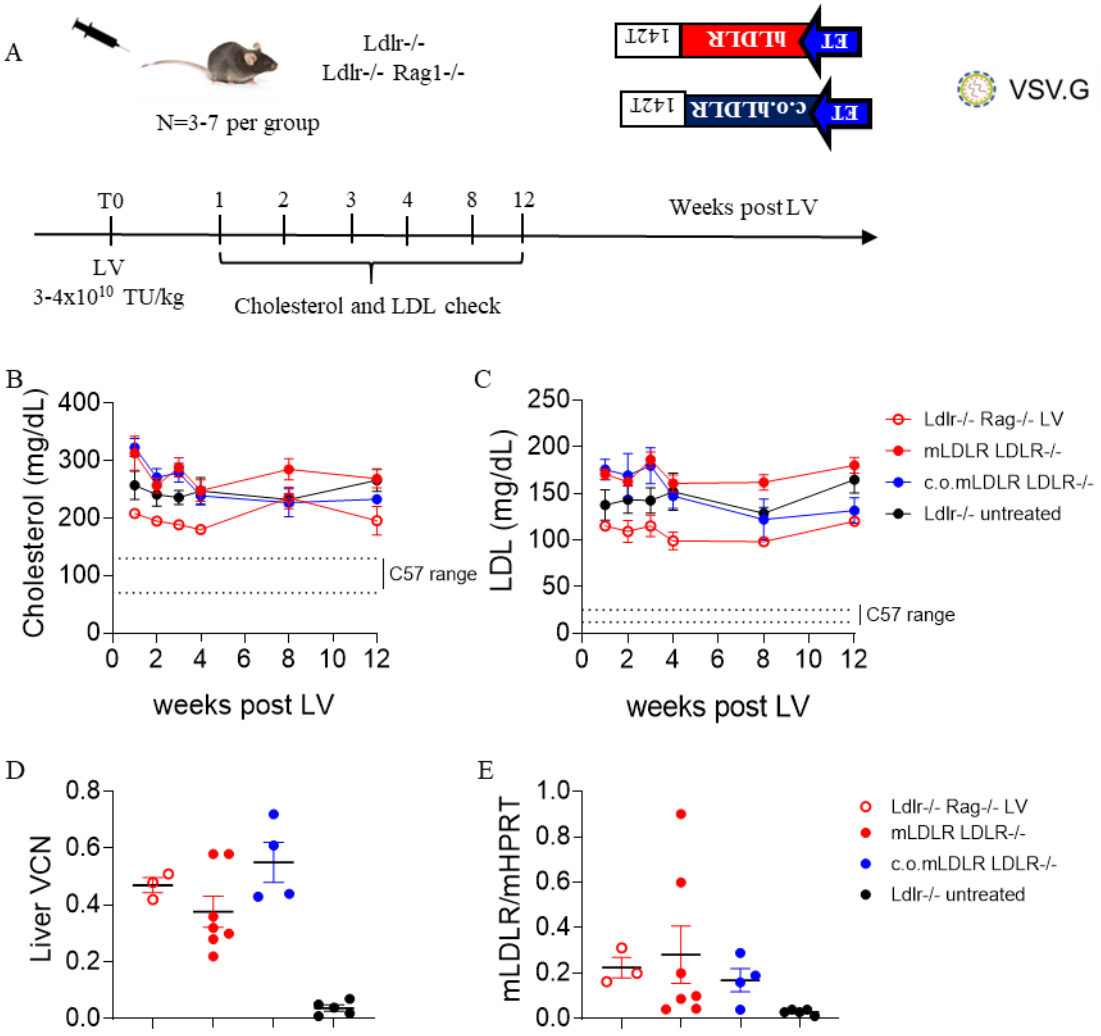


***Fig. 5:* mLdlr *gene transfer in adult* Ldlr$^{-/-}$ *mice fails to reduce LDL, independently on the immune system.** (**A**) Experimental design: 8-week-old mice,* Ldlr$^{-/-}$ *or* Ldlr$^{-/-}$ Rag1$^{-/-}$*, are treated with LV, pseudotyped with VSV.G, encoding mLDLR therapeutic transgene. 8-week-old mice,* Ldlr$^{-/-}$*, are treated with LV, pseudotyped with VSV.G, encoding c.o.mLDLR therapeutic transgene (2 independent experiments). Mean with SEM of total (**B**) and LDL (**C**) circulating cholesterol measured in the serum of experimental mice overtime. (**D**) Single values and mean with SEM of VCN measured in the total liver. (**E**) Single values and mean with SEM of expression analysis by quantitative PCR of* mLdlr *normalized on the endogenous* Hprt *gene on RNA extracted from the livers of experimental mice.*

Three months post GT, we determined the VCN in total liver DNA from treated mice (fig. 5D). It was comparable between immune competent and immune deficient mice, suggesting lack of immune response against the transgene product. Moreover, when we looked at RNA deriving from *Ldlr* expression, we detected it in the different groups (fig.

5E). Particularly, it was not higher in immune deficient mice. All together these data pointed towards subtherapeutic transduction efficiency in the adult mouse model.

3.2.3 mLdlr *gene transfer in young* Ldlr$^{-/-}$ *mice stably reduces LDL-C*

HoFH patients should be treated as soon as possible following diagnosis. For this reason, we moved to treat juvenile mice. We injected 2-week old mice with *mLDLR* or co.*mLDLR* a.s. oriented (fig. 6A).

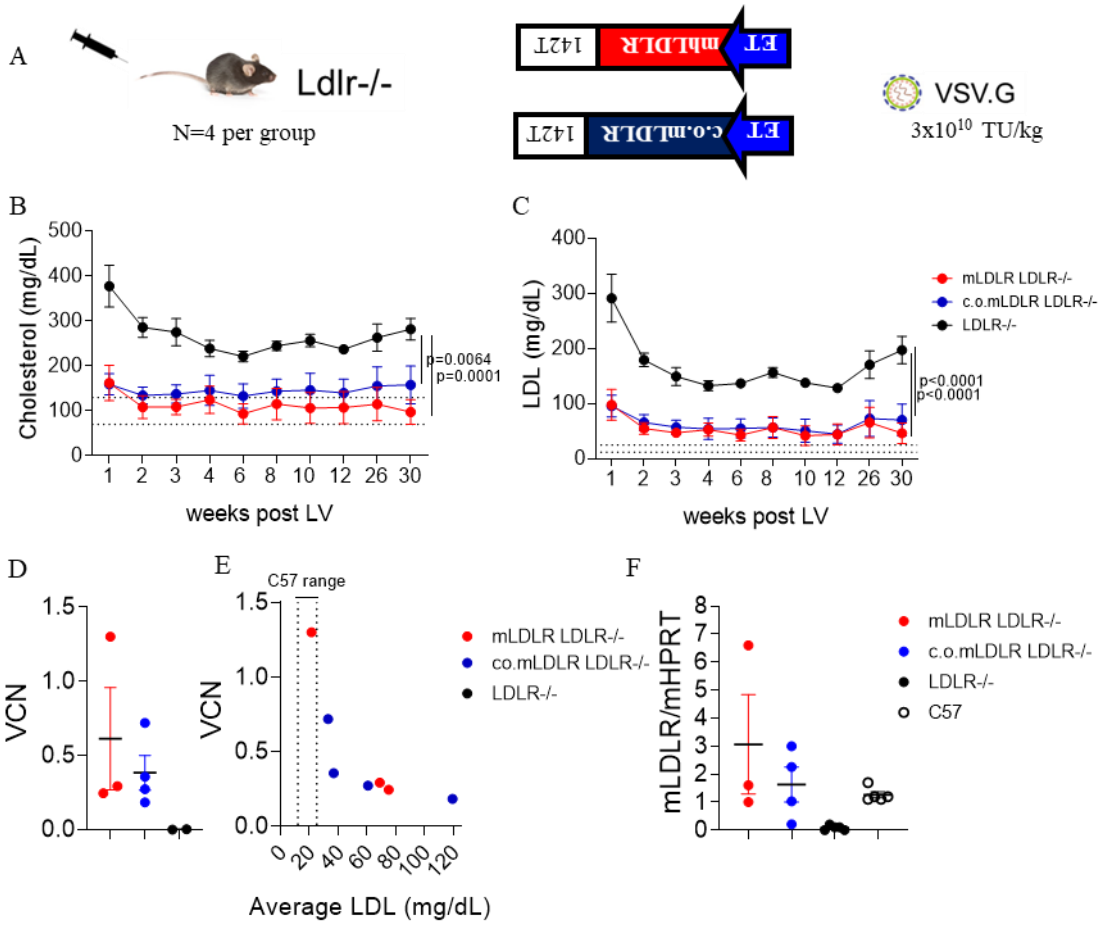


Fig. 6:* mLdlr *gene transfer in young* Ldlr$^{-/-}$ *mice stably reduces LDL-C. ***(A)*** *Experimental design: 2 weeks old mice,* Ldlr$^{-/-}$*, are treated with LV, pseudotyped with VSV.G, encoding mLDLR or c.o.mLDLR therapeutic transgene. Mean with SEM of total* ***(B)*** *and LDL* ***(C)*** *circulating cholesterol measured in the serum of experimental mice overtime. Two-way ANOVA with Tukey's multiple comparisons test.* ***(D)*** *Single values and mean with SEM of VCN measured in total liver of experimental mice.* ***(E)*** *Correlation between VCN and LDL circulating cholesterol (average of all values throughout experiment).* ***(F)*** *Single values and mean with SEM of expression analysis by quantitative PCR of* mLdlr *normalized on the endogenous* Hprt *gene on RNA extracted from*

the livers of treated mice. RNA from liver of random adult C57 mice was used as control, for assessing Ldlr *level of expression in a normal healthy adult mouse liver.*

Blood samples were collected overtime, to assess possible cholesterol reduction. We observed a rapid decrease in total cholesterol and LDL, maintained throughout the experiment up to 7 months post GT, when mice were euthanized (fig. 6 B, C). VCN in total liver showed an inverse correlation compared to circulating LDL-C amounts (fig. 6D): indeed, the higher the gene transfer, the lower the circulating LDL-C throughout experiment (fig. 6 E). *Ldlr* RNA was measured in the liver of treated mice. The treated mice where cholesterol and LDL-C were normalized showed a liver expression of *Ldlr* higher than C57 mice, confirming that, to compensate the lack of LDLR in the extra-hepatic tissues, corrected hepatocytes should work slightly more than normal hepatocytes (fig. 6F). Previous data from our group indicate that higher hepatocytes gene transfer is achieved in neonates and juvenile mice, compared to adults ((Milani *et al.*, 2022) and unpublished data). It is probably for this reason that we did not achieve phenotypic correction in adults when treating the mice at the same dose *per* kg.

3.2.4 mLdlr *gene transfer in young* Ldlr$^{-/-}$ *mice fully normalizes LDL-C and protects from ATH, even after a diet challenge*

In order to define the LV dose required to achieve full normalization in total cholesterol and LDL-C amounts, we next treated juvenile mice at a slightly higher LV dose. Since we obtained correction of the phenotype, even using the wild type *mLdlr* sequence (non c.o.), we selected that one for future experiments. We injected 12 mice with *mLdlr* LV (fig. 7A). We confirmed cholesterol reduction in the first weeks following GT. All treated mice showed complete normalization in total cholesterol (fig. 7B), most of the mice even in LDL-C (fig 7C). To stress the system and understand if a counter-selection of corrected hepatocytes might occur in challenging conditions, we started feeding 6 of the 12 treated mice, together with untransduced *Ldlr*$^{-/-}$and C57 controls, with high cholesterol high carbohydrate diet (referred to as Western Diet, WD). The challenge lasted 3 months. Mice were put back to standard chow diet for an additional month, to assess if total cholesterol and LDL-C were reduced back to their values pre-challenge once WD was discontinued (fig. 7D, E). After an additional month, all the mice were euthanized.

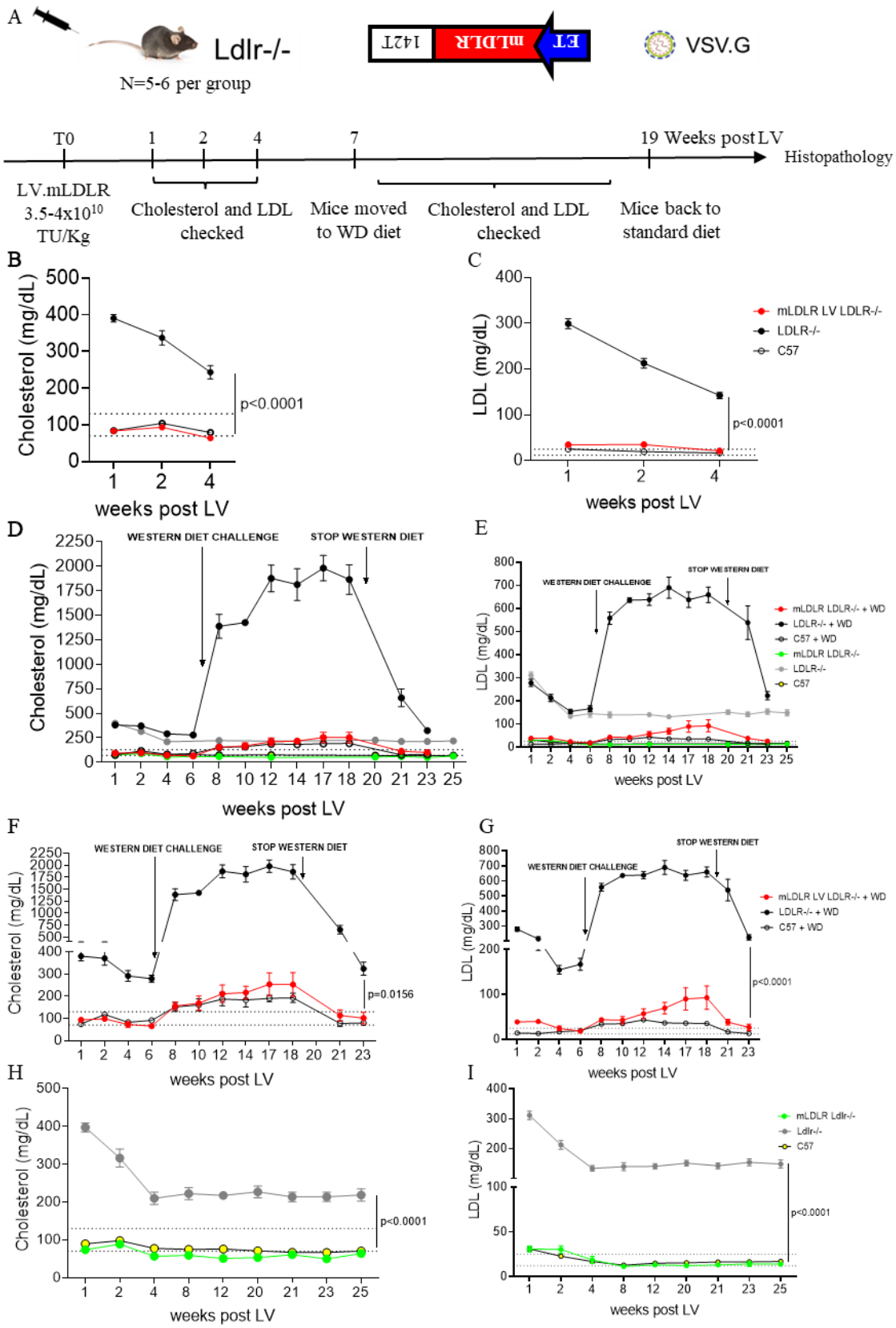

A
Ldlr-/-
N=5-6 per group
ET
mLDLR
1421T
VSV.G
T0
1
2
4
7
19 Weeks post LV
Histopathology
LV.mLDLR
3.5-4x10^10
TU/Kg
Cholesterol and LDL
checked
Mice moved
to WD diet
Cholesterol and LDL
checked
Mice back to
standard diet
B
Cholesterol (mg/dL)
p<0.0001
weeks post LV
C
LDL (mg/dL)
mLDLR LV LDLR-/-
LDLR-/-
C57
p<0.0001
weeks post LV
D
WESTERN DIET CHALLENGE
STOP WESTERN DIET
Cholesterol (mg/dL)
weeks post LV
E
WESTERN DIET CHALLENGE
STOP WESTERN DIET
LDL (mg/dL)
mLDLR LDLR-/- + WD
LDLR-/- + WD
C57 + WD
mLDLR LDLR-/-
LDLR-/-
C57
weeks post LV
F
WESTERN DIET CHALLENGE
STOP WESTERN DIET
Cholesterol (mg/dL)
p=0.0156
weeks post LV
G
WESTERN DIET CHALLENGE
STOP WESTERN DIET
LDL (mg/dL)
mLDLR LV LDLR-/- + WD
LDLR-/- + WD
C57 + WD
p<0.0001
weeks post LV
H
Cholesterol (mg/dL)
p<0.0001
weeks post LV
I
LDL (mg/dL)
mLDLR Ldlr-/-
Ldlr-/-
C57
p<0.0001
weeks post LV

Fig. 7:* mLdlr *gene transfer in young* Ldlr$^{-/-}$ *mice subsequently challenged with WD. ***(A)*** *Experimental design: 2 weeks old mice,* Ldlr$^{-/-}$*, are treated with LV, pseudotyped with VSV.G, encoding mLDLR transgene, and bled to assess normalization of total and LDL cholesterol. Starting from week 7 after LV, mice are challenged with WD for 3 months. Total and LDL cholesterol are monitored during challenge. At week 19, mice are put back to standard diet for one additional month, before being sacrificed for histopathological analysis. Mean with SEM of total and LDL circulating cholesterol measured in the serum of experimental mice during the first weeks following administration (**B**, **C**) and throughout the whole experiment (**D**, **E**). (**F**) Total and LDL (**G**) cholesterol focused only on WD groups; total (**H**) and LDL (**I**) cholesterol focused only on non-WD groups. Two-way ANOVA with Tukey's multiple comparisons test.*

Following challenge, all GT treated mice showed levels of total cholesterol comparable to C57, while LDL-C levels were slightly increased overtime in 2 out of 6 mice.

The control untreated mice *Ldlr*$^{-/-}$ challenged showed a very pronounced increase in total cholesterol and LDL-C amounts (fig. 7F, G). Treated mice not challenged with WD maintained their total cholesterol and LDL-C normalized throughout the experiment (fig. 7H, I). After discontinuation of WD, all treated mice were back to their pre-challenge values.

Mice were euthanized and histopathological analysis of aortas and livers was performed. ATH was evaluated at the level of aortic sinus (fig. 8A), aortic arch (fig. 8B) and thoracic aorta (fig. 8C).

In aortic sinus, advanced atherosclerotic disease, with plaques showing accumulation of foamy macrophages, cholesterol crystals and fibrotic tissues involving all three aortic cusps was observed in all mice *Ldlr*$^{-/-}$ fed with WD, and scored as marked . ATH in aortic sinus of all *Ldlr*$^{-/-}$ mice receiving standard diet throughout the experiment was characterized by less extensive plaques, involving one or two aortic cusps, and was scored as minimal to mild. ATH was absent in C57 mice fed with standard diet as well as in those fed with WD. Mice treated with *Ldlr* LV not subjected to WD did not show any sign of ATH. Importantly, none of the mice treated with LV and challenged with WD showed any sign of ATH, either (fig. 8D).

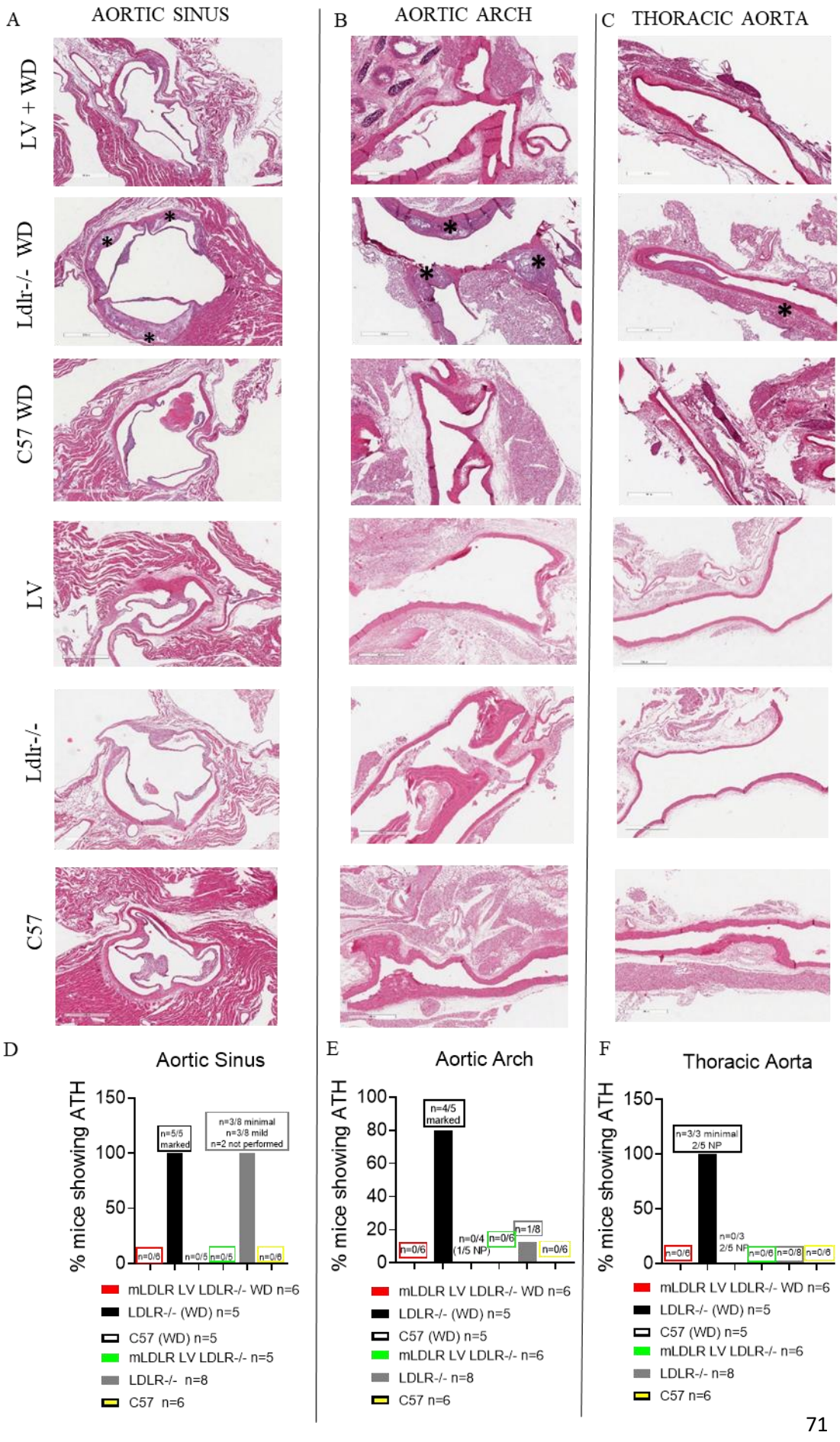

A
AORTIC SINUS
B
AORTIC ARCH
C
THORACIC AORTA
LV + WD
Ldlr-/- WD
C57 WD
LV
Ldlr-/-
C57
D
Aortic Sinus
% mice showing ATH
150
100
50
0
n=5/5 marked
n=3/8 minimal
n=3/8 mild
n=2 not performed
n=0/6
n=0/5
n=0/5
n=0/6
mLDLR LV LDLR-/- WD n=6
LDLR-/- (WD) n=5
C57 (WD) n=5
mLDLR LV LDLR-/- n=5
LDLR-/- n=8
C57 n=6
E
Aortic Arch
% mice showing ATH
100
80
60
40
20
0
n=4/5 marked
n=0/6
n=0/4 (1/5 NP)
n=0/6
n=1/8
n=0/6
mLDLR LV LDLR-/- WD n=6
LDLR-/- (WD) n=5
C57 (WD) n=5
mLDLR LV LDLR-/- n=6
LDLR-/- n=8
C57 n=6
F
Thoracic Aorta
% mice showing ATH
150
100
50
0
n=3/3 minimal
2/5 NP
n=0/6
n=0/3
2/5 NP
n=0/6
n=0/8
n=0/6
mLDLR LV LDLR-/- WD n=6
LDLR-/- (WD) n=5
C57 (WD) n=5
mLDLR LV LDLR-/- n=6
LDLR-/- n=8
C57 n=6

Fig. 8:* mLdlr *LV treated* Ldlr$^{-/-}$ *mice are protected from ATH, even when fed with WD. *Representative H&E images of atherosclerosis assessment at the level of (**A**) aortic sinus, (**B**) aortic arch, (**C**) thoracic aorta, detected in experimental mice, with the following vertical order:* Ldlr$^{-/-}$ *LV treated + WD,* Ldlr$^{-/-}$ *+ WD, C57 + WD,* Ldlr$^{-/-}$ *LV treated,* Ldlr$^{-/-}$*, C57. * = Atherosclerotic plaque. Frequency and grade of atherosclerosis (ATH) detected in the different experimental groups in aortic sinus (**D**), aortic arch (**E**) and thoracic aorta (**F**).*

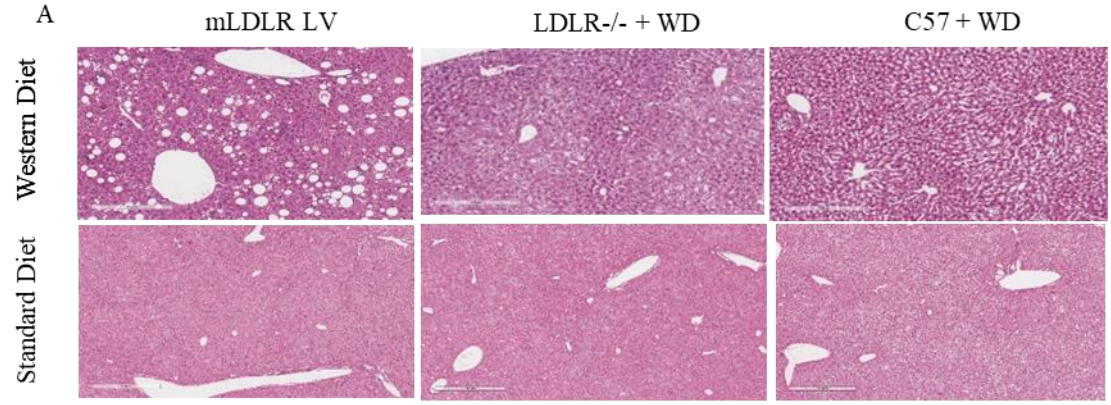
In aortic arch, marked ATH was present in 4 out of 5 *Ldlr*$^{-/-}$ mice fed with WD, and in 1 out of 8 *Ldlr*$^{-/-}$ mice, graded as minimal in severity. Again, no sign of ATH was seen in C57 or *Ldlr*$^{-/-}$ mice treated with LV, with or without WD challenge (fig. 8E).

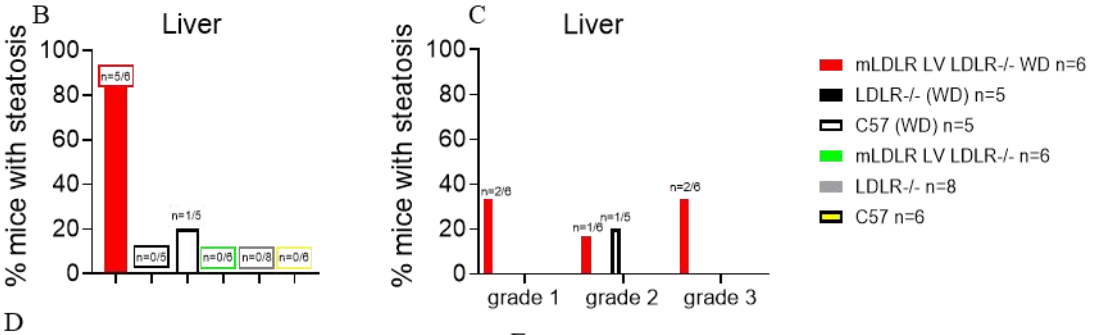
Descending thoracic aorta showed minimal ATH in 3, out of the 4 analyzed, *Ldlr*$^{-/-}$ mice challenged with WD analyzed, while no ATH was seen in *Ldlr*$^{-/-}$ mice. Again, no sign of ATH was seen in C57 nor *Ldlr*$^{-/-}$ mice treated with LV, fed with or without WD (fig. 8F).

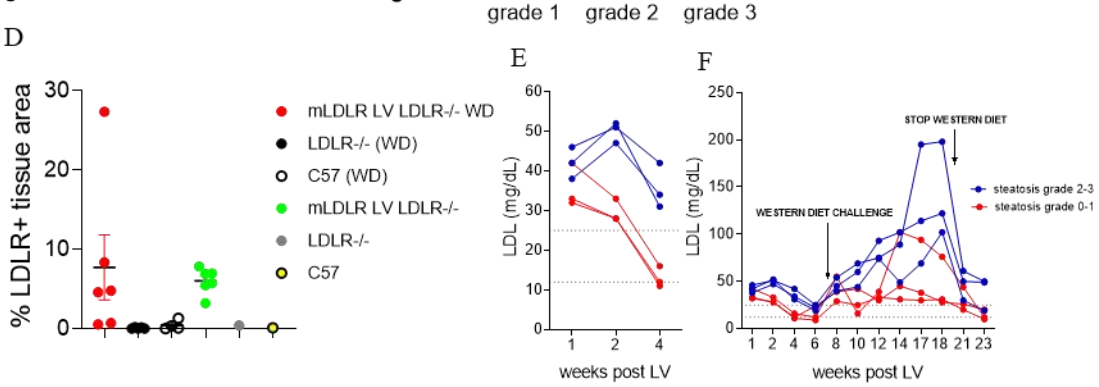
Reasons for reduced ATH in *Ldlr*$^{-/-}$ untreated mice, compared to humans carrying mutations in *LDLR* gene, reside in compensatory mechanisms which protects mice, as already mentioned above (see 1.4.3.1) (Getz & Reardon, 2006).

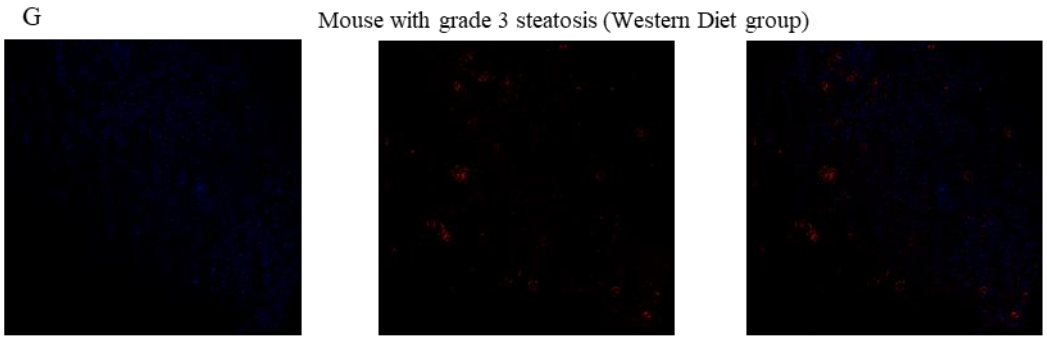
We then evaluated if the higher LDL-C clearance required by LV corrected hepatocytes induced liver steatosis, by performing histopathology analysis (fig. 9A). Liver sections of mice treated with *mLdlr* LV and challenged with WD showed minimal to moderate lipid macro-micro vacuolation of hepatocytes in 5 out of 6 mice. Mild lipid macro-micro vacuolation of hepatocytes was observed in 1 out of 5 C57 mice challenged with WD. *Ldlr*$^{-/-}$ challenged mice seemed protected from liver steatosis, possibly because LDL were accumulating in arterial walls, while being incapable of accessing hepatocytes. C57 and *Ldlr*$^{-/-}$ mice not challenged did not show signs of liver steatosis. Importantly, none of *Ldlr*$^{-/-}$ LV treated mice not challenged showed any liver steatosis, indicating that, in a standard diet condition, cholesterol clearance almost exclusively by hepatocytes is a feasible strategy (fig. 9B). Concerning challenged treated mice showing lipid vacuolation, in a scale from 1 to 5, 1/6 was not showing any steatosis, 2/6 were assigned to grade 1, 1/6 to grade 2, 2/6 to grade 3. The C57 mouse showing lipid vacuolation was scored as grade 2 (fig. 9C).

We then evaluated the % of tissue area positive for transgene derived LDLR (fig. 9D), by immune fluorescence analysis.


A
mLDLR LV
LDLR-/- + WD
C57 + WD
Western Diet
Standard Diet


B
Liver
% mice with steatosis
n=5/6
n=0/6
n=1/5
n=0/6
n=0/6
n=0/6
C
Liver
% mice with steatosis
n=2/6
n=1/6
n=1/5
n=2/6
grade 1
grade 2
grade 3
mLDLR LV LDLR-/- WD n=6
LDLR-/- (WD) n=5
C57 (WD) n=5
mLDLR LV LDLR-/- n=6
LDLR-/- n=8
C57 n=6


D
% LDLR+ tissue area
mLDLR LV LDLR-/- WD
LDLR-/- (WD)
C57 (WD)
mLDLR LV LDLR-/-
LDLR-/-
C57
E
LDL (mg/dL)
weeks post LV
F
LDL (mg/dL)
STOP WESTERN DIET
WESTERN DIET CHALLENGE
steatosis grade 2-3
steatosis grade 0-1
weeks post LV


G
Mouse with grade 3 steatosis (Western Diet group)

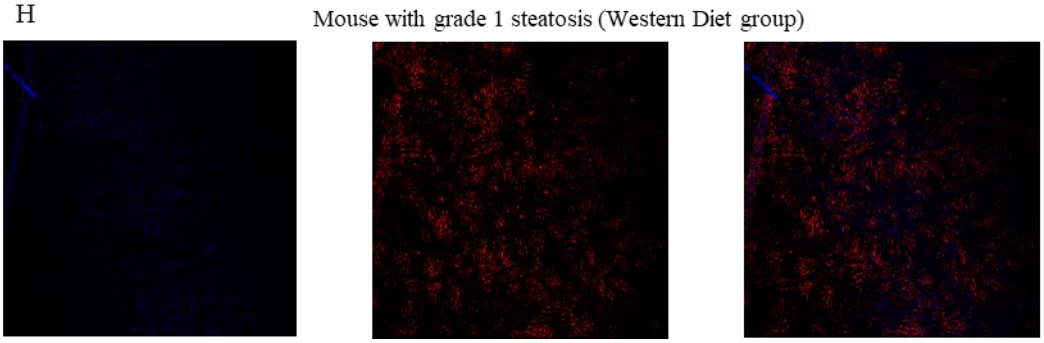

H
Mouse with grade 1 steatosis (Western Diet group)

Fig. 9: Histopathological analysis of the liver of LV treated* Ldlr$^{-/-}$ *mice challenged or not with WD. ***(A)*** *Representative H&E images of liver tissue. Left part of the panel: LV treated* Ldlr$^{-/-}$ *mice. Middle part of the panel:* Ldlr$^{-/-}$ *mice. Right part of the panel: C57 mice. Upper part of the panel: mice subjected to WD challenge; lower part of the panel: mice kept on standard diet throughout the whole experiment.* ***(B)*** *Frequency of liver steatosis in experimental mice.* ***(C)*** *Frequency of specific grade of liver steatosis in experimental mice.* ***(D)*** *Single values and mean with SEM of percentage of tissue area LDLR positive. Images analyzed using MATLAB software* ***(E)*** *Starting and overall* ***(F)*** *LDL-C levels of LV treated mice showing high or low/absent levels of steatosis at the end of experiment.* ***(G-H)*** *Representative images of immunofluorescence analysis of transgene derived mLDLR in the liver of LV treated mice. Nuclei are marked in blue by Hoechst staining, left panels. Immunostaining with anti-mLDLR (red), middle panel. Merged: right panels.*

We confirmed that, to normalize total and LDL cholesterol, liver *Ldlr* expression must be higher in LV treated *Ldlr*$^{-/-}$ mice than in C57 (fig. 9D).

C57 signal was indeed almost undetectable in this experimental setting. We then tried to correlate, in the 6 mice treated with LV and challenged with WD, i) LDL-C circulating amounts, ii) grade of liver steatosis, iii) percentage of LDLR positive area. Interestingly, the mice with less decrease in circulating LDL-C in the first weeks following LV treatment (fig. 9E) were the ones showing slight LDL-C progressive increase throughout the challenge, and higher grade of liver steatosis (fig. 9F). Indeed, we observed an inverse correlation between the grade of steatosis and the transgene positive tissue area (fig. G, H).

All these observations suggest that the higher the number of genetically corrected hepatocytes, the lower the cholesterol capture required by each hepatocyte, the lower the liver steatosis at the time of liver harvest. The fact that the two mice displaying progressive increase in LDL-C were two of the three showing higher grade of steatosis possibly suggests a progressive, stressful, accumulation of cholesterol and potentially triglycerides. The same mice were even the ones showing the lowest tissue positive area. Taken together these data suggest that the highest the liver mass corrected, the lower the work each hepatocyte will have to face, and the best will be its fitness.

3.2.5 Long term efficacy and safety following Ldlr *LV GT in young* Ldlr$^{-/-}$ *mice*

Once assessed the efficacy of this strategy, we set out to assess its safety, as the 4th pillar of an optimal GT (see 1.1). To this aim, we treated 2-week-old mice with mLDLR encoding a.s. LV and followed them long-term, for 1 year post LV (fig. 10A).

We confirmed normalization of total (fig. 10B) and LDL circulating cholesterol (fig. 10C) in treated mice. Normalization was stable and maintained throughout the experiment. At the end of experiment, livers were collected for histopathological analysis, VCN and RNA analysis.

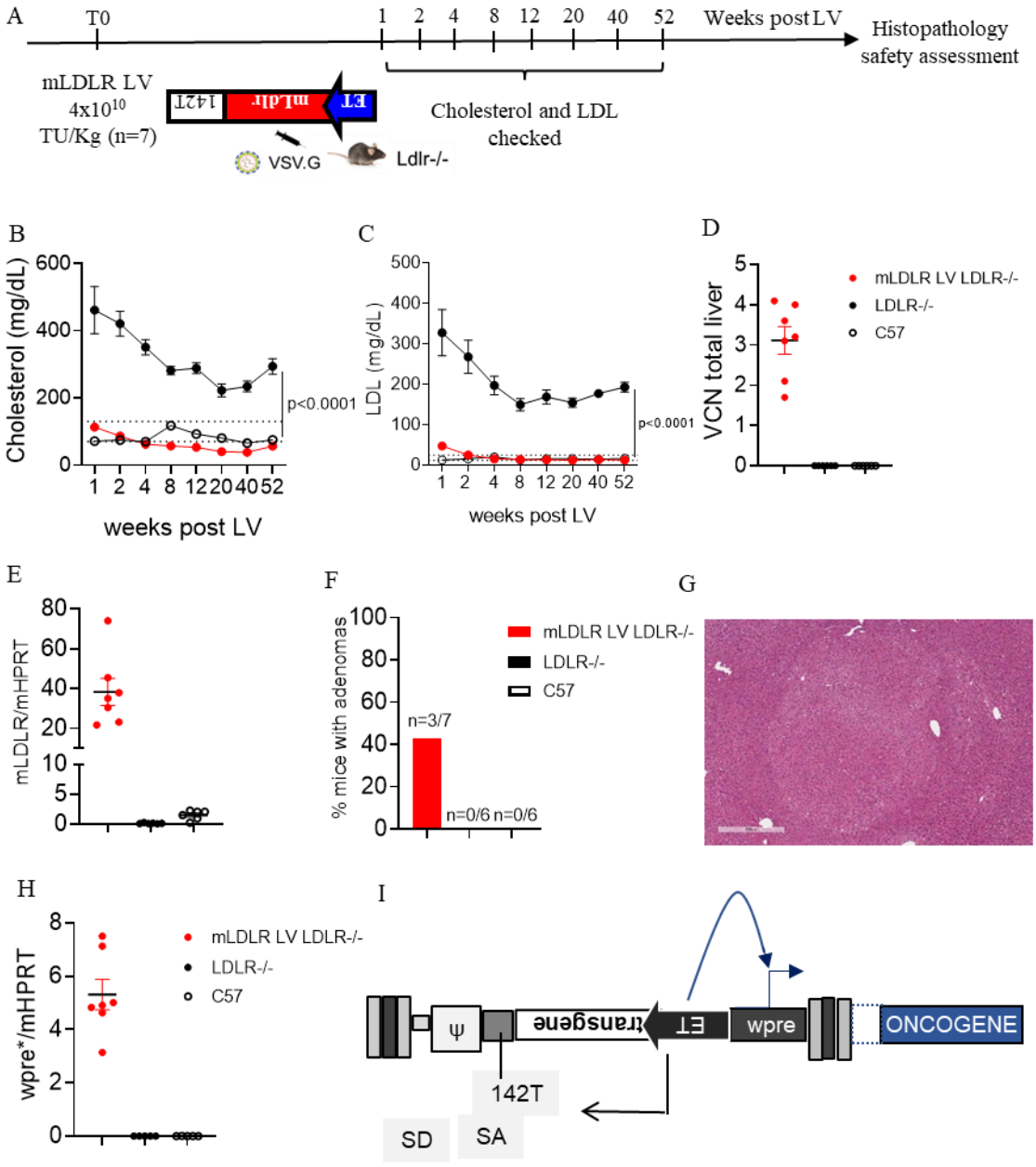


Fig. 10:* mLdlr *gene transfer in young* Ldlr$^{-/-}$ *mice: 1 year follow up. (A) *Experimental design: 2 weeks old mice,* Ldlr$^{-/-}$*, are treated with LV, pseudotyped with VSV.G, encoding mLDLR AS (4*x10^{10}*TU/Kg), monitored overtime for cholesterol and LDL, and sacrificed 1 year post LV. Total (**B**) and LDL (**C**) cholesterol in the serum of experimental mice overtime. Two-way ANOVA with Tukey's multiple comparisons test. (**D**) Single values and mean with SEM of VCN measured in the total liver of experimental mice (**E**) Single values and mean with SEM of expression analysis by quantitative PCR of mLdlr or WPRE (**H**) normalized on the endogenous hprt gene on RNA extracted from the livers of treated mice. (**F**) Frequency of adenomas detected in the experimental mice. (**G**) Representative image of adenoma found in one of mLdlr a.s. LV treated mice. Scale: 500um. (**I**) Schematic representation of LV antisense oriented, used for this set of experiments.*

VCN on total liver showed copies ranging from 1.7 to 4.1 (fig. 10D). *Ldlr* transgene derived RNA confirmed the necessity to express more receptor in comparison to the liver of a C57, to fully normalize circulating LDL. We then performed histopathological analysis.

Unexpectedly, we found microscopic adenomas in 3/7 LV treated mice (fig. 10F, G). Since no adenomas were detected in untreated control mice, it is likely that the new a.s. cassette that we selected to apply LV GT to FH could be the reason for this outcome. *ET* present in our cassette comprises promoter and enhancer sequences, to ensure high level of expression of the downstream transgene. In this novel configuration, *ET* ends up being next to *Wpre** sequence. Interestingly, when we evaluated if transcription was occurring in the opposite direction compared to the transgene (i.e. toward *Wpre**), we found a positive signal when using *Wpre** probe (fig. 10 H). *Wpre** expression was around 7-fold lower, compared to *Ldlr*. *Wpre** signal was around 5-fold higher than *Hprt*, used as normalizer. These data suggest that LV with this kind of configuration are genotoxic in this disease model, thus we had to discard the a.s. cassette as a strategy for liver directed GT for the treatment of FH (fig. 10I).

3.2.6 Expression of LDLR *inhibitor rescues productivity of sense-oriented LV, which fully normalize LDL-C in* Ldlr$^{-/-}$ *mice*

As already mentioned, all previous work from our group used LV with cassettes in sense orientation, showing absence of genotoxicity, with different transgenes and even in

challenging conditions (tumor prone or tumor promoted mice) (Cantore *et al.*, 2015). Since a.s. oriented cassettes showed oncogenicity one year post GT in *Ldlr*$^{-/-}$ mice, we had to reconsider the use of LV with sense-oriented cassette, thus set out to rescue productivity of LV with *LDLR* sense-oriented cassette. As said before, PCSK9 is the natural inhibitor of LDLR, thus we speculated that addition of PCSK9 during LV production may rescue the titer. The assumption was the following: PCSK9 interacts with LDLR, mediating its degradation before its exposure on the membrane of the cells, thus reducing the interaction between LDLR and VSV.G and the re-infection of producer cells by LV released in the supernatant. To avoid PCSK9 accumulation in the supernatant of producer cells and its co-injection together with the LV *in vivo*, we used a non-secreted GOF PCSK9 variant, reported to be responsible for FH (Homer *et al*, 2008). We made a test by transfecting 293T cells with standard LV plasmid mix, with or without the addition of PCSK9 encoding plasmid. We collected LV-containing supernatant. Importantly, infectious titer showed to be 5-fold higher when PCSK9 plasmid was added, both with standard and c.o.LDLR transgene, compared to standard transfection (fig. 11A). Interestingly, by looking at the a.s. oriented LDLR-encoding LV, we observed a detrimental effect of PCSK9 on the infectious titer, which was 4.4-fold lower compared to the titer of LV without PCSK9. In LV encoding LDLR a.s., LDLR is not expressed by producer cells. Thus, the LDLR exposed on the membrane derives exclusively from 293T cells expression, since they need to capture cholesterol for their membranes. In LDLR a.s. LV production, PCSK9 addition might induce over-degradation of LDLR, ultimately leading to insufficient cholesterol uptake by 293T cells and reduced cell viability and capability to produce LV particles. Despite a.s. oriented cassette still gave rise to the highest infectious titer, the addition of PCSK9 to sense-oriented cassettes proved to be a valuable strategy to improve yield of LDLR encoding LV in standard configuration. For the reasons mentioned before, using the murine *Ldlr* sequence would be preferable in the mouse model (Kassim *et al.*, 2013). Thus, we tested if human PCSK9 was able to rescue even the titer of mLDLR-encoding LV. The experiment was designed just like the previous one. We confirmed the increase in infectious titer of hLDLR-encoding LV, and the detrimental effect of PCSK9 addition on LV productions where LDLR is not overexpressed. However, we observed a minimal if any advantage in infectious titer of mLDLR encoding LV, indicating only partial interaction between human GOF PCSK9 and murine LDLR (fig. 11B).

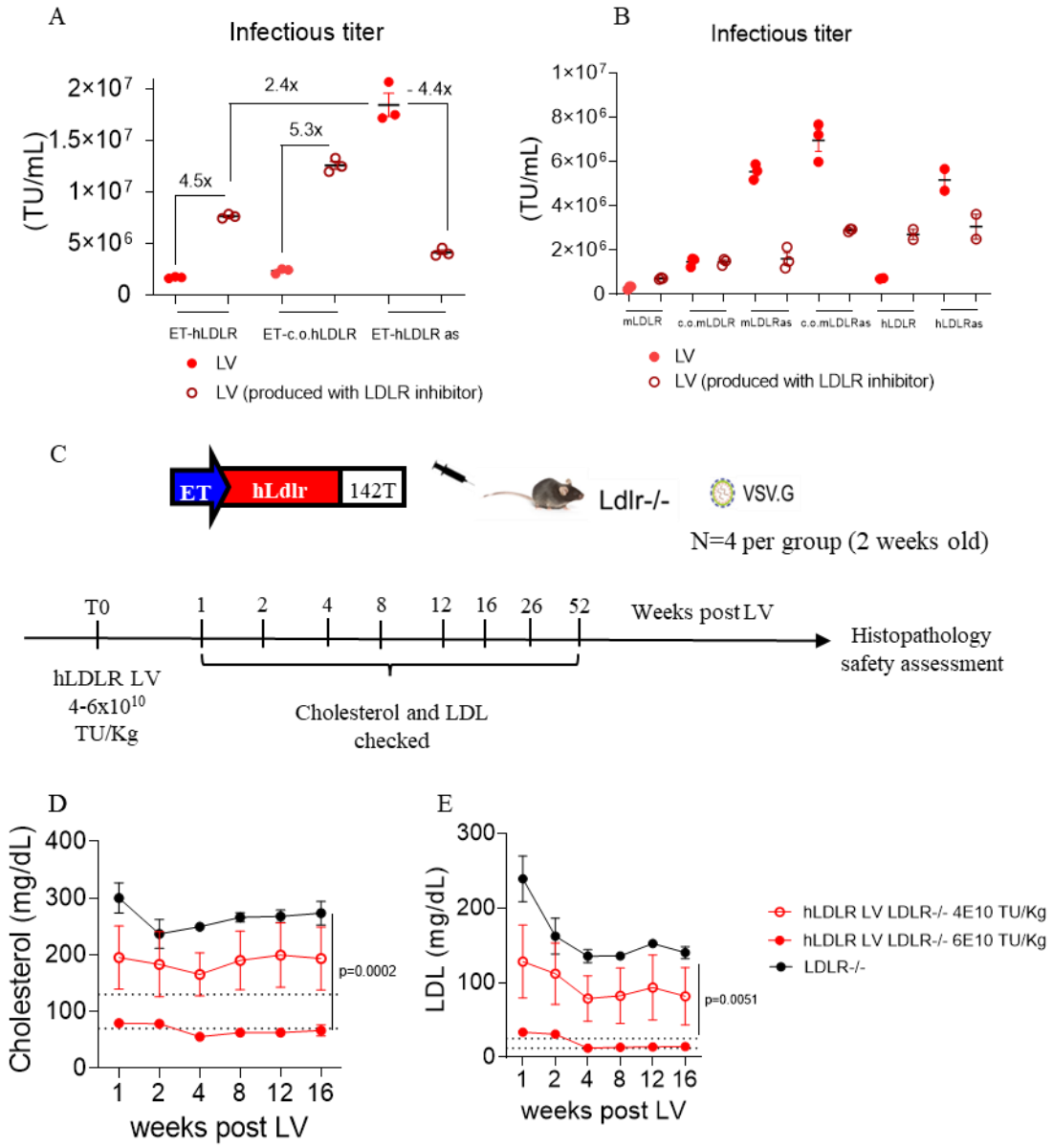


Fig. 11. Expression of LDLR inhibitor rescues productivity of sense-oriented LV, which fully normalize LDL-C in* Ldlr$^{-/-}$ *mice. *(**A**) Single values and mean with SEM of infectious titer of non-concentrated hLDLR LV, produced through transient transfection with (empty red dots) or without (full red dots) the addition of hLDLR non-secreted inhibitor (hPCSK9 S127R). (**B**) Single values and mean with SEM of infectious titer of non-concentrated mLDLR LV, produced through transient transfection with (empty red dots) or without (full red dots) the addition of hLDLR non secreted inhibitor (hPCSK9 S127R). (**C**) Schematic representation of* in vivo *experimental design: hLDLR i.v. injection in juvenile mice (dose: 4-6x10^{10}TU/Kg), followed overtime. (**D**) Total and LDL (**E**) circulating cholesterol in the serum of experimental mice overtime. Two-way ANOVA with Tukey's multiple comparisons test.*

Finally, to show therapeutic effect by treating *Ldlr*$^{-/-}$ mice, we produced *hLDLR* encoding LV, adding PCSK9 in the transfection mix. Since expected interaction between murine LDL and human LDLR is lower compared to mLDLR, we treated 2-week-old mice at therapeutic dose observed with previous experiments using mLDLR, and a higher dose (fig. 11C). Total and LDL cholesterol circulating in the serum were then monitored longitudinally (fig 11D, E). Importantly, all mice at the higher dose showed full normalization of total cholesterol and LDL-C, while mice at the lower dose showed intermediate phenotype. Total cholesterol and LDL-C were stable overtime, until last time point analyzed (4 months post LV).

3.3 Endowing transduced hepatocytes with a selective advantage

As already mentioned in this work and as already shown for FH, increasing the potency of gene transfer is crucial for GT. Lowering the dose required for achieving therapeutic purposes would result in reduction in dose-dependent toxicities and immunogenicity, carrying about the non-trivial consequence of reduction of costs associated with manufacturing. Towards this aim, we tested different strategies, aiming at increasing transgene output *a priori* or *a posteriori* (on-demand). Concerning the latter, in order to increase the amount of genetically modified hepatocytes *a posteriori*, and improve our control on the quantity of transgene product, we set out to endow transduced hepatocytes with a selective advantage over untransduced ones. As already mentioned, we exploited a strategy based on paracetamol metabolism (described in 1.5.4 and in (Vonada *et al.*, 2021). To test this strategy, we used LV cassettes encoding for secreted transgenes, hFIX or hFVIII, to monitor their levels longitudinally.

3.3.1 Selectable LV GT is feasible for HB

We generated "selectable" LV carrying, next to the *hFIX* transgene, a short hairpin RNA (shRNA) against cytochrome *P450 reductase* (*Cypor*). We then treated adult wild-type mice with selectable LV expressing hFIX, modified as above.

Nine mice were injected at two different doses. In the first weeks following GT blood samples were collected to assess their hFIX circulating amounts (fig. 12A). Then, they were split: 5 mice *per* dose were assigned to selection process, 4 mice *per* dose were left

non-selected. From week 5 post GT, mice selected were injected intra-peritoneally (i.p.) with toxic doses of paracetamol.

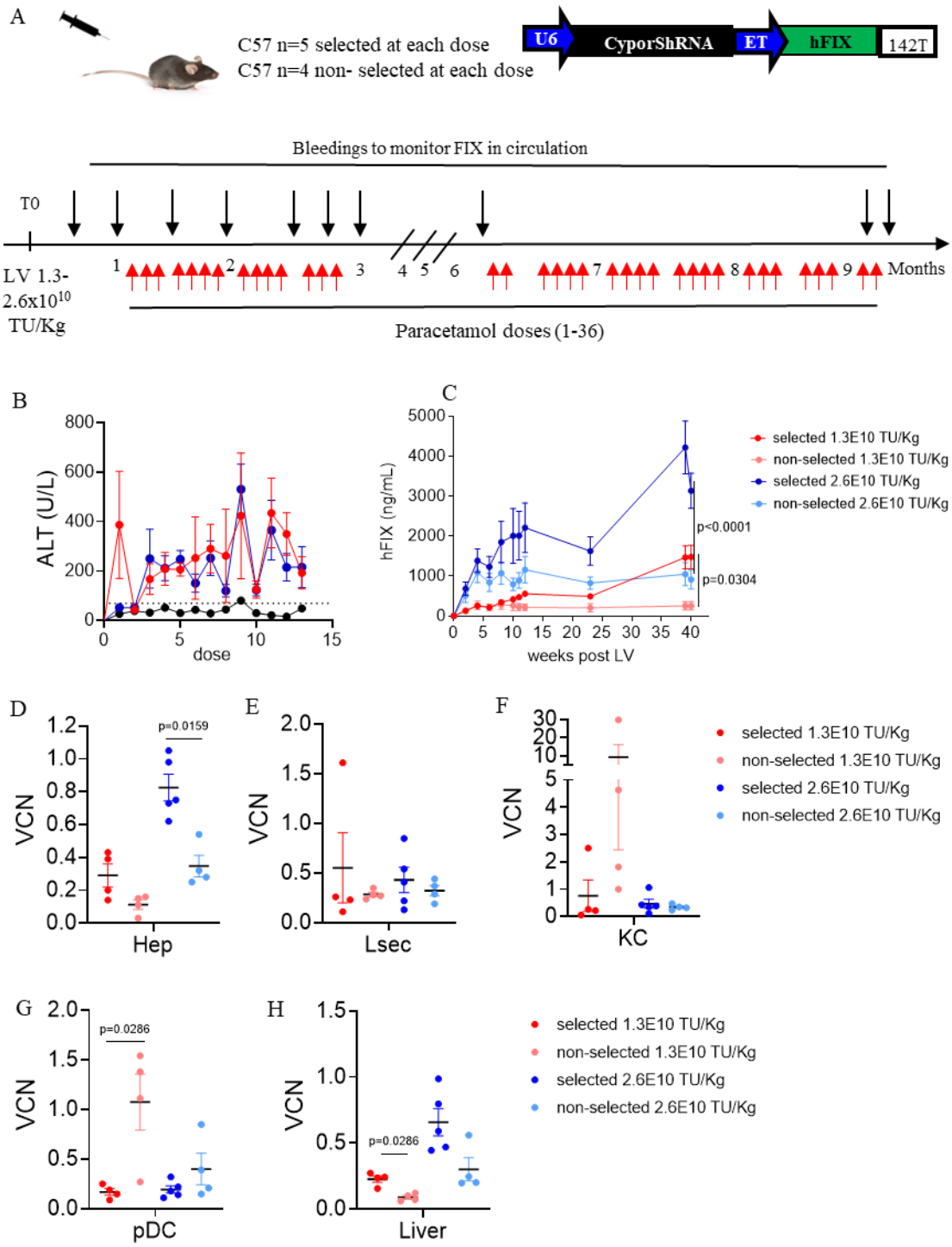


Fig. 12: Paracetamol-mediated selection of LV-transduced hepatocytes using hFIX transgene. *(A) Experimental design: 8-week-old mice were treated with* U6 shCypor-ET hFIX *LV. Once reached transgene plateau, some of them started being selected through i.p. injection*

*of paracetamol. (**B**) Mean with SEM of ALT measured in the serum of experimental mice 6-7 hours after paracetamol injection. (**C**) Mean with SEM of hFIX antigen measured in the plasma of LV treated C57 mice overtime. Two-way ANOVA with Sidak's multiple comparisons test. (**C**) Single values and mean with SEM of VCN measured in fractionated and FACS-sorted liver subpopulations: hepatocytes (**D**), LSEC (**E**), KC (**F**) pDC (**G**), or total liver (**H**) of treated mice, 10 months after LV administration. Mann-Whitney test.*

To confirm liver damage, alanine aminotransferases (ALT) were monitored in the serum of treated mice 6-7 hours after each paracetamol injection (fig. 12B). Selected mice, both in the low LV dose group and in the high LV dose group showed a clear positive selection already after 12 paracetamol doses, as highlighted by increase in hFIX amounts overtime, compared to mice non-selected, showing stable unchanged hFIX amounts (fig. 12C). Selection was then stopped for three months, to monitor hFIX stability over time. It turned out that the hFIX increase due to the selection was maintained overtime. Mice were then subjected to additional 23 paracetamol doses, to assess if selection could be induced again *on demand*. Mice showed an additional increase in circulating hFIX levels (fig. 12C). Ten months post GT, they were euthanized, and liver cell subpopulations sorted. Consistent with increased hFIX output, we found higher LV VCN in sorted hepatocytes and total liver of selected mice, compared to their counterparts left unselected (fig. 12D, H). VCN in the other liver subpopulations were not different, with the exception of pDC in the low dose group (fig. 12E, F, G). Interestingly, mean VCN of sorted hepatocytes of selected mice was 0.3 for low LV dose treated mice and 0.8 for high LV dose treated mice, suggesting approximately 30-80% of transduced hepatocytes, if we assume the vast majority of transduced hepatocytes to carry a single copy of LV. hFIX circulating amounts, in humans, are 5000 ng/mL (defined as 100%). We showed in this experiment that 0.3 Hep VCN corresponded to ~1500 ng/mL (please compare fig. 12C and fig. 12D), 30% of hFIX. In addition, we showed that 0.8 Hep VCN corresponded to ~4000 ng/mL, 80% of hFIX. Based on these data, we can estimate that one copy of *ET.FIX* would lead to hFIX circulating amounts comparable to the ones deriving from 2 copies of endogenous FIX promoter.

3.3.2 Selectable LV GT is feasible for HA

To confirm the feasibility of the strategy for different diseases, we generated "selectable" hFVIII encoding LV carrying, together with hFVIII transgene, a short hairpin RNA (shRNA) against cytochrome P450 reductase (Cypor). We treated newborn HA mice (*F8*$^{-/-}$) with selectable LV expressing hFVIII, modified as above (fig. 13A). Just as before, blood samples were collected to assess their starting hFVIII circulating amounts (fig. 13B).

Then, they were assigned to selection or non-selection group. From week 8 post GT, mice to be selected were injected i.p. with paracetamol. We monitored ALT during selection (fig. 13C). Selected mice showed a clear positive selection, as highlighted by increase in hFVIII levels overtime, compared to mice non-selected, showing stable unchanged hFVIII amounts (fig. 13D), with a 6-fold increase compared to their amounts pre-selection (fig. 13E) and 8-fold increase compared to their un-selected counterparts (fig. 13F). Importantly, in selected mice, hFVIII circulating amounts turned from being sub-therapeutic to therapeutic (>10 ng/mL). At the end of experiment, LV VCN was higher in hepatocytes and total liver of selected compared to unselected mice, reflecting the higher transgene amounts (fig. 13G, H). VCN in the other liver subpopulations was not different (fig. 13I, J, K). Interestingly, mean VCN of sorted hepatocytes of selected mice was ~0.5, suggesting approximately 50% of transduced hepatocytes, if we assume most of the transduced hepatocytes to carry a single copy of LV. hFVIII amounts, in humans are 100 ng/mL (defined as 100%), We showed in this experiment that 0.5 Hep VCN corresponded to ~25 ng/mL, the 25% of hFVIII (please compare fig. 13D and G). Based on these data, we can estimate that one copy of ET.hFVIII (non-codon optimized) would lead to hFVIII circulating amounts comparable to the ones deriving from 1 copy of endogenous FVIII promoter. Thus, the VCN required to achieve 100% of FVIII would be 2 copies *per* hepatocyte. Overall these data confirm and expand the previously reported paracetamol as a valuable strategy for achieving positive selection of transduced hepatocytes. This goal was reached with two different mouse models (C57 and HemoA mice) treated at different age (as adults or as neonates). Importantly, the positive selection of corrected hepatocytes was detected at molecular level, with a VCN higher in the liver and sorted hepatocytes of selected mice, compared to non-selected counterparts.

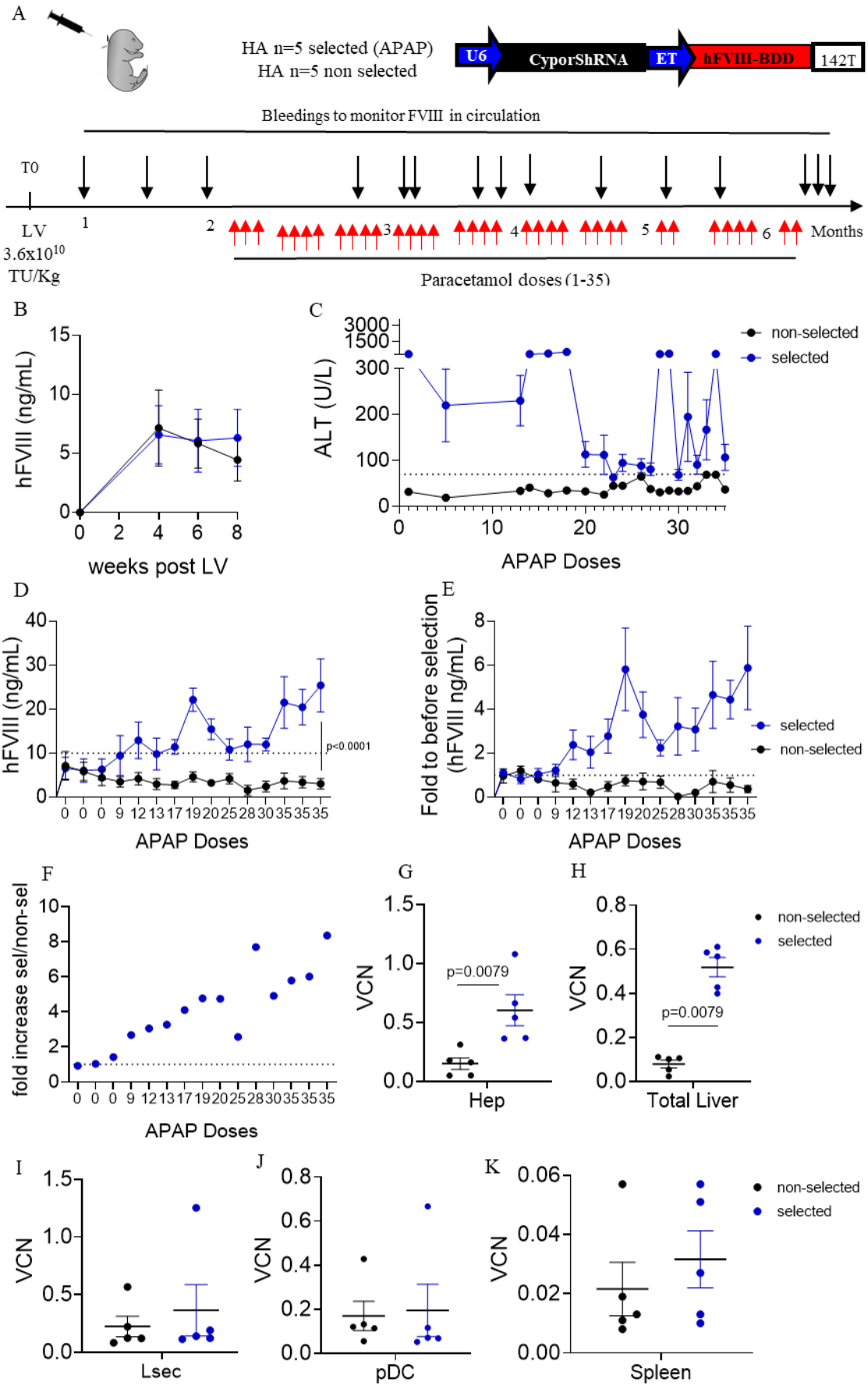

A
HA n=5 selected (APAP)
HA n=5 non selected
U6
CyporShRNA
ET
hFVIII-BDD
142T
Bleedings to monitor FVIII in circulation
T0
LV
3.6x10^10
TU/Kg
1
2
3
4
5
6
Months
Paracetamol doses (1-35)
B
hFVIII (ng/mL)
weeks post LV
C
ALT (U/L)
non-selected
selected
APAP Doses
D
hFVIII (ng/mL)
p<0.0001
APAP Doses
E
Fold to before selection (hFVIII ng/mL)
selected
non-selected
APAP Doses
F
fold increase sel/non-sel
APAP Doses
G
VCN
p=0.0079
Hep
H
VCN
p=0.0079
Total Liver
non-selected
selected
I
VCN
Lsec
J
VCN
pDC
K
VCN
Spleen
non-selected
selected

Fig. 13: Paracetamol-mediated selection of LV-transduced hepatocytes using* hFVIII *transgene. *(**A**) Experimental design: 2-days-old* f8$^{-/-}$ *mice were treated with* U6 shCypor-ET hFVIII *LV. Once reached transgene plateau, some of them started being selected through i.p. injections of paracetamol. (**B**) Mean and SEM of hFVIII measured in the plasma of experimental mice during the first weeks post LV. (**C**) Mean with SEM of ALT measured in the serum of experimental mice 6-7 hours after paracetamol injection. (**D**) Mean with SEM of hFVIII antigen measured in the plasma of LV treated HA mice overtime. Two-way ANOVA with Sidak's multiple comparisons test. (**E**) Single values and mean with SEM of fold of increase in hFVIII amounts after starting the selection protocol, compared to values pre-selection. (**F**) Fold increase of selected mice, on non-selected ones overtime, during selection process. Single values and mean with SEM of VCN measured in fractionated and FACS-sorted liver subpopulations: hep (**G**), LSEC (**H**), pDC (**I**), total liver (**J**) or spleen (**K**) of treated mice, 7 months after LV administration. Mann-Whitney test.*

3.3.3 Selectable LV GT is feasible at different ages but stably impairs CYP450 activity

We treated neonatal C57 mice with LV expressing hFIX, modified as before to become selectable. Eight mice were injected at two different doses (fig. 14A). Again, in the first weeks following GT, blood samples were collected to assess their hFIX circulating amounts (fig. 14B). Then, mice were split in 2 groups: 4 mice *per* dose were assigned to selection process, 4 mice *per* dose were left non-selected. From week 12 post GT, mice to be selected were injected i.p. with paracetamol. We monitored ALT during selection (fig. 14C). Since starting hFIX level were already high, indicating a large initial mass of transduced liver, increase in hFIX amounts were more modest than seen with previous experiments (fig.14D). As said before (see 1.5.4), following selection, corrected hepatocytes are expanded, especially/exclusively in zone 3 (the pericentral zone), where CYP450 enzymes are expressed at highest extent. Cypor downregulation in corrected hepatocytes could imply that the activity of all CYP450 may be impaired. Indeed, pericentral-enriched-corrected hepatocytes would stably downregulate Cypor, the redox obliged partner of all microsomal P450. To test if this was happening, 1 year after LV administration, we injected caffeine in the experimental mice and monitored its reduction following conversion in its metabolites, as a read out of CYP450 residual activity. Caffeine metabolism requires activity of several CYP450, which convert caffeine in theobromine, paraxanthine and theophylline (Nehlig, 2018).

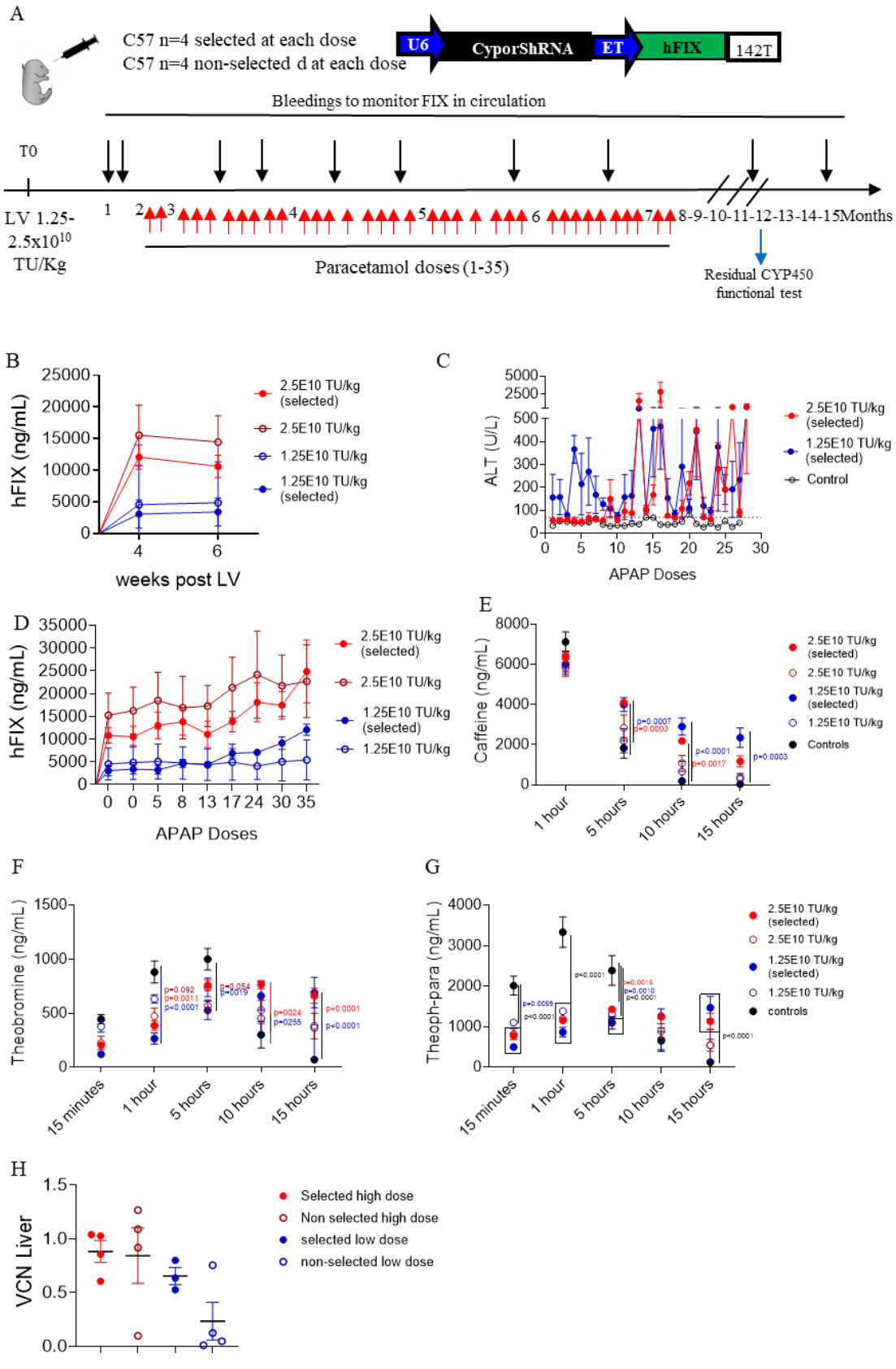

A
C57 n=4 selected at each dose
C57 n=4 non-selected d at each dose
U6
CyporShRNA
ET
hFIX
142T
Bleedings to monitor FIX in circulation
T0
LV 1.25-2.5x10^10 TU/Kg
1 2 3 4 5 6 7 8-9-10-11-12-13-14-15Months
Paracetamol doses (1-35)
Residual CYP450 functional test
B
hFIX (ng/mL)
weeks post LV
2.5E10 TU/kg (selected)
2.5E10 TU/kg
1.25E10 TU/kg
1.25E10 TU/kg (selected)
C
ALT (U/L)
APAP Doses
2.5E10 TU/kg (selected)
1.25E10 TU/kg (selected)
Control
D
hFIX (ng/mL)
APAP Doses
2.5E10 TU/kg (selected)
2.5E10 TU/kg
1.25E10 TU/kg (selected)
1.25E10 TU/kg
E
Caffeine (ng/mL)
1 hour
5 hours
10 hours
15 hours
2.5E10 TU/kg (selected)
2.5E10 TU/kg
1.25E10 TU/kg (selected)
1.25E10 TU/kg
Controls
F
Theobromine (ng/mL)
15 minutes
1 hour
5 hours
10 hours
15 hours
G
Theoph-para (ng/mL)
15 minutes
1 hour
5 hours
10 hours
15 hours
2.5E10 TU/kg (selected)
2.5E10 TU/kg
1.25E10 TU/kg (selected)
1.25E10 TU/kg
controls
H
VCN Liver
Selected high dose
Non selected high dose
selected low dose
non-selected low dose

Fig. 14: Paracetamol-mediated selection of LV-transduced hepatocytes in neonatal mice and evaluation of CYP450 functionality. *(**A**) Experimental design: 2-days-old mice were treated with* U6 shCypor-ET hFIX *LV. Once reached transgene plateau, some of them started being selected through i.p. injection of paracetamol. (**B**) Mean and SEM of hFIX measured in the plasma of experimental mice during the first weeks post LV. (**C**) Mean with SEM of ALT measured in the serum of experimental mice 6-7 hours after paracetamol injection. (**D**) Mean with SEM of hFIX antigen measured in the plasma of LV treated C57 mice overtime. Caffeine (**E**), theobromine (**F**), theophylline-paraxanthine (**G**) amounts in the circulation of selected, non-selected and untreated mice, following i.p. injection of 1mg/kg of caffeine, 1 year post LV. Two-way ANOVA with Dunnett's multiple comparisons test vs controls. (**H**) Single values and mean with SEM of VCN measured in the total liver of experimental mice, 1.3-year post LV. Mann-Whitney test.*

Their conversion in subsequent metabolites once again requires, among others, the activity of CYP450. Experimental mice were injected with caffeine (1mg/kg) then the rate of caffeine clearance was monitored. While untreated mice showed rapid decline in circulating caffeine amounts, almost undetectable 10 hours after the injection, selected mice showed a clear reduction in caffeine conversion, with the low-dose-selected-mice being the ones with the highest caffeine amounts throughout the assay. Since this group was the one showing highest selection occurring, this is in line with increased replacement of pericentral hepatocytes with corrected-CYP450 impaired LV positive hepatocytes (fig.14E). By looking at caffeine metabolism, theobromine and paraxanthine-theophylline, the trend was confirmed. Indeed, untreated mice showed progressive increase in metabolites amounts (peaking at 1-5 hours), followed by a decline and being almost undetectable 15 hours post injection. In contrast, experimental mice showed delay in metabolites formation and conversion, with selected mice being the most impaired in this metabolism (low-dose-selected-mice still did not even reach the peak of metabolites concentration 15 hours after the injection) (fig. 14F, G). At 1.3 years after LV injection mice were euthanized and VCN was measured (fig. 14H).

The same experimental design was applied to 2-week-old mice, to confirm feasibility of this strategy at this different age (fig. 15A). Again, mice were monitored during the first weeks post GT (fig. 15B), then they were split and selection started. We monitored ALT during selection (fig. 15C) and hFIX increase following paracetamol injections (fig. 15D). Even in this case, the starting hFIX circulating amounts were quite high, and the selection modest.

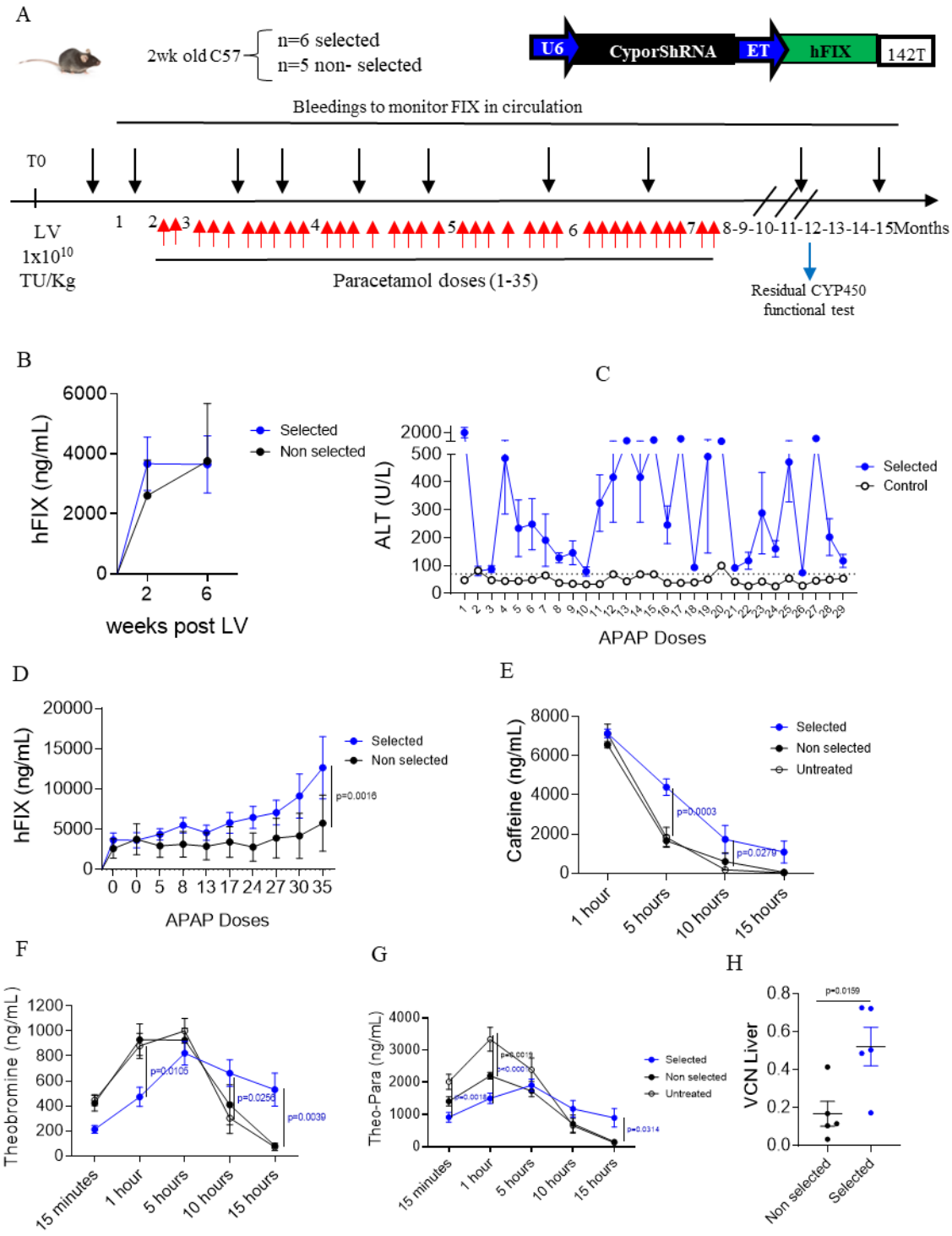


Fig. 15: Paracetamol-mediated selection of LV-transduced hepatocytes in juvenile mice and evaluation of CYP450 functionality. *(**A**) Experimental design: 2-weeks-old mice were treated with* U6 shCypor-ET hFIX *LV. Once reached transgene plateau, some of them started being selected through i.p. injection of paracetamol. (**B**) Mean and SEM of hFIX measured in the plasma of experimental mice during the first weeks post LV. (**C**) Mean with SEM of ALT measured*

*in the serum of experimental mice 6-7 hours after paracetamol injection. (**D**) Mean with SEM of hFIX antigen measured in the plasma of LV treated C57 mice overtime. Caffeine (**E**), theobromine (**F**), theophylline-paraxanthine (**G**) amounts in the circulation of selected, non-selected and untreated mice, following i.p. injection of 1mg/kg of caffeine, 1 year post LV. Same controls as for caffeine assay reported in figure 14, since all the animals were injected with caffeine the same day. Two-way ANOVA with Dunnett's multiple comparisons test vs controls. (**H**) Single values and mean with SEM of VCN measured in the total liver of experimental mice, 1.3-year post LV. Mann-Whitney test.*

One year post GT, experimental mice were injected with caffeine (1mg/kg) and bled in the following hours, to monitor caffeine rate of clearance. We confirmed the reduced CYP450 activity of "selectable LV" treated mice. Indeed, caffeine rate of clearance was slower in selected mice (fig. 15E), just like it was slower the appearance and elimination of its metabolites theobromine (fig. 15F) and paraxanthine-theophylline (fig. 15G). When mice were euthanized, VCN of total liver was higher in selected mice compared to non-selected (fig. 15H).

3.3.4 Selectable LV GT allows for >50-fold increase in transgene output, when starting from very low transgene amounts

Selection of transduced hepatocytes is a strategy inducing, by definition, clonal expansions. Indeed, the integrations due to the initial gene transfer would be progressively enriched. What remain to be determined is the nature of those integrations. If the expansion of one integration at the expense of another is by chance, if it is promoted by the localization of the hepatocyte carrying that integration or if specific LV integrations induce in those hepatocytes a proliferative advantage. Thus, to assess the safety of this strategy, we wanted to make an integration site analysis. We treated three groups with selectable LV hFIX: one group at a dose and two groups at 5-fold lower dose. Then, one of the two groups at the lower dose started being selected (fig.16A). Mice were monitored during the first weeks post GT (fig. 16B), then they were split, and selection started. We monitored ALT during selection (fig. 16C) and hFIX increase following paracetamol injections (fig. 16D). As suggested before, the lower the starting LV dose, the lower the initial liver gene transfer, the higher the selection following paracetamol injection. Indeed, in this experiment, up to 50-fold increase in hFIX circulating amounts were

obtained. This was not due to the higher number of paracetamol doses (70 against 35-36 of the previous experiments). Indeed, just a few mice received that number of doses: mice kept to be selected just until their hFIX amounts were comparable to the ones observed in the mice treated at the 5-fold higher dose (fig. 16E).

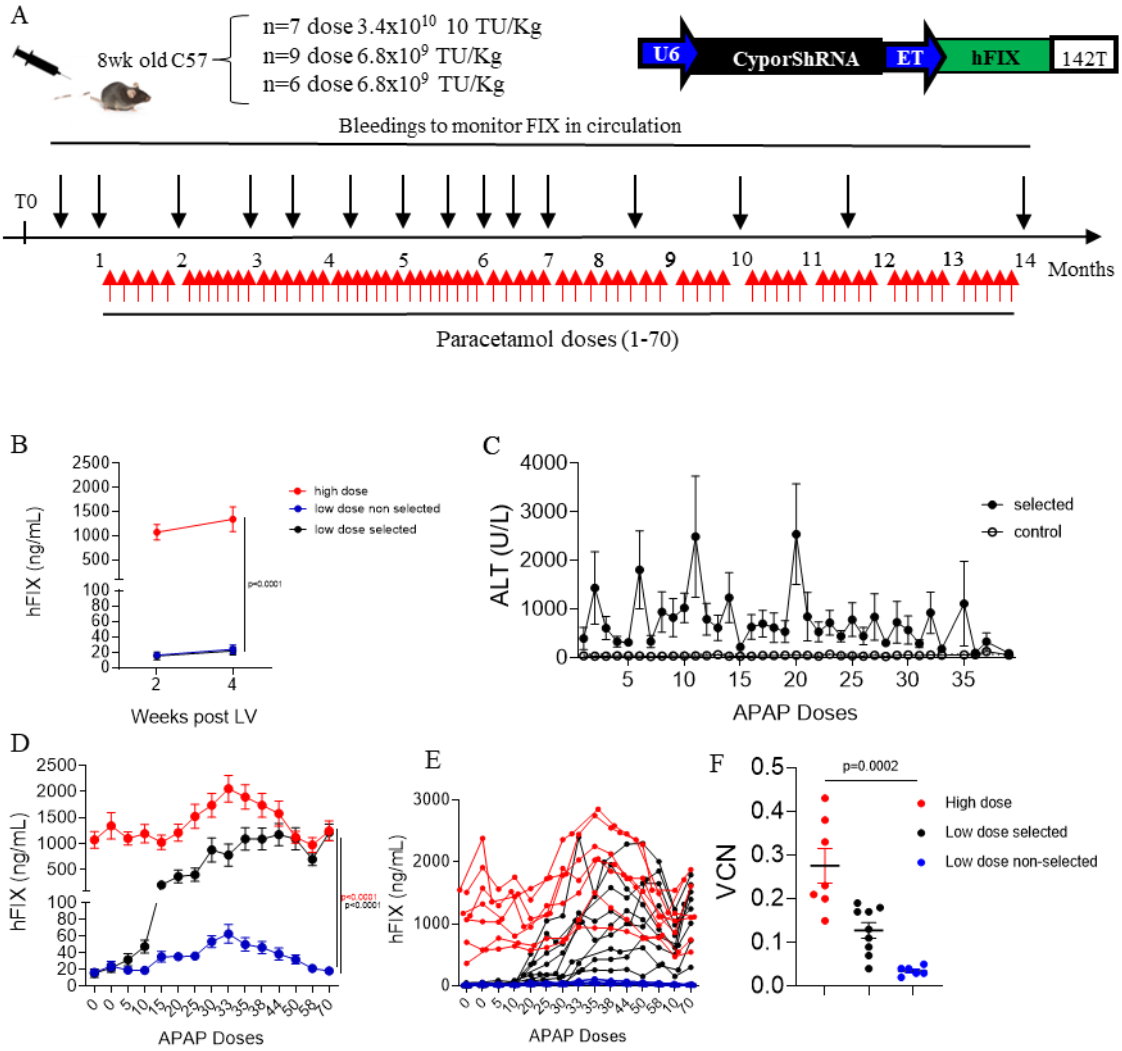


Fig. 16: Paracetamol-mediated selection of LV-transduced hepatocytes is most effective when starting from very low transgene amounts. *(**A**) Experimental design: 8 weeks-old mice were treated with* U6 shCypor-ET hFIX *LV. Once reached transgene plateau, some of them started being selected through i.p. injection of paracetamol. (**B**) Mean and SEM of hFIX measured in the plasma of experimental mice during the first weeks post LV. (**C**) Mean with SEM of ALT measured in the serum of experimental mice 6-7 hours after paracetamol injection. (**D**) Mean with SEM of hFIX antigen measured in the plasma of LV treated C57 mice overtime. Two-way ANOVA with Tukey's multiple comparisons test. (**E**) Single values and mean with SEM of VCN measured in the total liver of experimental mice, 1.3-year post LV. Kruskal-Wallis test with Dunn's multiple comparisons test.*

Concerning variability, however, it was challenging to obtain for all the mice a precise ultimate hFIX value. Indeed, despite the high number of doses of paracetamol administered, some mice did not escalate like the others (fig. 16E). VCN on total liver confirmed higher values in the mice treated a starting higher dose, compared to the mice non selected treated at the lower dose. Mice selected showed intermediate VCN. Despite the same mean of circulating hFIX in group treated at high dose and group selected, the difference in VCN was probably due to the nPC contribution to the VCN of high dose treated group (fig. 16F).

Selection of corrected hepatocytes *a posteriori* through paracetamol administration is an intriguing concept, despite some remaining concerns as further discussed below (see 4.5).

3.4 Transduction enhancers: targeting anti-viral pathways

As highlighted above , increasing the potency of hepatocytes gene transfer following *in vivo* GT would be crucial, to i) reduce the doses to be administered and to ii) face liver diseases where majority of liver mass must be corrected for therapeutic purposes (see also 1.5).

With the purpose of finding safe and promising enhancer of transduction, we focused on anti-viral pathways, possibly responsible for reduced efficiency of entry, retro-transcription, integration of LV.

Bortezomib is a proteasome inhibitor with anti-inflammatory properties. It may decrease KC activation and improve transduction in specific cell types (see also 1.5.2).

MarI is a mAb against IFNARI. Since this signal is crucial for the activation of innate immune response, its administration before LV administration might increase gene transfer potency by reducing viral sensing (see also 1.5.1).

3.4.1 MarI and Bortezomib as single treatments increase LV gene transfer potency

To test these two compounds, we used a transgene applied to a disease for which LV dose reduction would be important: HA. Indeed, we used hFVIII as transgene, since it gives the double advantage of i) making possible longitudinal measurements and ii) representing a challenging transgene for GT, since its sequence is particularly long, LV

carrying its sequence display quite low infectious titers and high doses are requested to achieve phenotypic correction (Milani *et al.*, 2022).

However, hFVIII is highly immunogenic. Thus, experiments were performed using or Alb-F8*R593C mice. Alb-F8*R593C lack murine FVIII but express a human version of hFVIII with missense mutation, resulting in hemophilia. The protein is translated, but non secreted and not functional (0% activity). Since however it is translated, immune system is reported to be tolerant towards exogenously delivered functional hFVIII (Bril *et al*, 2006).

We injected adult Alb-F8*R593C mice i.v. with Bortezomib (1mg/kg) or saline one-hour before c.o.hFVIII-BDD LV administration (fig. 17A). We then compared the circulating secreted hFVIII amounts in mice pre-treated with Bortezomib with those of mice treated at the same LV dose but without Bortezomib pre-treatment.

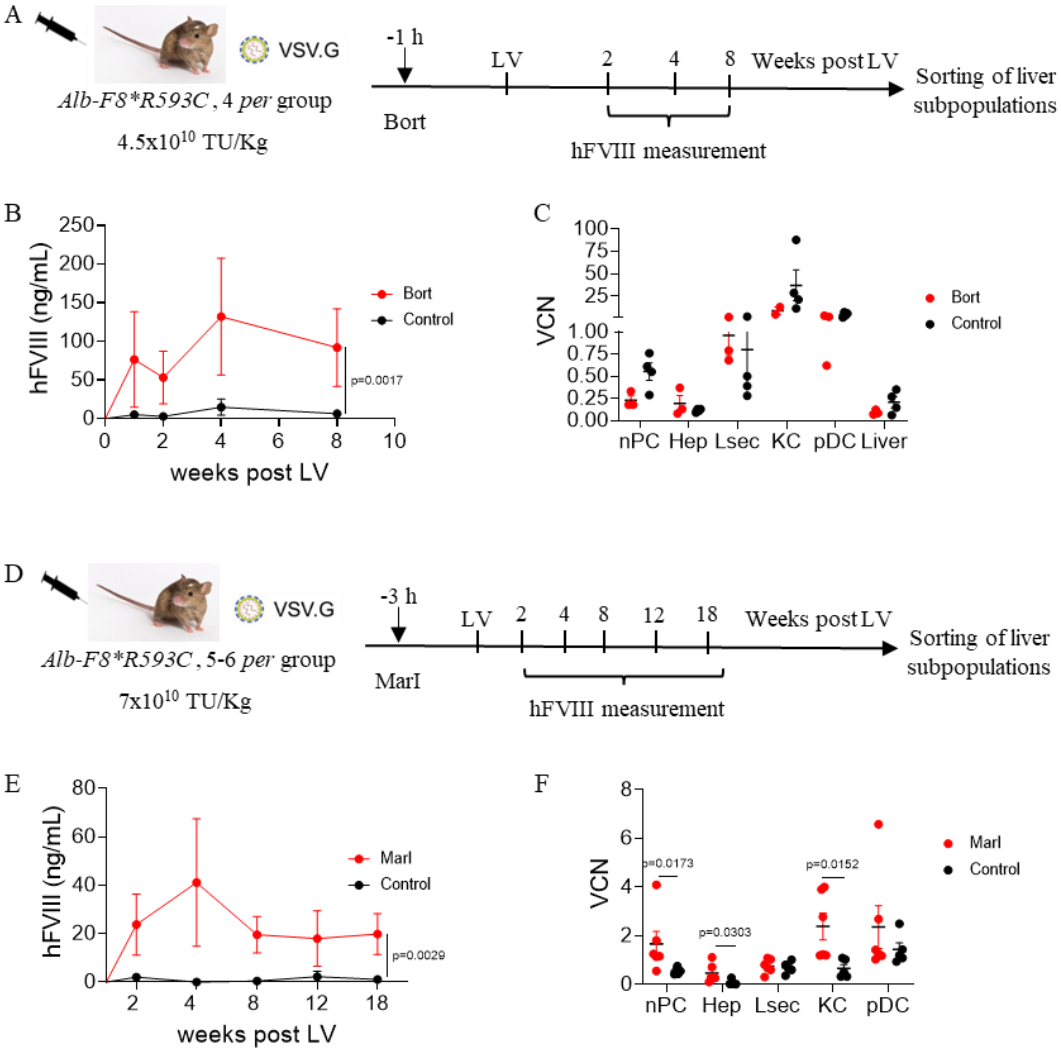


Fig. 17: Bortezomib and MarI, as single treatments, enhance LV GT potency *(**A**) Experimental design: 8 weeks old Alb-F8*R593C mice are injected i.v. with Bortezomib (1mg/kg) or saline 1 hour before receiving c.o.*hFVIII *LV i.v., dose: $4.5x10^{10}$. Then, hFVIII is monitored in treated mice longitudinally. (**B**) Mean with SEM of hFVIII antigen measured in the plasma of LV treated mice overtime (n=4* per *each group). Two-way ANOVA. (**C**) Single values and mean with SEM of VCN measured in fractioned and FACS-sorted liver subpopulations: nPC, Hep, LSEC, KC, pDC of experimental mice, total liver of experimental mice, pre-treated with MarI (red dots) or with saline (controls, black dots), 3 months post LV. Mann-Whitney test. (**D**) Experimental design: 8 weeks old Alb-F8*R593C mice are injected i.v. with MarI (1mg/mouse) or saline 3 hour before receiving c.o.*hFVIII *LV i.v., dose: $7x10^{10}$. Then, hFVIII is monitored in treated mice longitudinally. (**E**) Mean with SEM of hFVIII antigen measured in the plasma of LV treated mice overtime (n=5-6* per *each group). Two-way ANOVA. (**F**) Single values and mean with SEM of VCN measured in fractioned and FACS-sorted liver subpopulations: nPC, Hep, LSEC, KC, pDC of experimental mice, pre-treated with MarI (red dots) or with saline (controls, black dots), 5 months post LV. Mann-Whitney test.*

Mice pre-treated with Bortezomib showed higher circulating hFVIII amounts, compared to the group receiving exclusively LV. The advantage was maintained throughout the experiment (fig. 17B). We then compared the VCN in total liver, and sorted liver cell subpopulations detected in Bortezomib pre-treated mice with the ones detected in mice injected with the same LV dose but without Bortezomib pretreatment (fig. 17C).

We observed a trend of decrease in VCN of KC and pDC of Bortezomib pre-treated mice, possibly indicating reduced capture of LV by phagocytes or toxicity in those cells. However, no increase was observed in sorted hepatocytes.

We then moved to MarI. We injected adult Alb-F8*R593C mice with MarI (1mg/mouse) or saline 3 hours prior LV co.*hFVIII*-BDD administration (fig.17D). We compared the circulating secreted hFVIII amounts in mice pre-treated with MarI with the ones circulating in mice treated at the same dose of LV without pre-treatment with MarI. hFVIII circulating amounts were higher in MarI pre-treated mice, throughout the experiment (fig. 17E). We then compared the VCN in total liver, and sorted liver cell subpopulations detected in MarI pre-treated mice with the ones detected in mice injected with the same LV dose (fig. 17F). We detected higher VCN in sorted hepatocytes,

showing improvement of transduction and reflecting the higher hFVIII transgene output trend throughout the experiment.

3.4.2 Lack of additive/synergistic effect in enhancing LV gene transfer of MarI and Bortezomib

Given the increased transgene output and transduction efficiency observed with the FVIII transgene, we decided to test MarI and Bortezomib in combination, to evaluate if the administration of both prior LV could enhance the potency of liver gene transfer more than the two treatments tested separately. Adult mice were injected either with MarI three hours before, with Bortezomib one hour before or with the combination of the two before injection of LV. Blood samples were then collected overtime to assess hFIX circulating amounts (fig. 18A).

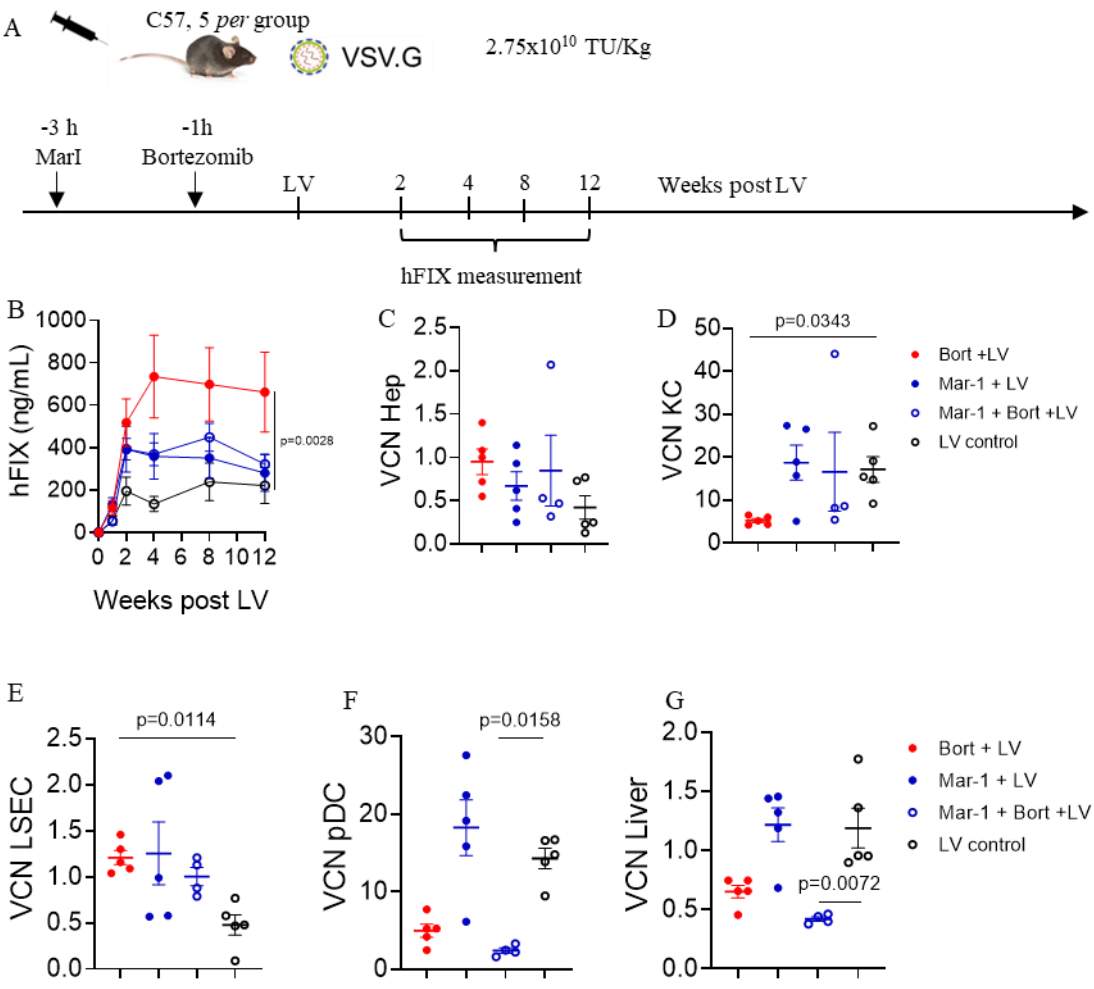


Fig. 18: MarI and Bortezomib used in combination fail to give additional advantage in LV gene transfer. *(**A**) Experimental design: 8 weeks old mice are injected or not with MarI 3 hours before and/or Bortezomib 1 hour before receiving hFIX-IRES-GFP LV i.v. Then, hFIX is monitored in treated mice longitudinally. (**B**) Mean with SEM of hFIX antigen measured in the plasma of LV treated mice overtime (n=5* per *each group). Two-way ANOVA with Dunnett's multiple comparisons test vs control. Single values and mean with SEM of VCN measured in fractionated and FACS-sorted liver subpopulations: hepatocytes (**C**), KC (**D**) LSEC (**E**), pDC (**F**) and total liver (**G**) of treated mice, 3 months after LV administration. Kruskal-Wallis test with Dunn's multiple comparisons test over controls.*

We confirmed hFIX amounts of Bortezomib pre-treated mice to be higher than controls. However, while we observed a trend of increase in the MarI treated group, the advantage appeared to be less prominent. Importantly, the combination of the two treatments before LV administration did not give any additional advantage, suggesting that Bortezomib could have an effect even on reducing IFN signal, thus explaining its higher beneficial effect on GT, compared to MarI, and the lack of additive/synergistic effect when used in combination.

We then sorted the liver cell subpopulations. Bortezomib pre-treated mice showed a skewing in LV subpopulation targeting, with a reduced VCN in KC (fig. 18D) and pDC (fig. 18F), a trend of increase in hepatocytes (fig. 18C) and an increase in LSEC (fig.18E).

3.5 Transduction enhancers: fasting

Fasting was reported as a procedure leading to higher transgene output, following AAV GT (Hosel *et al.*, 2017; Moulay *et al*, 2010), possibly due to the activation of autophagy (see also1.5.3). Despite the differences existing between AAV and LV, we decided to test this procedure in the context of *in vivo* liver-directed LV GT.

3.5.1 Fasting increases LV gene transfer to hepatocytes in vivo

To test if fasting had an impact on LV transduction, we fasted C57 mice for 24 hours. Since we were expecting the fasted mice to weigh less than their non-fasted counterparts at the time of LV administration, we decided to include in the experiment three groups of mice: i) 8 weeks old mice fasted for 24 hours, ii) 8 weeks old mice non-fasted, iii) 6 weeks old mice (weighting less than the others), non-fasted.

Then, they were injected i.v. with LV expressing hFIX. Blood samples were collected overtime to monitor hFIX circulating amounts (fig. 19A). Fasted mice were the ones with highest weights, one day before LV administration, while their weight was comparable to 6 weeks old mice at the time of LV administration (fig. 19B). Importantly, we observed circulating hFIX amounts to be higher in fasted mice, throughout the experiment (last timepoint: 3 months post LV), compared to both control groups, 6 and 8-weeks-old non-fasted mice (fig. 19C). At end of experiment, however, VCN in sorted hepatocytes was similar in fasted and non-fasted mice. Please note, however, that, considering the very high VCN in KC (around 30), even a 1% contamination of KC in hepatocytes may possibly mask changes in VCN of hepatocytes (fig. 19D). To assess if biodistribution might be different in fasted mice, we assessed VCN in other organs and found it to be comparable to control mice (fig. 19E).

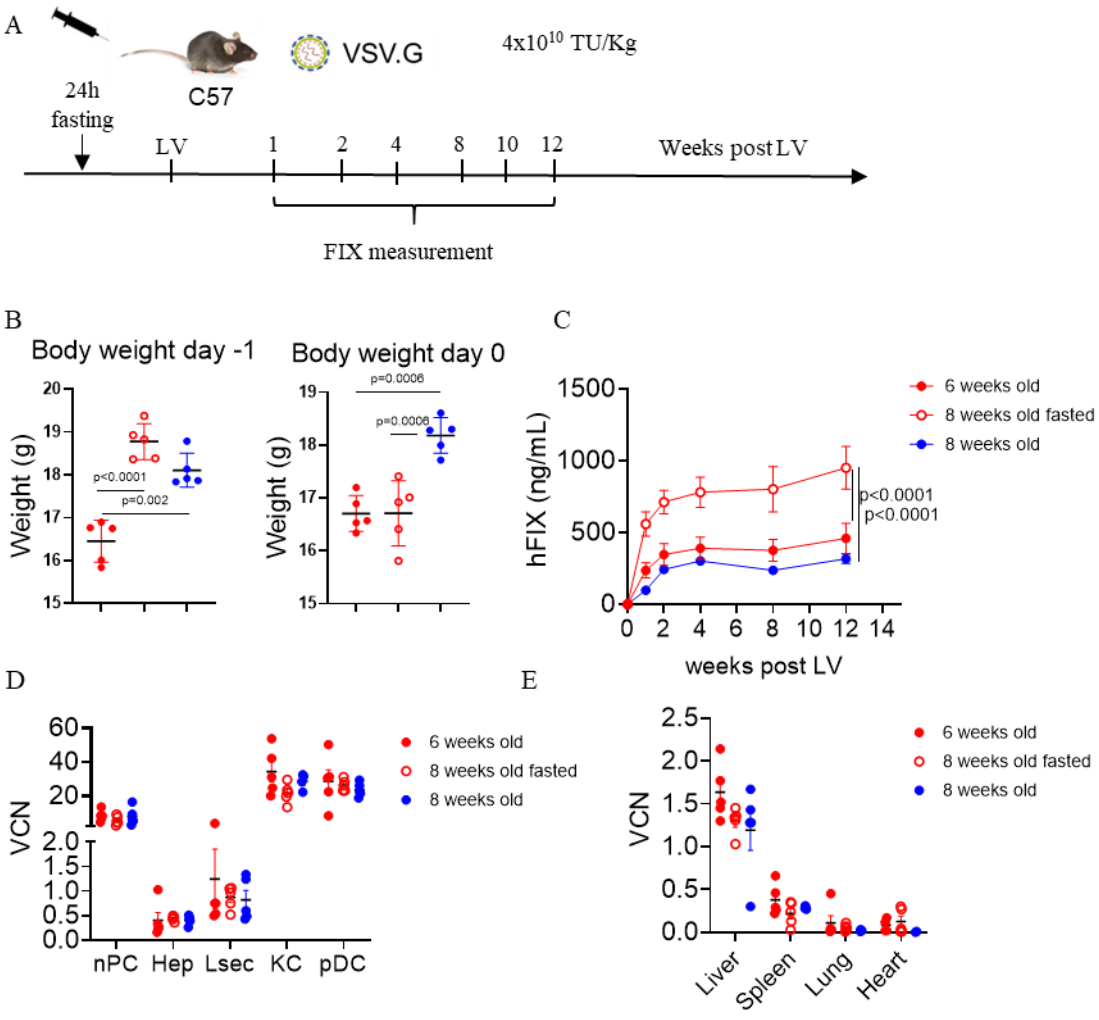


Fig. 19: Fasting increase LV gene transfer, independently on body weight: *(**A**) Experimental design: 8 weeks old mice are fasted 24 hours. Then, they are injected i.v. with* hFIX *LV, together with 8 weeks old mice non-fasted and 6 weeks old mice non-fasted and their circulating hFIX are monitored longitudinally. (**B**) Mice weight 24 hours prior LV injection and at the time of LV injection. (**C**) Mean with SEM of hFIX antigen measured in the plasma of LV treated mice overtime (n=5* per *each group). Two-way ANOVA with Tukey's multiple comparisons test. (**D**) Single values and mean with SEM of VCN measured in the annotated organs. (**E**) Single values and mean with SEM of VCN measured in FACS-sorted nPC, hepatocytes, LSEC, KC, pDC. Kruskal-Wallis test with Dunn's multiple comparisons test.*

To visualize a possible higher transgene positive area in fasted mice, we then injected i.v. C57 mice with a LV encoding hFIX-IRES-GFP.

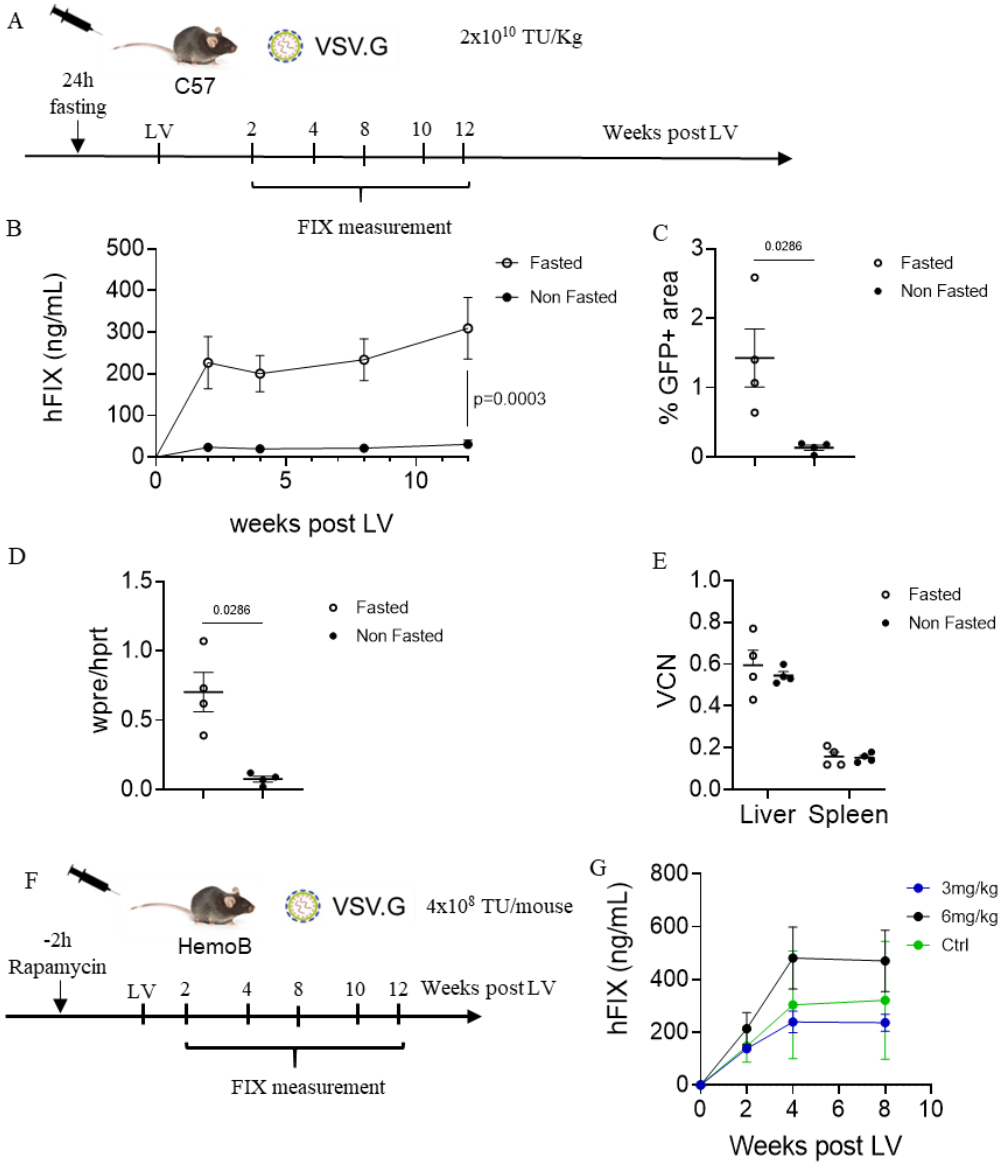


Fig. 20: Fasting-mediated increase in LV gene transfer is unrelated to autophagy *(**A**) Experimental design: 8 weeks old mice are fasted 24 hours. Then, they are injected i.v. with hFIX-IRES-GFP LV, together with 8 weeks old mice non-fasted. Their circulating hFIX are monitored longitudinally. (**B**) Mean with SEM of hFIX antigen measured in the plasma of LV treated mice overtime (n=4* per *each group). Two-way ANOVA with Sidak's multiple comparisons test. (**C**) Single values and mean with SEM of percentage of liver area expressing GFP by immunofluorescence analysis 3 months after LV administration, Mann-Whitney test. (**D**) Single values and mean with SEM of expression analysis by quantitative PCR of WPRE normalized on the endogenous hprt gene on RNA extracted from the livers of treated mice. Mann-Whitney test. (**E**) Single values and mean with SEM of VCN measured in total liver and spleen of LV treated mice. Mann-Whitney test. (**F**) Experimental design: 8 weeks old* $f9^{-/-}$ *mice are injected with rapamycin (3 or 6 mg/kg) or saline. 2h later, they are injected i.v. with* hFIX *LV. Their circulating hFIX are monitored longitudinally. (**G**) Mean with SEM of hFIX antigen measured in the plasma of LV treated mice overtime (n=4* per *each group).*

The addition of internal ribosome entry site (IRES) sequence to a construct is a valuable strategy allowing multi-cistronic gene expression starting from a single mRNA. Even though the expression of the second gene is less efficient, since it is not cap-dependent (compared to the first gene) (Al-Allaf *et al*, 2019a), it looked a good compromise, since we could detect i) circulating hFIX amounts longitudinally and ii) visualize transduced area at the end of experiment (fig. 20A).

We confirmed the higher transgene output for fasted mice with this different construct (fig. 20B). Moreover, percentage of tissue positive area (fig. 20C) and RNA derived from LV (fig. 20D) were higher in fasted mice, compared to non-fasted counterparts, reflecting a higher gene transfer in fasted mice. Once again, in total liver, VCN was comparable between the two groups (fig. 20E).

To then assess if the higher transgene output was due to autophagy induction, as suggested in the past in the context of AAV (Hosel *et al.*, 2017), we tested the autophagy inducer rapamycin, in an *in vivo* experiment. Adult hemophilia B mice were injected i.v. with either 3 mg/kg, 6 mg/kg or saline. 2 hours later, they were injected with LV (fig. 21 F). Mice were then bled overtime, to compare hFIX circulating amounts among the different groups. However, we did not observe an advantage due to the pre-treatment with rapamycin (fig. 21.G), possibly implicating a reason different from autophagy for the advantage in LV mediated liver GT observed through fasting.

3.5.2 Fasting impacts on LDLR pathway

In an effort to understand the reasons behind higher gene transfer in fasted mice, we then decided to monitor mice during fasting, and to look at LDLR pathway.

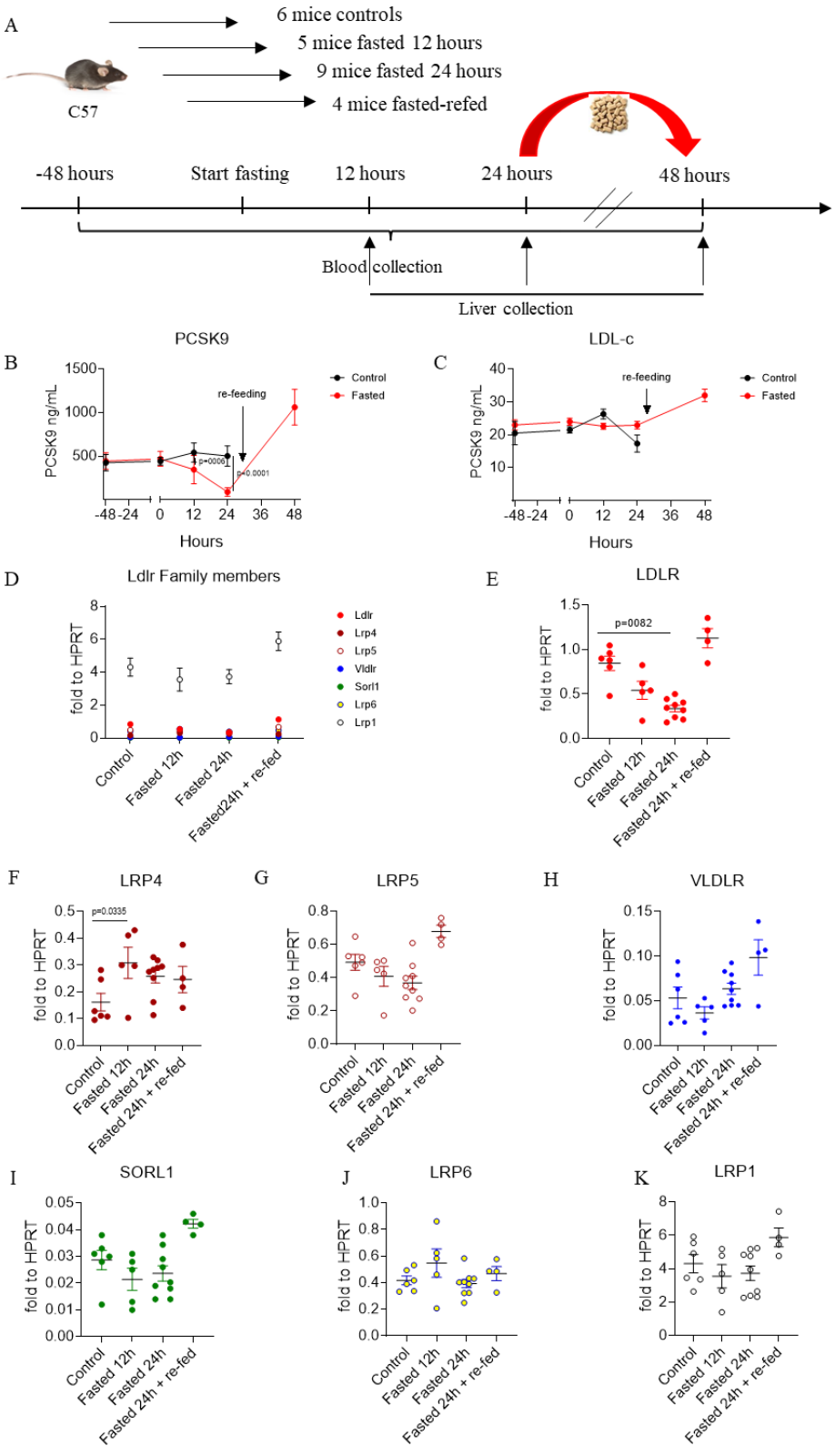


Fig. 21: Monitoring LDLR pathway over fasting. *(**A**) Experimental design: 8 weeks old mice are fasted 12 or 24 hours and euthanized or re-fed for additional 24 hours. LDLR pathway is monitored overtime. (**B**) Mean with SEM of mPCSK9 antigen and LDL-C (**C**) measured in the serum of experimental mice overtime. Two-way ANOVA with Sidak's multiple comparison test. (**D**) Single values and mean with SEM of expression analysis by quantitative PCR of Ldlr (**E**), Lrp4 (**F**), Lrp5 (**G**), Vldlr (**H**), Sorl1 (**I**), Lrp6 (**J**), Lrp1 (**K**), normalized on the endogenous hprt gene on RNA extracted from the livers of C57 or* Ldlr$^{-/-}$ *mice. Kruskal-Wallis test with multiple comparisons over control group.*

Groups in the experiment were the following: i) mice used as control and fed *ad libidum*, ii) mice fasted 12 hours and then euthanized, iii) mice fasted 24 hours and then euthanized, iv) mice fasted 24 hours, re-fed for additional 24 hours and then euthanized (fig. 22A).

Circulating PCSK9 amounts were reduced overtime during fasting (fig. 23B). In contrast, LDL-C circulating amounts were comparable over fasting (fig. 22C).

Both PCSK9 and LDL-C showed compensatory positive feedback, once food was given back to the mice, with amounts higher than in control mice.

We then looked at the liver of experimental mice and performed gene expression analysis on *Ldlr* and *Ldlr FM* (fig 22D). *Ldlr* RNA followed the same trend as PCSK9, being reduced overtime over fasting (fig. 23E). The other family members showed to be less to not affected by fasting. Some of them showed instead the trend of increased expression following re-feeding (fig. 23 E - K). Put together, the higher gene transfer observed in *Ldlr*$^{-/-}$ mice and reduction of *Ldlr* over fasting, condition again related to higher transgene output, may suggest that lower amounts of LDLR improve rather than impair LV transduction *in vivo* in the liver. LDLR could act as a scavenger receptor for LV, with another receptor, present on *Ldlr*$^{-/-}$ mice just as in C57 mice, whose levels are not impacted by fasting, being a better receptor.

3.6 Transduction enhancers in combination, in C57 and *Ldlr*$^{-/-}$ mice

Once identified three different enhancers of transduction (MarI, Bortezomib, fasting), which proved to be effective with different transgenes tested, we wondered if the three transduction enhancers had an additive or even synergistic effect when combined. Since we were also interested in comparing/confirming the advantage of these enhancers in the

Ldlr$^{-/-}$ mouse model, we used C57 and *Ldlr*$^{-/-}$ divided in the following experimental groups (Table 2).

According to the groups, mice were either faster for 24 hours, injected with MarI 3 hours before LV and/or injected with Bortezomib 1-hour before LV. Circulating hFIX amounts were then monitored longitudinally (fig. 23A).

Table 2

	C57 experimental groups							*Ldlr*$^{-/-}$ experimental groups						
	I	II	III	IV	V	VI	VII	I	II	III	IV	V	VI	VII
LV	x	x	x	x	x	x	x	x	x	x	x	x	x	x
MarI		x			x		x		x			x		x
Bort			x			x	x			x			x	x
Fasting				x	x	x	x				x	x	x	x

In C57, compared to LV only, MarI and Bortezomib, as single treatments before LV administration confirmed to enhance transgene output (fig 23B, C).

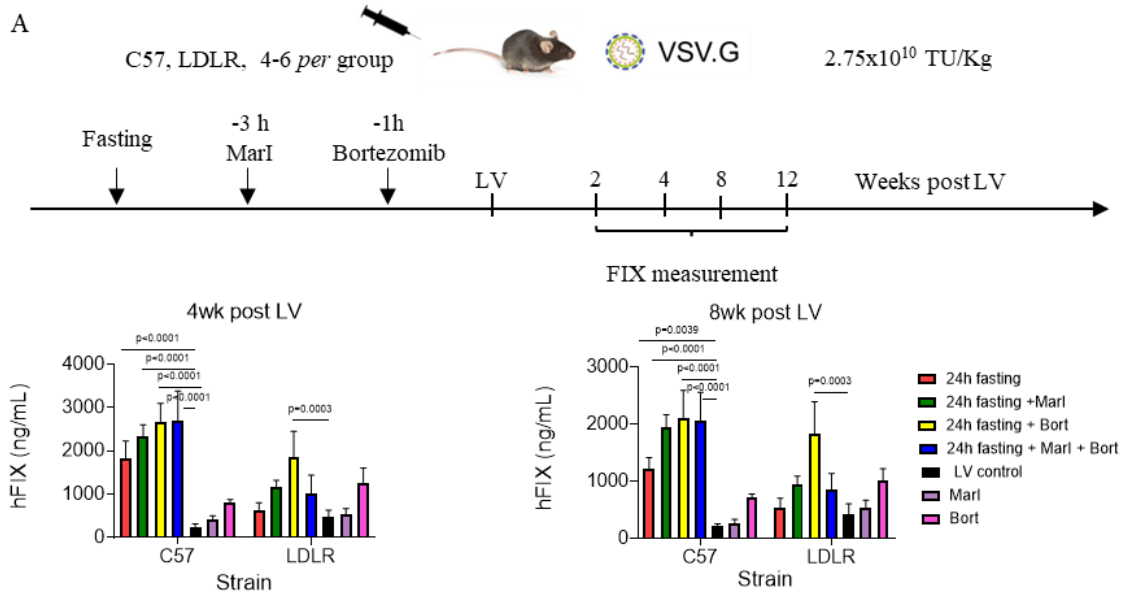


Fig. 22: Transduction enhancers additive effect in C57 and* Ldlr$^{-/-}$ *mice ***(A)*** *Experimental design: 8 weeks old mice C57 or Ldlr*$^{-/-}$ *(n=4-6* per *each condition) are injected with Bortezomib and/or MarI and/or fasted for 24 hours, before receiving LV (dose 2.75x10*^{10} *TU/Kg) i.v. Then, hFIX is monitored in treated mice longitudinally.* ***(B)*** *Mean with SEM of hFIX antigen measured in the plasma of LV treated mice overtime (4wk post LV timepoint).* ***(C)*** *Mean with SEM of hFIX*

antigen measured in the plasma of LV treated mice overtime (8wk post LV timepoint). Two-way ANOVA with Dunnett's multiple comparisons test vs LV control, performed for each of the two strains used.

The best outcome following single enhancement treatment was however reached with fasting, where transgene amounts were 7.5-fold higher than in control mice treated with LV alone. Moreover, combination of MarI and fasting and combination of Bortezomib and fasting proved to induce an additional advantage in terms of transgene output, 9.5-fold higher and 11-fold higher than LV controls, respectively.

While it was already clear, at least in the time window observed, that MarI and Bortezomib effect was not additive (see 3.5.2), we found out that the combination of fasting, MarI and Bortezomib administration was not inducing any additional advantage compared to the combination of fasting + MarI or fasting + Bortezomib.

Moving to *Ldlr*$^{-/-}$, firstly we confirmed the higher transgene output in *Ldlr*$^{-/-}$, compared to C57. Moreover, while MarI and Bortezomib showed to give an advantage, the effect of fasting was minimal/mild. Even when combined with fasting, MarI and Bortezomib showed milder increase in *Ldlr*$^{-/-}$ than C57, compared to their use as single treatments.

The greatest advantage, for *Ldlr*$^{-/-}$ mice, was achieved with the combination of fasting and Bortezomib, with an overall increase in transgene output of 4.3-fold. These data provide the great potential of a minimally invasive combination of treatments, which could be combined with LV for ensuring a GT with higher potency. Long term efficacy data and histopathological analysis will need to be further assessed before clinical translation.

4. DISCUSSION

4.1 LV mediated liver GT for FH

Despite all the therapeutic options available for people affected by HeFH, HoFH still lacks a definitive cure. For this reason, we set out to apply LV GT to this challenging metabolic disorder.

The results that we obtained in *Ldlr*$^{-/-}$ mice indicate that the dose required to normalize total cholesterol and LDL-C circulating amounts is 3.5-4x10^{10} TU/kg, in juvenile mice (see 3.2.4). When administering the same dose *per* kg in adults, we did not observe any decrease in circulating cholesterol or LDL. We have shown that LV-dose–response is more favorable in mice treated as newborns compared to mice treated as adults, suggesting better access and/or permissiveness to LV transduction in the former, a finding currently under active investigation in our group (Milani *et al.*, 2022) and unpublished data). Our results in *Ldlr*$^{-/-}$ mice are consistent with these data, as we observed reduced transduction efficiency in adults compared to juvenile mice. Indeed, even when adult immune-deficient *Ldlr*$^{-/-}$ mice were treated, efficacy was not observed (see 3.2.2), suggesting that lack of efficacy was not due to an immune response mounted against the LDLR or transduced hepatocytes.

In order to assess if *Ldlr* liver gene transfer strategy could resist challenging conditions, we fed the juvenile treated mice for 3 months with high fat high carbohydrate WD. The group fed with standard diet for the duration of the experiment did not show any sign of liver steatosis, or any alteration in total cholesterol and LDL-C circulating amounts, which were kept in normal range overtime. WD challenge induced atherosclerosis in all *Ldlr*$^{-/-}$ mice, while none of the LV-treated *Ldlr*$^{-/-}$ mice showed any atherosclerosis. Interestingly, the mice showing higher total cholesterol and LDL-C amounts, among the treated ones, before starting the challenge, were the ones displaying higher increase in LDL-C amounts throughout the challenge, higher grade of liver steatosis at the end of experiment and lower percentage of transduced liver area. These data point to the fact that, particularly for this disease, the highest the number of corrected hepatocytes, the better it would be. Indeed, the mice displaying a tissue LDLR-positive area of 5-8% were protected from steatosis, even despite the challenge. In the mice with more abundant transduced liver tissue, each hepatocyte had to internalize less LDL, and the reduced load of cholesterol and TG avoided steatosis. In contrast, our data suggest

that the mice with less transduced liver tissue had to overload few hepatocytes with LDL, with the consequence of inducing, in those hepatocytes, steatosis. We cannot exclude that the low percentage of LDLR positive tissue area in the two mice displaying highest LDL-C amounts throughout the WD challenge, was even the result of progressive loss of transduced hepatocytes, overloaded with LDL. However, despite the progressive slow increase in LDL-C during challenge, since LDL-C moved back to values pre-challenge when they started again eating standard diet, it is possible that the increase was the result of reduced activity of transduced hepatocytes in general, due to the stressful condition of the challenge (see 3.2.4).

Since we prioritized histopathology analysis of the aorta in this experiment, we had to perfuse the mice with paraformaldehyde, thus, we could not evaluate VCN and *Ldlr* RNA amounts in their livers. However, from the experiment at sub-therapeutic dose (see 3.2.3) it is possible to extrapolate that, to normalize LDL-C, the liver of *Ldlr* LV treated *Ldlr*$^{-/-}$ mice must express the receptor more than hepatocytes of healthy mice, because of the residual lack of extrahepatic contribution to the clearance of circulating cholesterol. Thus, a potential GT in humans affected by HoFH should instruct the liver to work more than the liver of a healthy person. We do not consider this as an issue, since, even in case of WD challenge, a portion of mice had steatosis comparable to WT mice, but we reckon that high percentage of corrected hepatocytes will be needed for ensuring them to be fit.

4.2 The risk of insertional-mutagenesis in LV-mediated liver GT

Given the urgency of early-in-life treatment for HoFH (atherosclerosis develops in childhood), we consider an integrating platform to be preferable for GT applied to this disease. LV turned out to be safe when used to target the hematopoietic system. Throughout the years, to further improve the safety profile of these vectors, viral-derived promoters and enhancers, used at the beginning to drive transgene expression, were replaced with cellular promoters and regulatory sequences. Indeed, a plethora of preclinical studies highlighted the cause-effect relationship between viral promoters/enhancers, clonal expansion and oncogenesis, following integration of LV (Poletti & Mavilio, 2021; Tucci *et al*, 2022).

Three of the current approved gene therapies are based on LV (Zynteglo, Skysona, Libmeldy, see Table 1). Among them, Skysona is the only one where transgene is not

driven by a cellular promoter. Indeed, it is driven by murine myeloproliferative sarcoma virus U3 enhancer/promoter region. Skysona had to pay the fee of this choice and is the only LV GT drug labeled with a black box warning by FDA, since cases of hematological malignancies were reported (https://www.fda.gov/media/161640/download). Despite the warning, the FDA deemed that the risk/benefit ratio of the therapy remained in favor of the latter in this indication. Choosing the right promoter is crucial for GT purposes, and usage of stronger promoters to ensure higher transgene expression does not mean getting in turn higher chances of curing the disease.

In our long-term experiment (see 3.2.5), adenomas were found in the livers of 3/7 mice 1 year after LV administration when using the LV with *Ldlr* cassette in a.s. orientation. The *ET* enhancer/promoter present in the hepatocyte specific cassette is made of synthetic transthyretin promoter and hepatocyte specific enhancer sequences. *Wpre** was kept in the construct, to enhance vector titer. In this configuration, *wpre** ends up between *ET* and LTR. It is known that, if *ET* promoter is located inside LTR, the construct becomes genotoxic, due to *ET* activating nearby genes following integration (Cantore *et al.*, 2015; Ranzani *et al*, 2013). In our construct, despite *ET* not being within LTR, it was located back-to-back with wpre* and LTR. As already mentioned, genotoxicity occurs mediated by enhancers or promoter activities. In our experiment, we identified RNA signal not only when using probes amplifying *Ldlr* transgene, but also when using the probe amplifying the wpre* sequence. This was unexpected, since *ET* and *Ldlr* were in a.s. orientation. Wpre* sequence present in LV, as said before, has been mutated to prevent woodchuck hepatitis virus X peptide expression (Kingsman *et al.*, 2005; Zanta-Boussif *et al.*, 2009). However, 3 ATG and a transcription start site are still present in the sequence that we are currently using. While this might not be an issue when *wpre** is downstream the transgene, it might be in this different configuration. By detecting *wpre** signal at RNA level, we showed a considerable amount of read-through transcription. If LV integrates nearby oncogenes, and *ET* allows the transcription of the cassette to occur even in opposite direction compared to the transgene of interest, it may continue through the LTR, possibly running into splice donor sites, ending up matching with inappropriate splice acceptor sites. The weak polyadenylation signal present in the LTR may not be active in this scenario, and a stable RNA comprising part of the LV genome and part of the host-derived genome could be generated, thus ultimately resulting in overexpression of the oncogene nearby the LV insertion site. Further molecular studies assessing the pattern of

LV integration and the presence of possible hybrid transcripts should be performed to further dissect the mechanism of insertional mutagenesis mediated by the LV with the *Ldlr* cassette in a.s. configuration. In line with this speculation, we obtained similar results in a different setting using a GFP transgene in a.s. orientation. More specifically, we found hepatocellular adenomas 1 year after i.v. LV administration, in C57 mice treated as neonates with LV containing a cassette in a.s. orientation, while no adenomas were found where the LV contained the same GFP transgene cassette but in the canonical sense orientation.

An additional contributing factor to this unexpected result might reside in the LDLR transgene expression cassette. Indeed, a constitutive, not regulated, expression of LDLR, might induce an excessive cholesterol intrahepatic amount, possibly causing cellular stress favoring adenoma formation. However, since constitutive life-long over-physiological expression of LDLR has been reported in a healthy Scandinavian family (Bjornsson *et al*, 2021), we tend to exclude that the adenomas were related to the supra-physiological LDLR expression. For this reason, the only modification to the construct that we considered crucial was to find an *escamotage* to move back to sense-oriented LV expressing *LDLR*, as discussed below.

4.3 Rescue in productivity of sense-oriented LDLR encoding LV

Other groups highlighted the difficulties encountered when trying to produce LDLR encoding LV (Al-Allaf *et al*, 2010). Since the overexpressed LDLR protein during LV production is not compatible with yields of LV required for *in vivo* administration, most of our results were obtained using a novel, previously undescribed in the context of liver GT, design to avoid transgene expression during LV production: the a.s. orientation of the cassette. However, for the already mentioned safety reasons, it was crucial to go back to sense-oriented design. The *escamotage* of using PCSK9 GOF non-secreted variant as additional plasmid during vector production, its subsequent interaction with LDLR and the consequent degradation of the receptor, allowed us to rescue the infectious titer of LDLR LV in sense orientation, ultimately obtaining yields far good enough for *in vivo* use. Interestingly, infectious titer of a.s. oriented cassette encoding LDLR LV were decreased. This may be due to PCSK9-mediated degradation of LDLR, which is synthetized by the cells for capturing cholesterol from the medium, required to build more

plasma membranes, during proliferation. As a consequence, cell viability and the capability to produce LV may be reduced.

As already mentioned, the homology between mLDLR and hLDLR is 78% at the amino acid sequence level (Kassim *et al.*, 2013). Thus, we somehow expected that a higher LV dose was required for normalizing total and LDL cholesterol of *Ldlr*$^{-/-}$ mice, when hLDLR was used as transgene. Even though long-term histopathologic analysis will be crucial to ensure the safety of this strategy, all our historical safety data have been collected using this kind of LV configuration. Thus, we do not expect genotoxicity in the mice treated with sense-oriented cassette. If this will be confirmed, this configuration would become a promising candidate for further research towards a possible clinical translation.

4.4 Future directions of HoFH treatment by *in vivo* liver-directed LV GT

Before starting a clinical trial, the paradigm requires to test larger animal models, if possible. This strategy allows to confirm the feasibility of the procedure, using a model more similar to humans. Thus, the pillars of a successful GT must be confirmed even in this new model: efficacy, durability, immune tolerability and safety. Concerning FH, the best larger animal model is the rabbit. Dr. Yoshio Watanabe accidentally identified a hyperlipidemic male rabbit in 1973. He devoted nearly all his income to the establishment of a hyperlipidemic colony and named his rabbits as Watanabe Heritable Hyperlipidemic Rabbits (WHHR). This model has been used worldwide for hyperlipidemic studies. The genetic cause turned out to be a deletion in *LDLR* gene, responsible for loss of four amino-acids required for efficient binding of LDL (Yamamoto *et al*, 1986). WHHR display LDL-C circulating amounts similar to those of HoFH patients, develop fatty intimal streaks and later complicated atherosclerotic lesions. Indeed, unlike *Ldlr*$^{-/-}$ mice, and as human beings, they express *Apobec* exclusively in enterocytes. Thus, VLDL generated in the liver carries exclusively APOB100 and once turned into LDL, can be internalized exclusively through LDLR. It would be crucial, in the future, to validate our LV GT strategy in this spontaneous larger animal model. Indeed, it would be possible to assess even if competition in trafficking to the membrane of the transgenic LDLR would occur. Rabbits are not supposed to be restricted to lentiviral infections, thus evaluating LV-mediated GT should be feasible (Filice *et al*, 1988). In the past, there has been a work

describing the usage of LV carrying *LDLR* for the treatment of WHHR. However, the reduction in total and LDL cholesterol was mild (Kankkonen *et al*, 2004).

Evaluation of LV transduction of cells from HoFH patients, with different types of *LDLR* mutations, *in vitro* may be considered in the future to confirm the efficiency of VSV.G LV-mediated gene transfer. Peripheral blood cells may be relatively easy to obtain from patients. Alternatively, mice engrafted with hepatocytes derived from HoFH patients would be a good experimental model, however it will require the availability of viable hepatocytes from the explanted liver, following a liver transplantation procedure.

Likely, the best therapy for HoFH patients would be gene transfer of *LDLR*, with the following features: i) long lived, administered once throughout the patient life; ii) administered during infancy, since the sooner the treatment the better the outcome; iii) targeting the liver, but instructing it to work more than a normal liver, since liver transplant is not fully curative; iv) targeting the highest possible percentage of hepatocytes to avoid excessive stress for the few corrected. Genome editing, to restore physiologic LDLR activity, could be an option, however, it should be considered that the efficiency of editing is still relatively low compared to gene transfer and that the correction of the liver, even at high efficiency, would not be curative if physiological expression is restored. Indeed, as mentioned above, overexpressing the LDLR in a large fraction of hepatocytes would be necessary for an effective treatment of HoFH. Besides reducing circulating cholesterol by inducing LDL intake by hepatocytes, *LDLR* gene transfer to the liver would bring about the additional advantage of suppressing cholesterol synthesis by hepatocytes: incorporation of cholesterol indeed could cause inhibition of HMG-CoA reductase, since cholesterol synthesis is not needed anymore (Brown & Goldstein, 1974). *LDLR* gene transfer induces a constitutive expression of LDLR, in contrast with the tight regulation of LDLR in mice and humans and with its lower expression by hepatocytes. For this reason, it could be speculated that the higher the percentage of hepatocytes corrected, the higher the chance to normalize LDL-C even using a weaker, potentially including regulatory sequences, promoter. However, cases of hypocholesterolemia, due to deletion of the regulatory 3' region of *LDLR* gene have been reported. Despite the loss of regulatory elements, these individuals were not showing any health concern (Bjornsson *et al.*, 2021), thus further justifying the therapeutic strategy of LDLR gene transfer.

4.5 Selection of corrected hepatocytes mediated by paracetamol

In liver GT, the doses needed to reach therapeutic expression represent a challenge from the manufacturing point of view, together with bringing about the increased risk of immune responses. Because of these reasons we decided to test a strategy to select corrected hepatocytes, to expand them *a posteriori*, to potentially ensure for each future patient the chance of reaching therapeutic transgene amounts.

We showed that positive selection through paracetamol administration is feasible in different mouse strains (C57, *F8*$^{-/-}$) and at different ages (mice treated as neonates, juvenile, adults), confirming and expanding previous results about this strategy. Overall, we showed here that it is possible to select genetically corrected hepatocytes *a posteriori*, achieving a remarkable up to 50-fold increase in transgene output, thus allowing to substantially reduce the therapeutic dose with positive consequences on manufacturing, costs and potential acute toxicities related to the GT procedure.

The selection process can be stopped without impacting transgene amounts and can be re-started *on demand*. We showed that transgene product fold-increase, throughout selection, is higher when starting from very low doses. We can speculate that, since in case of few corrected hepatocytes, most of the drug will end up in non-corrected hepatocytes, these will be damaged and replaced. The higher the percentage of starting corrected hepatocytes, the lower the chances of inducing damage in the non-corrected ones.

Paracetamol is a drug proven to be safe throughout the decades of its commercialization. It is cheap and assumed orally. Moreover, it can be assumed by both adults and pediatric patients. Moreover, an antidote exists: N acetyl cysteine. Thus, in a clinical perspective, in case ALT measurement would be too high, it could be taken *on demand*, to avoid the liver damage to be excessive. The delivery of a therapeutic gene *in cis* with a siRNA downregulating *Cypor* activity is thus a valuable strategy to achieve a strong selection.

This selection protocol is not showing the same efficacy in all the mice, with the opposite situation of immediate and rapid selection of some, and slow and delayed of others. Still, it allowed to obtain hFVIII activity in the therapeutic range, starting from sub-therapeutic hFVIII amounts, thus being potentially transformative in some particularly challenging GT settings.

We have shown that there is no linear correlation between increased LV dose and increased transgene outcome (see fig. 16). This is expected and our group previously showed to be due to the saturation of KC, particularly in adult mice, which uptake massively LV at low doses, while increasing the dose allows the vector to reach hepatocytes more efficiently. Indeed, the mice in the group then subjected to selection, while treated at a dose 5-fold lower that the others, showed circulating hFIX starting amounts 50-fold lower. This must be kept in mind when approaching this strategy: selection will have to be intensive, to reach the transgene amounts obtained with a starting dose 5-fold higher.

It will be interesting to perform integration site analysis of selected mice and un-selected counterparts. As it is designed, this strategy is inducing clonal expansions. Thus, it is expected the following outcome: higher number of integrations, each one low represented, in mice treated at a standard/high dose; lower number of integrations, each one low represented, in mice treated at low doses and left non-selected; low number of integrations, highly represented, in the low dosed mice subjected to selection. What remains to be clarified is the nature of these integrations: are all the clones represented to the same extent? Are the most expanded clones carrying mutations near/into potential oncogenes? Or the expanded clones are carrying LV integrations in safe places, which happen to be expanded just because of their location in the liver? Integration sites analysis should help answering these questions.

Together with the long toxic regimen required to achieve corrected hepatocytes expansion, downregulation of all microsomal CYP450 activity remains an important limitation for the translatability of this strategy. The caffeine assay was used as a proof of concept, to clarify that, once a portion of pericentral hepatocytes is replaced with corrected Cypor downregulating hepatocytes, their CYP450 activity will be impaired. This has several implications, among others: CYP450 activity is necessary for cholesterol synthesis, bile acids excretion in the bile canaliculus, for most of xenobiotics metabolism. Liver-specific *Cypor*$^{-/-}$ mice have been generated several years ago. They are vital and fertile, even though fertility and litter sizes are reduced, compared to C57. Moreover, liver *Cypor*$^{-/-}$ mice display 90% reduction in bile acids excretion, reduced circulating cholesterol and, importantly, massive fat accumulation into the liver (Henderson *et al*, 2003). Among the possible strategies to restore CYPOR activity to normal, once selection is completed, one might be flanking the portion of LV cassette containing *U6* and *Cypor*

shRNA with LoxP sites. Once selection protocol is over, the *Cre* recombinase could be delivered as mRNA through LNP, to excide exclusively the portion of LV containing the shRNA sequence. Thus, the transgene would continue being expressed, but CYP450 activity would be restored.

Another limitation of this strategy is the exclusive enrichment of zone 3 hepatocytes. As a matter of fact, if a genetic disease requires correction of periportal hepatocytes, this strategy would be vain, since hepatocytes in the wrong zone will be enriched over time.

Lastly, this strategy is inducing death of hepatocytes by necrosis. Even though paracetamol is one of the safest drugs on the market, with liver toxicity as only side effect in case of overdose, we reckon that the best strategy to positively select corrected hepatocytes should aim to apoptosis of non-corrected hepatocytes further than necrosis.

4.6 Inhibition of proteasome activity and IFN signaling before LV enhance hepatocyte gene transfer

In line with the already mentioned issue of high doses of LV required for therapeutic purposes, in this work we looked for antiviral pathways to be counteracted for enhancing the potency of gene transfer to hepatocytes. We identified IFNARI and proteasome inhibitions to efficiently increase gene transfer.

In the past, higher liver gene transfer was reported in mice *IfnaRI*$^{-/-}$. In our experiments, we observed an increase when a single dose of MarI (anti IFNARI mAb) was administered to the mice before LV. The mechanism might be explained as follows: IFN induction, mainly mediated by pDC, restricts hepatocytes transduction because of an anti-viral state activation. Thus, MarI may facilitate successful LV steps following entry into hepatocytes.

The second antiviral pathway that we targeted was the proteasome, once again with the challenging *hFVIII* used as transgene. Proteasome inhibition was reported in the past as good strategy to improve LV transduction in stem cells, and the explanation was the possible delay in particles degradation, thus able to escape from endosomes for a longer period of time, ultimately leading to increased nuclear translocation (Santoni de Sio *et al.*, 2006; Santoni de Sio *et al*, 2008).

Even in this case, a single dose of Bortezomib prior to LV was sufficient to observe an increase in hFVIII circulating amounts, compared to the amounts of controls. These

results were observed despite the still high variability in hFVIII transgene derived output among mice (Milani *et al.*, 2022).

These two transduction enhancers did not show an additive effect, when used in combination, at least in the window of time that we tested. The lack of synergy, together with the higher outcome obtained with Bortezomib compared to MarI may suggest that Bortezomib increases gene transfer impacting on IFN pathway and beyond. Indeed, Bortezomib reduces both function and survival of pDC, the major producers of IFN type I (Hirai *et al*, 2011). VCN of sorted pDC showed to be lower in Bortezomib and Bortezomib + MarI pre-treated mice, compared to control and MarI pre-treated mice. Thus, while MarI may render hepatocytes insensitive to IFN signaling, Bortezomib may indirectly abolish IFN signaling by transiently reducing the functionality of their cellular source, consequently improving hepatocytes transduction.

Just like in pDC, VCN on sorted KC proved to be lower than in controls in Bortezomib pre-treated mice. Two are the main possible explanations for this KC outcome: i) impaired phagocytic capability, ii) enhancement in toxicity, with subsequent replacement by non-transduced progenitors (Anan *et al*, 2006).

Bortezomib treated mice showed a skewing in the distribution of liver VCN, compared to controls, since we observed higher VCN in LSEC and a trend of increase even in VCN of hepatocytes. LSEC and particularly hepatocytes VCN of Bortezomib + MarI mice were less different from controls, as highlighted even by circulating hFIX amounts.

The positive impact of Bortezomib even on LSEC, which came out as bystander discovery, might be particularly useful for the treatment of diseases due to LSEC impairment, like Von Willebrand Disease or even HA, since FVIII is normally synthetized by this subcellular type. Indeed, there are groups focused on liver GT for HA with the aim of targeting LSEC, to mediate FVIII expression by the cellular type that, physiologically, is responsible for its synthesis (Merlin *et al*, 2019).

4.7 Fasting before LV enhance gene transfer and induces additive effect if combined with proteasome inhibition

Fasting was the third transduction enhancer that we identified. At the beginning of this project, when we did not know that we could obtain gene transfer in mice lacking LDLR, we thought that strategies aiming to increase LDLR may be exploited to obtain higher

gene transfer by LV. Since fasting was reported to increase LDLR both at RNA and protein level in hamsters (Wu *et al*, 2012), we decided to test this procedure.

When subjecting mice to 24 hours of fasting, we consistently obtained an advantage in circulating hFIX amounts (spanning from 2 to 10-fold transgene output increase in the different experiments). We also observed higher RNA expression deriving from the liver, confirming that the higher circulating transgene amounts were deriving, as expected, from hepatocytes. We did not show higher VCN in sorted hepatocytes, possibly due to contamination with nPC. Still, we cannot exclude this outcome to be partially due to different pattern of integration of LV when entering hepatocytes of mice fasted for 24 hours. Chromatin conformational changes are indeed occurring during fasting (Bideyan *et al*, 2021; Goldstein & Hager, 2015). LV might integrate in different *loci*, compared to standard conditions, wide open during fasting. However, if this is the reason, following re-feeding, these regions should be maintained in conformation of open-highly accessible chromatin, since the advantage in expression is maintained long term. However, even if this is occurring, higher gene transfer is taking place as well, since we observed and higher tissue transduced area.

We observed strong gene expression reduction in PCSK9 and LDLR during fasting. Indeed, in mice, in contrast to hamsters, all genes subordinated to transcription factor SREBP2 activity reduce their expression (Horton *et al*, 1998). As a consequence, at the time of LV administration, fasted mice displayed very low *Ldlr* gene expression and higher LV gene transfer. This is in line with our findings in the mouse model *Ldlr*$^{-/-}$, which are even better transduced than wild type mice.

Ldlr FM expression remained unchanged over fasting. PCSK9 has been reported to inhibit not only LDLR but also other family members (VLDLR, LRP1) (Canuel *et al*, 2013; Poirier *et al.*, 2008). Thus, concerning fasting, one could speculate that LDLR FM, despite being transcribed at the same extent during fasting or feeding, would end up being more exposed on membrane of hepatocytes during fasting, because of their reduced PCSK9-mediated degradation. By using them, LV might thus access hepatocytes more efficiently. However, in *Ldlr*$^{-/-}$ mice, PCSK9 circulating amounts are >10-fold higher than those of wild type mice, considering that lack of LDLR means reduced internalization of PCSK9 into hepatocytes and reduced degradation (Ason *et al*, 2014). This means that in those mice, even LDLR FM are even less available for interaction with VSV.G, compared to C57. Altogether, if LDLR and LDLR FM are indispensable for efficient VSV.G LV

entry, there is no way gene transfer could be higher in mice lacking LDLR. The results that we kept collecting throughout this project on efficient gene transfer into hepatocytes and LSEC of *Ldlr*$^{-/-}$ point toward the possibility that another, more efficient, receptor, might be able to ensure VSV.G LV entry into target cells.

Fasting was also reported to increase liver gene transfer in AAV GT context. In that case, the explanation was the over-activation, induced by fasting, of autophagy, which is required for efficient AAV transduction (Hosel *et al.*, 2017). The positive effect of induction of autophagy was described as possibly related to enhanced transport of AAV towards the nuclei and increased vesicular acidification, providing beneficial acidic environment for AAV. However, when we tested a known inducer of autophagy, Rapamycin, before LV, we did not observe any advantage in transgene derived hFIX amounts following LV injection.

We still lack a definitive answer to explain the advantage of gene transfer following fasting. Still, this non-invasive, cost-effective practice proved to be effective in enhancing gene transfer using different transgenes (hFIX, GFP). Thus, it could represent a valuable strategy to enhance potency of gene transfer in context of LV mediated liver GT. Healthy adults, monitored over 48 hours of fasting, showed PCSK9 amounts and cholesterol synthesis (expressed as lathosterol-to-cholesterol ratio) to be reduced overtime, again indicating reduced activity of SREBP2 transcription factor, thus resembling what was observed by us (Browning & Horton, 2010). Interestingly, even in humans, no reduction in LDL-C was observed, at the beginning. Then, starting from 16 hours of fasting, they steadily increased. This is possibly due to reduction in LDLR, resulting in accumulation of residual LDL in circulation. Based on these similarities, fasting might be translated to humans as a strategy to enhance gene transfer during LV in vivo GT.

When we tested the three transduction enhancers in combination, we identified 24 hours of fasting and Bortezomib administration 1 hour before LV injection to be the best combination to achieve the highest gene transfer. This combination led to a remarkable increase in hFIX transgene circulating amounts of 11-fold. The hFIX transgene used in the experiment was a codon optimized version of hFIX, so the advantage derived from enhancers could be slightly amplified. Thus, the increase, if looking at tissue positive area, could be of a lesser extent. Still, fasting and Bortezomib could be crucial to face more challenging diseases, where most of the liver mass must be corrected to obtain a therapeutic outcome. Long term histopathological analysis will be crucial for assessing

the safety of this combination, even if, being a one-time regimen, it is unlikely to have negative impacts long-term.

When trying to apply these transduction enhancers to *Ldlr*$^{-/-}$ mice, interestingly, fasting turned out to be less/not efficacious. Different reasons could explain this finding:

i) hepatocytes of mice lacking LDLR could be unresponsive to fasting, thus unable to be reprogrammed.

ii) LDLR, despite the very efficient interaction with VSV.G, might actually be detrimental for LV transduction, acting as a scavenger receptor. If this is the case, its reduction over fasting would be beneficial for mice with a functional LDLR, while it would be neutral in mice without LDLR. What seems to be clear is that: LDLR is not required for efficient liver gene transfer, *Ldlr*$^{-/-}$ mice transgene output is higher than the one observed in C57 at same dose. However, while C57 are fasted, transgene output is higher than that of *Ldlr*$^{-/-}$ meaning that, even if lacking LDLR is beneficial for LV gene transfer purposes, the advantage induced by fasting is related even to other, up to now still unknown, reasons.

iii) KC might be partially incapable of internalizing LV, due to cholesterol overload subsequent to lack of LDLR. However, when sorting liver subpopulations of C57 and *Ldlr-/-* mice treated with LV, we did not find a difference in KC VCN between the two strains.

iv) membrane trafficking and vesicular transport inside hepatocytes of *Ldlr*$^{-/-}$ and fasted mice may be altered in such a way to favor entry and trafficking of LV capsids, ultimately improving LV transduction efficiency.

4.8 Conclusions

LV are attractive vehicles for liver directed GT. They offer the distinctive advantage of integrating in the genome of target cells. Thus, they could be potentially used to treat pediatric patients with a single administration, last life-long, and face diseases which would be life-threatening in childhood. Moreover, pre-existing immunity is <1%, thus vast majority of patients could benefit from a potential *in vivo* LV GT.

In this work, we successfully enhanced the efficiency of LV-mediated hepatocyte gene transfer, thus paving the way to expanding its *in vivo* applicability. We faced the challenging FH as disease model, and in parallel we tested different approaches to

enhance the potency of liver gene transfer by LV, once again with the aim of broadening its possible applications. Since the new transgene we faced, LDLR, is tied hand in glove with VSV.G, used to pseudotype LV, we had to overcome different challenges related to this approach (very low infectious titers, changing of LV configuration). Despite all these complications, we succeeded in using the same LV configuration shown to be safe in the past. Insertional mutagenesis remains a concern for integrating vectors. It should be noted, however, that with the sense-oriented LV design, LV-mediated liver gene transfer did not result in liver carcinogenesis even in mice treated as newborns, genetically tumor-prone or tumor-promoted, followed for long time (over 1 year) (Cantore *et al.*, 2015; Milani *et al.*, 2022). Moreover, analysis of LV integrations in the liver of mice, dogs and NHP did not show clonal expansions or enrichment of integrations nearby cancer genes (Cantore *et al.*, 2015; Cesana *et al*, 2021; Milani *et al.*, 2019), thus overall suggesting a very low risk of insertional mutagenesis.

In this work we utilized small animal models. We performed, to our knowledge, the first effective LV-mediated liver GT in *Ldlr*$^{-/-}$ mice and showed long-term therapeutic benefit, even in case of WD challenge. We showed that FH is a particularly challenging disease, since targeted hepatocytes will have to clear the cholesterol of a healthy liver plus the cholesterol conventionally cleared by extra-hepatic tissues, meaning that the work will have to be superior to that of a normal liver. Indeed, since it has been shown that liver transplantation is not fully corrective in HoFH patients, we assume that overexpressing LDLR in a large portion of hepatocytes would be required in a GT setting. Site-specific correction of *LDLR* in its endogenous locus may not be as effective as viral-vector mediated gene transfer in this case, because physiological LDLR expression would not be sufficient. Ideally, the gene transfer procedure should be performed as soon as possible after diagnosis, to prevent accumulation of damage and reduce the risk of CVD. For this reason, the use of integrating vectors, such as LV, may be preferred, as it would allow stable LDLR expression following a single administration and potentially lasting for the entire life of the recipient. In a future in which GT has shown to benefit FH, its application to non-genetic forms of dyslipidemias may also be considered. As mentioned above, beyond FH there is acquired hypercholesterolemia. Some conditions could trigger it as bystander effect, including type II diabetes and aging. In type II diabetes, insulin is produced, but tissues become insensitive to it. As a result, adipose tissue and skeletal muscle are induced to undergo lipolysis, to release FFA in the circulation. Cholesterol

and TG levels, thus, increase as a bystander effect. In the context of type II diabetes or spontaneous increase in LDL-C due to aging, a GT intervention such as inactivation of *PCSK9* or *LDLR* gene transfer may become beneficial.

This work was also focused on finding strategies to increase the potency of GT, with both the aim to tackle, in the future, challenging liver diseases requiring high percentage of liver corrected tissue and to allow reducing the doses required for therapeutic efficacy in case of non-cell-autonomous diseases like hemophilia. We validated the strategy of selection of corrected hepatocytes, previously shown to be effective in neonatal mice (Vonada *et al.*, 2021), at different ages of treatment and using different transgenes. Our data suggest that such an approach may not reach the clinics, in the way it is currently designed. It would be desirable to replace necrosis with apoptosis and restore Cypor activity after selection, to favor its clinical application. However, both these aspects will likely take time for being optimized. Enhancing the potency of liver gene transfer *a priori*, by usage of transduction enhancers prior to LV administration will likely be accepted more easily, if proven to be as safe as LV alone. Fasting of the mice for one day, short inhibition of IFN signaling and proteasome activity proved to be effective in enhancing gene transfer to hepatocytes, with the combination of fasting and Bortezomib being the most promising combination (11-fold increase in transgene output, compared to LV alone).

Despite the remaining unknowns and lack of long-term safety data, genetic therapies bear the potential to revolutionize medicine and positively impact on people suffering from several different diseases. Besides efficacy and safety, wide adoption of gene therapies in the clinical practice in the future will also depend on evolution of the current regulatory and reimbursement framework and propensity to innovation of all the involved stakeholders, including physicians, patients, and policy makers.

5. MATERIAL AND METHODS

5.1 Plasmid generation

Plasmids used for this work were either already available in the lab, or they were generated through standard cloning techniques, inserting into backbones, already available, inserts derived from other pre-existing plasmids or derived from gene synthesis required *ad hoc*. LV sense-oriented *ET-hLDLR-wpre** (both standard and co) were generated starting from LV-*ET-FIX* Padua-wpre* (Cantore *et al.*, 2015), by substituting *FIX* sequence with *LDLR* sequence. *hLDLR* cDNA sequences were synthetized through GenScript, in accordance with the sequence available online (NCBI>CCDS Database). Codon optimization was performed by GenScript, and sequence optimized for both human and mouse was selected. Both final LV were generated by digesting backbone and insert with NheI HF - SalI HF (New England Biolabs). LV Anti-sense *hLDLR* (both standard and co) were generated using LV anti-sense ET-GFP-wpre as backbone (unpublished). GFP was replaced with hLDLR or co.*hLDLR* using NheI HF – SalI HF. *mLdlr* cDNA sequences were synthetized through GenScript in accordance with the sequence available online (NCBI>CCDS Database). Codon optimization was performed by GenScript, and sequence optimized for mouse was selected. LV sense-oriented *ET-mLdlr*-wpre* (both standard and co) were generated starting from LV-*ET-FIX* Padua-*wpre** (*Cantore et al, 2015)*, by substituting *FIX* sequence with *LDLR* sequence. *FIX* was removed BsiWI HF – SalI HF and replaced with *mLdlr* BsiWI HF – XhoI (XhoI is compatible with SalI). LV anti-sense-oriented *ET-mLdlr-wpre** (both standard and co) were generated starting from LV anti-sense *ET-co.FVIII-wpre** (unpublished), by substituting *FVIII* sequence with *mLdlr* sequence. *FVIII* was removed MluI HF – SalI HF and replaced with *mLdlr* MluI HF – XhoI (XhoI is compatible with SalI). LV sense-oriented *U6-Cypor shRNA-ET-co.hFIX* Padua-*wpre** was generated starting from LV - sense oriented *U6-Cypor shRNA-ET-coFIX-wpre** (Vonada *et al.*, 2021), by substituting coFIX sequence with co.*hFIX*.Padua sequence (NheI HF – SalI HF). LV sense-oriented *U6-Cypor-shRNA-ET-hFVIII-wpre** was generated starting from LV sense oriented *U6-Cypor* shRNA-co.*FIX*.Padua sequence, used as backbone (NheI HF – SalI HF). Co.*FIX*.Padua was replaced with *FVIII* NheI HF– SalI HF deriving from LV-*FVIII-wpre** (Milani *et al.*, 2022).

5.2 Plasmid DNA purification

Large-scale amounts of plasmids DNA, required during vector generation, were obtained using Machaery-Nagel-endotoxin-free high purity plasmid maxi preparation system. Purification was performed in accordance with manufacture's instructions. Plasmids were subsequently resuspended in TE (10mM TrisHCl, pH8, 1 mM EDTA). Packaging and envelope plasmids were generated by Nature Technology Corporation. Small-scale amounts of plasmids DNA, required during screening of colonies following cloning, were obtained using Wizard® Plus SV Minipreps DNA Purification System (Promega). Colonies were subsequently screened by enzymatic digestion and sequencing.

5.3 Cell line cultures

Human embryonic kidney 293 cells, expressing the large T antigen (HEK293T) were employed for vector production and titration. They were cultured in Iscove's modified Dulbecco's medium (IMDM, Corning), supplemented with penicillin/streptomycin (100 international units, IU/mL), Lonza. 10% fetal bovine serum (FBS, Euroclone) was added. Human hepatoma cells (Huh7) and murine Hepa1.6 hepatoma cells, used for *ex vivo* assessment of transduction efficiency, were subjected to the same culture conditions as HEK293T. The two cell lines were kept in incubators humidified (37°C, 5% CO2). The two cell lines were detached using PBS 0.05% trypsin 4mM EDTA.

5.4 LV production

Third generation SIN LV were generated through calcium-phosphate based HEK 293T transfection. 24h prior transfection, 8-10 million cells were seeded in a 15cm plate (or 4-6 in a 10 cm plate). Medium was changed with 22.5mL of fresh one, 2 hours prior transfection. Cells were transfected with a mix containing the plasmids required, resuspended in 0.1X TE-supplemented cell culture grade water (Sigma), to a final volume of 1.25 mL per dish. Plasmids amounts were the following: pMDL/RRE, 12.5 µg/plate; pCMV.REV, 6.25 µg/plate; PMD2.VSV.G or pBA.AcMNPV.gp64, 9 µg/plate; pAdvantage plasmid, 15 µg/plate; transfer plasmid, 35 µg/plate. In case of further addition of *PCSK9* plasmid (either pMD2.*PCSK9* or pMax.*PCSK9*), its amount per plate was 15 µg. Plasmid mix was aliquoted in 15 mL tubes (one tube per one dish) pre-filled with 150 µL $CaCl_2$ 2.5 M. Then, transfection was achieved through dropwise addition of

1.25 mL of 2X HBS (100 mM Hepes, 281 mM Nacl, 1.5 mM Na_2HPO_4, pH 7.12, prepared *in house*) to each tube, followed by the transfer of the entire volume into the culture medium of a HEK293T plate. Cultured medium was replaced with fresh one 14-16 hours post transfection. LV was collected after additional 30 hours, filtered (0.22 µm, Millipore) and ultra-centrifuged (Beckman Optima XL-100K Ultracentrifuge) for 2 hours, using polyallomer tubes (Beckman), at 20 000 g at 20°C. LV-containing pellets were resuspended in PBS, reaching a concentration of 500X, pooled, aliquoted and stored at -80° before being titrated.

Concerning the experiments where to be transfected were 10 cm plates: 4-6 million cells were seeded 24 hours before; medium was replaced, 2 hours prior transfection, with 10 mL of fresh one; medium was replaced, 14-16 hours after transfection, with 8 mL of fresh one. Plasmids amounts were the following: pMDL/RRE, 5 µg/plate; pCMV.REV, 2.5 µg/plate; PMD2.VSV.G or pBA.AcMNPV.gp64, 4 µg/plate; pAdvantage plasmid, 7.5 µg/plate; transfer plasmid, 15 µg/plate. In case of further addition of *PCSK9* plasmid, its amount per plate was 7.5µg. Plasmid mix was aliquoted in tubes pre-filled with 50 µL $CaCl_2$ 2.5 M. Then, 500 µL of 2X HBS were added dropwise to each tube, followed by the transfer of the entire volume into the culture medium of a HEK293T plate. Collection was performed 30 hours post transfection. In this context, titrations were done on non-concentrated cells supernatant.

5.5 LV titration

LV titration was performed as previously described (Milani *et al.*, 2022). LV titer was determined by assessing integrated copies of LV, by droplet digital PCR (ddPCR) in HEK293T cells, transduced and kept in culture for 10 days. 75 000 HEK293T cells were seeded in 6 wells plates one day prior transduction, assuming them to be 100 000 at the time of transduction. They were then transduced with 10-fold serial dilutions (ranging from 10^{-3} to 10^{-7}) of LV, prepared in fresh medium in the presence of polybrene (at a final concentration of 8 µg/mL. 10 days after transduction, i.e. following dilutions/loss of plasmids, which could alter the result, contained in the LV prep, the cells were collected and the their DNA extracted.

5.6 ddPCR and VCN determination

VCN was determined as previously described (Milani *et al.*, 2022). Extraction of genomic DNA (gDNA) from transduced cells lines and mice organs was obtained through Maxwell 16 or Maxwell 48 DNA purification kit (Promega), in accordance with manufacturer's instructions. gDNA from primary liver murine sorted subpopulations was extracted through QIAamp DNA micro kit (Qiagen) or QIAamp DNA mini kit (Qiagen), in accordance with manufacturer's instructions. VCN per diploid genome was defined starting from 15-20 ng DNA, following the reading through QX200 Droplet Digital PCR System (Biorad), in accordance with the manufacturer's recommendations (usage of each of the primers at concentration of 900 nM, probe at 250 nM). Primers and probes sequences used for LV detection were the following:

- HIV Fw: 5'-TACTGACGCTCTCGCACC-3'
- HIV Rv: 5'- TCTCGACGCAGGACTCG-3'
- HIV Pr 5'-(FAM)-ATCTCTCTCCTTCTAGCCTC-(MGBNFQ)-3'

They were designed to bind the primer binding site (PBS) present in all LV.

To quantify human gDNA, GAPDH was used (Applied Biosystems Hs00483111_cn). To quantify murine gDNA, Semaphorin 3A (Sem3A) was used. Primers and probes sequences to detect Sem3A were the following:

- Sema Fw: 5'- ACCGATTCCAGATGATTGGC-3'
- Sema Rv: 5'- TCCATATTAATGCAGTGCTTGC-3'
- Sema Pr: 5'-(HEX)-AGAGGCCTGTCCTGCAGCTCATGG-(BHQ1)-3'

For VCN determination, the following formula was employed: $VCN = \frac{ng\ LV}{ng\ gDNA} 2$. Infectious titer was calculated with the formula $TU/_{ml} = \frac{VCN \times 100.000}{1/dilution\ factor}$. LV physical particles were measured by p24 ELISA assay (Perkin Elmer). Infectivity was determined as the ratio between infectious titer and physical particles.

5.7 Gene expression assays

Murine organs, murine primary sorted hepatocytes and LSEC were stored at -80°C in RLT+ buffer (Qiagen) solution, suggested for RNA extraction. In case of organs, 300 µl of RLT+ were added every 25 mg tissue piece. In case of cells, 250 µl of RLT+ were

added by default. Organs were homogenized using gentleMACS™ M Tubes (MACS Miltenyi Biotec, 130096335). Tubes were inserted in gentleMACS™ Octo Dissociator (Miltenyi Biotec) and protocol selected was gentleMACS program RNA_02, suggested for frozen tissues. Homogenized tissues were subsequently loaded into Maxwell® RSC simplyRNA tissue cartridges and RNA was extracted using simplyRNA tissue method.

Cells RNA was extracted using RNeasy+ mini kit (Qiagen), in accordance with manufacturer's instructions. DNA was digested on columns through RNase-Free DNase Set (Qiagen). Retro transcription was performed using SuperScript IV VILO Master Mix with EzDNase Enzyme (Thermo Fisher), in accordance with manufacturer's instruction. Each sample was retro-transcribed in two wells, one containing the enzyme (RT+), and one without the enzyme (RT-). cDNA was analyzed by ddPCR as described above, using probe systems. RT- signal was subtracted from RT+ signal, resulting in true signal. For LV derived *Wpre**, *mLdlr*, co.*mLDLR*, custom primers and probe were used. For all the other genes, commercially available primers and probes were used. As normalizer, commercial *Hprt* primers and probe were used. Gene expression levels were calculated with the formula $ng\ cDNA\ gene/ng\ cDNA\ normalizer$.

Custom primers and probe, designed and used, were the following:

- *Wpre** Fw: 5'- GGCTGTTGGGCACTGACAAT -3'
- *Wpre** Rv: 5'- ACGTCCCGCGCAGAATC -3'
- HIV Pr 5'-(FAM)- TTTCCATGGCTGCTCGCCTGTGT -(MGB)-3'

- *mLdlr* Fw: 5'- CCATCCTGGCTTCGGCAA -3'
- *mLdlr* Rv: 5'- AGGAACTGGCGGCTGAAG -3'
- *mLdlr* Pr: 5'-FAM- GAGCTCGTCCTCTGTGGTCT -(MGB)-3'

- co.*mLdlr* Fw: 5'- GTAGCCATCCTGAGACCTGC -3'
- co.*mLdlr* Rv: 5'- GCTGTGGAGGAATTGGAGAC -3'
- co.*mLdlr* Pr:5'-FAM- GATGTGCAGCTCGTCCTCTG -(MGB)-3'

Commercial Biorad gene expression assays used were the following:

Ldlr	Mus Musculus, dMmuCPE5122114, FAM
Vldlr	Mus Musculus, dMmuCPE5114942, FAM
Lrp1	Mus Musculus, dMmuCPE5113466, FAM
Lrp1b	Mus Musculus, dMmuCPE5114778, FAM
Lrp2	Mus musculus, dMmuCPE5121668, FAM
Lrp4	Mus Musculus, dMmuCPE5195296, FAM
Lrp5	Mus Musculus, dMmuCPE5119884, FAM
Lrp6	Mus Musculus, dMmuCPE5098188, FAM
Sorl1	Mus Musculus, dMmuCPE5103740, FAM
Hprt	Mus Musculus, dMmuCPE5095493, VIC

5.8 Flow cytometry

Flow cytometry analyses were performed using FACSCanto analyzer (BD Biosciences), equipped with DIVA Software, as previously described (Milani *et al.*, 2022). Around 500 000 Huh7 and Hepa1.6 cells were harvested and washed with PBS. Staining was conducted in MACS buffer, incubating Huh7 and Hepa1.6 cells with *hLDLR* antibody for 20 minutes at 4°C. No rainbow beads (BD Biosciences) were used for calibration of the instrument detector, since hLDLR on Huh7 and Hepa1.6 was checked in a single experiment.

Data analysis was performed using FCS Express 6 software.

Antigen	*Fluorochrome*	*Clone*	*Company*	*Dilution*
hLDLR	APC	FAB2148A	R&D Systems	1:10

5.9 Mice experiments

Founder B6; 129S-7-Ldlr^{tm1Her}/J mice (referred to, in this thesis, as *Ldlr*$^{-/-}$) (Ishibashi *et al*, 1993), were obtained from the Jackson Laboratories (stock #:002207). Founder B6;129S-*F8*^{tm1Kaz}/J mice (referred to as HemoA or *F8* KO) (Bi *et al*, 1995) were obtained

from Jackson Laboratories (stock #004424). Founder *F8*^{tm1Kaz} Tg(Alb-F8*R593C)T4Mcal/J mice (referred to as HemoA-R593C) (Bril *et al.*, 2006) were obtained from The Jackson Laboratories (stock #017706). C57BL/6 mice were purchased from Jackson laboratories (stock #000664). NOD mice were purchased from Jackson Laboratories (stock #001976). Founder B6; 129S7-Rag1^{t1Mom}/J mice (referred to as *Rag1*$^{-/-}$ (Mombaerts *et al*, 1992) were obtained from Jackson Laboratories (stock #002216). *Ldlr*$^{-/-}$*-Rag1*$^{-/-}$ were generating by crossing *Ldlr*$^{-/-}$ homozygous mice with *Rag1*$^{-/-}$ homozygous mice. Starting from ear biopsies, genotype was determined following DNA extraction, using Maxwell 16 Mouse Tail DNA Purification Kit (Promega), in accordance with manufacturer's instructions. Thermal cycles used were the ones suggested in the protocols available in Jackson website. All mice were kept in specific pathogen free conditions. LV was administered in adult mice, males and females (7-10-weeks of age), through either tail vein or retro-orbital plexus (250 – 500 µL/mouse). LV was administered in newborn mice through temporal vein (25-30 µL/mouse). LV was administered in juvenile mice (2 weeks of age) through retro-orbital plexus (100 – 200 µL/mouse). Mice were bled from the retro-orbital plexus through capillary tubes. Blood was collected in 0.38% sodium citrate buffer, pH 7.4. Mice were euthanized by cervical dislocation at the scheduled time. All the procedures performed on mice were approved by Institutional Animal Care and Use Committee.

For fasting experiments, mice were starved for the number of hours indicated and then treated or not with LV.

For experiments with Bortezomib (Velcade), the drug (1mg/kg) was administered, once diluted in saline, i.v. 1 hour before LV administration.

For experiments with MarI (antiIFNARI Ab, clone MARI-5A3, Merk), the drug (1mg/kg) was administered, once diluted in saline, i.v. 3 hours before LV administration.

For the experiment with Rapamycin (CAS 53123-88-9 Calbiochem), the drug (3-6mg/kg) was administered, once diluted in ethanol, i.v. 2 hours before LV administration.

5.10 Paracetamol preparation and selection protocol

Acetaminophen (paracetamol; Sigma-Aldrich), was dissolved in saline at 13 mg/mL, filtered 0.22 µm and stored at room temperature for up to 1.5 month, or until precipitates formation was observed. Selection protocol was performed as previously described

(Vonada *et al.*, 2021). Mice were fasted overnight (for around 16 hours) before each acetaminophen administration. The morning of each injection, mice were weighted, and acetaminophen was given twice or once weekly. The starting dose of acetaminophen was 225 mg/Kg in males and 250 mg/Kg in females. ALT measurements of ongoing damage were made on bleedings performed 6-7 hours after acetaminophen injection. In case of ALT levels under 300 IU/L, the next dose was increased of 5-10 mg/kg. Once achieved ALT levels >300 IU/L, the dose was generally kept for the rest of the experiment. For most experiments, APAP doses were then kept constant. After fasting, is greater than 15% body weight was lost, APAP treatment was skipped.

5.11 Sorting of liver sub-populations

Fractioning of liver cellular subpopulations was performed as previously described (Milani *et al.*, 2019). Mice were dislocated and then perfused through inferior vena cava. Solutions used for perfusion were the following: PBS 0.5mM EDTA (~10 mL), HBSS (Hank's balanced salt solution, Gibco) 1% HEPES (4-(2-hydroxyethyl)-1-piperazineethanesulfonic acid) (~10 mL), HBSS 1% HEPES 0.03% collagenase IV (Sigma) (~16.5 ml). Livers were harvested and passed through a 100 μm cell strainer (BD Biosciences). Cellular suspension was centrifuged three times at 30, 25, 20 g for 3 minutes, to separate parenchymal cells (pelleted) from non-parenchymal cells, nPC (in the supernatant). Supernatant was centrifuged 7 minutes at 650g. Then, the cells were loaded in a Percol gradient 30%-60% and centrifuged 15 minutes at 1800g. nPC interface was collected and washed twice with HBSS 1% HEPES. Hepatocytes fraction was stained with the following antibodies, diluted in PBS, in 200μl of volume:

Antigen	*Fluorochrome*	*Clone*	*Company (code)*	*Volume*
CD31	APC	MEC 13.3	BD Biosciences (551262)	3 μl
CD45	APC	30-F11	BD Biosciences (559864)	3 μl
FC Block		2.4G2	BD Biosciences (553142)	5 μl

Hepatocytes were cleared from contaminants using FACAria Fusion (BD Biosciences).

nPC fraction was first incubated with FC Block and then stained with the following mix of antibodies, diluted in PBS, in 200 µl of volume:

Antigen	*Fluorochrome*	*Clone*	*Company (code)*	*Volume*
CD31	FITC	MEC 13.3	BD Biosciences (551262)	7 µl
CD45	e-fluor 450	30-F11	Invitrogen (48-0451-82)	7 µl
F4/80	PE	CI:A3-1	BD Biosciences (553142)	7 µl
CD45R/B220	PE-Cy5	RA3-6B2	BD Biosciences (553091)	7 µl
CD11c	PE-Cy7	N418	Invitrogen (25-0114-82)	7 µl

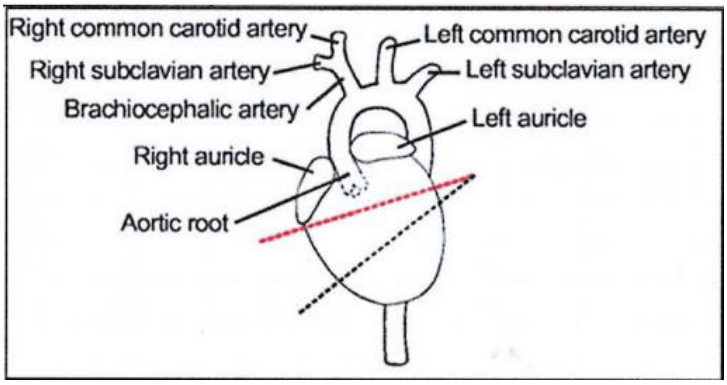
nPC subpopulations (LSEC, KC, pDC) were sorted by FACS, MOFLO-DAKO-Beckman Coulter.

5.12 Total cholesterol and LDL-C measurements

Mouse blood was centrifuged 5500 rpm for 15 minutes to collect serum, which was stored at -80°C. Cholesterol (#0018250540) and LDL-C (#0018256040) were used for the quantitative determination of the serum level with an International Federation of Clinical Chemistry and Laboratory Medicine optimized kinetic ultraviolet (UV) method in an ILab650 chemical analyzer (Instrumentation Laboratory), and there are expressed as mg/dl. SeraChem Control Level 1 and Level 2 (#0018162412 and #0018162512) were analyzed as quality control.

5.13 Aorta and liver collection for histopathology analysis

Mice were sacrificed through cervical dislocation. Mice were than perfused via left ventricle with the following solutions at subsequent steps: i) PBS EDTA (0.5 mM), 15mL ii) PFA (Paraformaldehyde, 50mL). Aorta, still attached to the heart, was subsequently dissected, and the tissue covering aorta removed. Liver and heart with aortic arch and thoracic (descending) aorta were stored in formalin and delivered to Pathology laboratory of GLP SR Tiget Test Facility. Samples were then processed as previously described (Cristofori *et al*, 2004). Livers were trimmed, embedded in paraffin wax, sectioned, mounted on glass slides and stained with hematoxylin and eosin (H&E). Aortic arch and descending thoracic aorta were cut; the heart was sectioned transversely just below the level of the atria (see red dotted line image below). Sequential 3-4 µm sections were cut from the apex towards the base of the heart. Every second serial section of the aortic root for each animal, over a distance of about 250 µm, was taken and the slides were stained with H&E, to see aortic valve leaflets.



Histopathological changes graded on a scale 1-5 as minimal (1), mild (2), moderate (3), marked (4), very marked (5); minimal referred to the least extent discernible and marked the greatest extent possible. The slides were independently peer-reviewed by an experienced pathologist, and a consensus reached on the findings and scores.

5.14 In vitro transduction experiments

HuH7 cells and Hepa1.6 cells were maintained under 37°C, 5% CO2 condition in Iscove's Modified Dulbecco's Medium (IMDM) supplemented with 10% FBS (Thermo Fisher Scientific, Waltham, MA). Cells were seeded into 6-well plates (1.5×10^5

cells/well) and transduced with LV variants at different MOI. Ten days post-LV transduction, cells were harvested and VCN was measured.

5.15 Dietary regimens

Starting from 4 weeks of age, all mice were fed ad libitum with VRF1 (P) by Special Diet Services. For the experiment with Western Diet Challenge, mice started being fed ad libitum with Envigo TD.88137 (0.2% total cholesterol) for three months. After that, they were put back on VRF1.

5.16 Mass spectrometry on caffeine and on its metabolites

Murine serum samples (50 µl) were spiked with 20 µl of $13C_3$-caffeine at 1 ng/µl and 28.5 µl of theobromine-d6 at 2.85 ng/µl. Theobromine, theophylline & paraxanthine and caffeine were quantified according to Mendes VM et al. (Mendes *et al*, 2019), with some modifications. Protein precipitation was performed by using Sirocco protein precipitation plate (Waters) with 150 µl ice-cold methanol added to the spiked samples. After shaking the plate for 1 minute, the vacuum was applied to collect the supernatants that were evaporated under N_2. The samples were resuspended in 100 µl 2% acetonitrile + 0.1 % formic acid and centrifuged at 14000xg for 10 min, transferred in vial and injected (10 µl) for LC-MS/MS analysis. Theobromine, theophylline & paraxanthine and caffeine were quantified in the serum samples by using calibration curves prepared with caffeine and theobromine (from 400 pg to10 ng as final injected quantity) dissolved in serum matrix and $13C_3$-caffeine or theobromine-d6 as internal standard to correct the extraction yield. Levels of each metabolite were profiled by liquid chromatography-mass spectrometry (LC-MS/MS) after 15 minutes, 1h, 5h, 10h, 15h upon caffeine infusion in mice using 4 technical replicates for each time points. Theobromine, theophylline & paraxanthine and caffeine quantification results are reported as ng/ml of serum. Samples were analyzed as previously described (Pieri *et al*, 2023), using the UPLC 1290 (Agilent Technologies) coupled to the TripleTOF 5600+ mass spectrometer (SCIEX) (ProMeFa, Proteomics and Metabolomics Facility, Ospedale San Raffaele, Milan, Italy). Chromatographic separations occurred on C18 column (ACQUITY UPLC HSS T3 column, Waters, 1.8 µm, 2.1 mm x 100 mm). Metabolites were separated using a flow rate set at 0.6 ml/min and a gradient of solvent A (water, 0.1% formic acid) and solvent

B (acetonitrile, 0.1% formic acid). The gradient, in positive mode, started from 2% B, increased up to 10 % B in 4 min, then increased up to 90 % B in 1 min, remained constant at 90% B for 1 min, decreased to 2% B in 0.1 min and remained at 2% B for 2 min. The column was set at 50°C, while the samples were kept at 4°C. Automated calibration was performed using an external calibrant delivery system (CDS) which infuses APCI positive calibration solution every 5 samples injection. Fμll scan spectra were acquired in the mass range from *m*/*z* 50 to 500 and the metabolites were analysed by scheduled product ions for the masses 181.07 (theobromine and theophylline&paraxanhine), 195.08 (caffeine), 187.10 (theobromine-d6) and 198.09 ($13C_3$-caffeine). The masses for each compound and the fragments used for the metabolite quantification are shown in Table 1. The source parameters were: Gas 1: 33 psi, Gas 2: 58 psi, Curtain gas: 35 psi, Temperature: 500 °C and ISVF (IonSpray Voltage Floating): 5500 V, DP: 80 V, CE: 40 V with a spread of 15V. MμltiQuant (version 2.1) from SCIEX was used to create the calibration curves and to quantify the metabolites.

Metabolite Name	Precursor Ion (MH+)	Fragment Ion (MH+)	RT (min)
Theobromine	181.07	138.06	3.19
Theophylline & Paraxanthine	181.07	124.05	3.93
Caffeine	195.08	138.06	5.56
Theobromine-d6	187.10	144.10	3.15
$13C_3$-caffeine	198.09	140.07	5.56

N.B. Theophylline and Paraxanthine were not separately detectable either by RT or by MS or MSMS.

5.17 Electron microscopy

Electron microscopy was performed as previously described (Milani *et al.*, 2017). Few microliters of ultra-centrifugated LV batches were absorbed an on glow discharged

carbon coated formvar copper girds. They were fixed for 20 minutes with paraformaldehyde 4%. Grids were washed in 50mM glycine in PBS and then blocked in 1% BSA in PBS. They were incubated with primary antibodiey anti-109 VSV.G, KeraFAST, 1:50) diluted in blocking buffer for 30-90 minutes. Following wash in 0.1% BSA in PBS, samples were incubated for 30 minutes with Protein A-gold (5 or 10 nm), fixed with 1% glutaraldehyde, stained with 2% uranyl acetate, air dried. The grids were subsequently observed with Zeiss LEO 512 transmission electron microscope. Images were acquired through 2k x 2k bottom-mounted slow-scan Proscan camera, controlled by EsivisionPro 3.2 software. For quantification of labeling density, random images of viral particles were taken at nominal magnification of 16k; gold particles associated to virions were manually counted using ImageJ. Virions were defined based on expected size (approximately 120nm) and an electron-dense core.

5.18 ELISA assays

ELISA assays were performed as previously described (Milani *et al.*, 2022). Mouse blood was centrifuged 6500 rpm for 6.5 minutes for plasma collection, then stored at -80°C. The concentration of human FVIII was determined in mouse plasma by an enzyme-linked immunosorbent assay (ELISA) specific for human FVIII antigen. Microtiter plates were coated with anti-hFVIII binding Ab (Green Mountain Antibodies #GMA8016, 0.2 µg/well in 0.1 M carbonate buffer, pH 9.6) over night at 4°C and then blocked 1 hour at room temperature with blocking buffer (PBS 0.05% Tween-20, 1M NaCl, 10% heat inactivated horse serum, Gibco). Plasma samples are diluted as needed starting from 1:10 in blocking buffer, added to wells (100µL/well) and incubated 2 hours at 37°C. hFVIII was detected by adding detection Ab (Affinity Biologicals, F8C-EIC-D) 1 hour at 37°C, followed by 5-10 minutes incubation with 100µL/well of TMB substrate (Surmodics). Reaction was blocked with HCl 1N (50µL/well) and absorbance of each sample was determined spectrophotometrically at 450nm, using a Multiskan GO microplate reader (Thermo Fisher Scientific) and normalized to antigen standard curve (ReFACTO, Pfizer, from 25ng/mL to 0.39ng/mL serially diluted 1:2 in blocking buffer; dilution was corrected with 10% HemoA murine plasma).

hFIX ELISA assay was used to assess hFIX concentration in mouse plasma samples (Affinity Biologicals, FIX-EIA), in accordance with manufacturer's protocol.

Absorbance of each sample was determined spectrophotometrically, using a Multiskan GO microplate reader (Thermo Fisher Scientific) and normalized to antigen standard curves.

5.19 Immunofluorescence imaging

Livers were harvested from mice, washed with PBS and fixed 4 hours in PBS 4% paraformaldehyde (PFA), then washed again in PBS before storage for at least 24 hours in 30% sucrose 0.02% sodium azide in H_2O. Livers were then frozen in OCT (optimal cutting temperature) compound (Killik, Bio Optica) and slices 5 µm thick were cut at cryostat (Histo-line MC5050), placed on Superfrost® Plus microscope slides (Thermo Scientific) and stored at -80°C. All the staining steps were performed protected from lights to preserve endogenous fluorescence. Slides were thawed at room temperature for at least 2 hours, then washed 3 times 5 minutes in PBS 0.1% X-Triton. Edges were drawn around the tissue using immunostaining pap pen (Sigma-Aldrich) to contain staining solutions. Blocking step was performed using PBS 0.1% X-Triton 1% bovine serum albumin (BSA) 5% FBS for 1 hour at room temperature in a humid chamber. Blocking solution was then substitute with mix containing primary antibodies in blocking solution and incubation was carried on for 12-16 hours at 4°C in a humid chamber. Primary antibodies mix solution was removed and slides were washed 3 times 5 minutes in PBS 0.1% X-Triton. Secondary antibodies were diluted in blocking solution together with Hoechst (Invitrogen, 1:20 000) and incubated for 1 hour at room temperature in a humid chamber. Slides were then washed in PBS and coverslip was added using Fluoromount-G (Invitrogen) as mounting medium. Slides were dried for 16 hours at room temperature or for longer at 4°C, and stored at 4°C before acquisition. The following antibodies were used for immunofluorescence staining:

Anti-mLDLR rabbit, monoclonal (Thermofisher MA5 29725, 1:500)

Anti-GFP rabbit, polyclonal (Invitrogen, A11122, 1:1000)

Anti-GFP chicken, polyclonal (Abcam, ab13970, 1:200)

Anti-Rabbit IgG Alexa Fluor (AF)647 donkey, polyclonal (Invitrogen, 1:1000)

Anti-Chicken IgY Alexa Fluor (AF)488 goat, polyclonal (Invitrogen, 1:1000)

Images were acquired using confocal microscope Leica TCS SP5, Leica TCS SP8 or Mavig Rs-G4 at 20X or 40X magnification. Images were analyzed using Image J or MATLAB software. A custom written Matlab pipeline was used to analyse the images. Briefly, for all the channels (LDLR, GFP positive and nuclei) we extract black and white masks of the cells/nuclei by background subtraction and then applying a fixed threshold. A mask of the tissue is obtained similarly on the image calculated as max projection across all the channels.

6. REFERENCES

Abifadel M, Varret M, Rabes JP, Allard D, Ouguerram K, Devillers M, Cruaud C, Benjannet S, Wickham L, Erlich D *et al* (2003) Mutations in PCSK9 cause autosomal dominant hypercholesterolemia. *Nat Genet* 34: 154-156

Adam RC, Mintah IJ, Alexa-Braun CA, Shihanian LM, Lee JS, Banerjee P, Hamon SC, Kim HI, Cohen JC, Hobbs HH *et al* (2020) Angiopoietin-like protein 3 governs LDL-cholesterol levels through endothelial lipase-dependent VLDL clearance. *J Lipid Res* 61: 1271-1286

Adhyaru BB, Jacobson TA (2018) Safety and efficacy of statin therapy. *Nat Rev Cardiol* 15: 757-769

Al-Allaf FA, Abduljaleel Z, Athar M, Taher MM, Khan W, Mehmet H, Colakogullari M, Apostolidou S, Bigger B, Waddington S *et al* (2019a) Modifying inter-cistronic sequence significantly enhances IRES dependent second gene expression in bicistronic vector: Construction of optimised cassette for gene therapy of familial hypercholesterolemia. *Noncoding RNA Res* 4: 1-14

Al-Allaf FA, Abduljaleel Z, Taher MM, Abdellatif AAH, Athar M, Bogari NM, Al-Ahdal MN, Al-Mohanna F, Al-Hassnan ZN, Alzabeedi KHY *et al* (2019b) Molecular Dynamics Simulation Reveals Exposed Residues in the Ligand-Binding Domain of the Low-Density Lipoprotein Receptor that Interacts with Vesicular Stomatitis Virus-G Envelope. *Viruses* 11

Al-Allaf FA, Coutelle C, Waddington SN, David AL, Harbottle R, Themis M (2010) LDLR-Gene therapy for familial hypercholesterolaemia: problems, progress, and perspectives. *Int Arch Med* 3: 36

Alonso R, Cuevas A, Mata P (2019) Lomitapide: a review of its clinical use, efficacy, and tolerability. *Core Evid* 14: 19-30

Altmann SW, Davis HR, Jr., Zhu LJ, Yao X, Hoos LM, Tetzloff G, Iyer SP, Maguire M, Golovko A, Zeng M *et al* (2004) Niemann-Pick C1 Like 1 protein is critical for intestinal cholesterol absorption. *Science* 303: 1201-1204

Anan A, Baskin-Bey ES, Isomoto H, Mott JL, Bronk SF, Albrecht JH, Gores GJ (2006) Proteasome inhibition attenuates hepatic injury in the bile duct-ligated mouse. *Am J Physiol Gastrointest Liver Physiol* 291: G709-716

Annoni A, Gregori S, Naldini L, Cantore A (2019) Modulation of immune responses in lentiviral vector-mediated gene transfer. *Cell Immunol* 342: 103802

Aronson SJ, Veron P, Collaud F, Hubert A, Delahais V, Honnet G, de Knegt RJ, Junge N, Baumann U, Di Giorgio A *et al* (2019) Prevalence and Relevance of Pre-Existing Anti-Adeno-Associated Virus Immunity in the Context of Gene Therapy for Crigler-Najjar Syndrome. *Hum Gene Ther* 30: 1297-1305

Ason B, van der Hoorn JW, Chan J, Lee E, Pieterman EJ, Nguyen KK, Di M, Shetterly S, Tang J, Yeh WC *et al* (2014) PCSK9 inhibition fails to alter hepatic LDLR, circulating cholesterol, and atherosclerosis in the absence of ApoE. *J Lipid Res* 55: 2370-2379

Barter PJ, Caulfield M, Eriksson M, Grundy SM, Kastelein JJ, Komajda M, Lopez-Sendon J, Mosca L, Tardif JC, Waters DD *et al* (2007) Effects of torcetrapib in patients at high risk for coronary events. *N Engl J Med* 357: 2109-2122

Bays HE, Moore PB, Drehobl MA, Rosenblatt S, Toth PD, Dujovne CA, Knopp RH, Lipka LJ, Lebeaut AP, Yang B *et al* (2001) Effectiveness and tolerability of ezetimibe in patients with primary hypercholesterolemia: pooled analysis of two phase II studies. *Clin Ther* 23: 1209-1230

Belalcazar LM, Merched A, Carr B, Oka K, Chen KH, Pastore L, Beaudet A, Chan L (2003) Long-term stable expression of human apolipoprotein A-I mediated by helper-dependent adenovirus gene transfer inhibits atherosclerosis progression and remodels atherosclerotic plaques in a mouse model of familial hypercholesterolemia. *Circulation* 107: 2726-2732

Bellinger A, Rhode E, Kathiresan S (2022) SEQUENTIAL IN VIVO CRISPR BASE EDITING OF THE PCSK9 AND ANGPTL3 GENES IN NON-HUMAN PRIMATES. *Journal of the American College of Cardiology* 79: 953-953

Berg P, Mertz JE (2010) Personal reflections on the origins and emergence of recombinant DNA technology. *Genetics* 184: 9-17

Bergmark BA, Marston NA, Bramson CR, Curto M, Ramos V, Jevne A, Kuder JF, Park JG, Murphy SA, Verma S *et al* (2022) Effect of Vupanorsen on Non-High-Density Lipoprotein Cholesterol Levels in Statin-Treated Patients With Elevated Cholesterol: TRANSLATE-TIMI 70. *Circulation* 145: 1377-1386

Bi L, Lawler AM, Antonarakis SE, High KA, Gearhart JD, Kazazian HH, Jr. (1995) Targeted disruption of the mouse factor VIII gene produces a model of haemophilia A. *Nat Genet* 10: 119-121

Bideyan L, Nagari R, Tontonoz P (2021) Hepatic transcriptional responses to fasting and feeding. *Genes Dev* 35: 635-657

Bissig-Choisat B, Wang L, Legras X, Saha PK, Chen L, Bell P, Pankowicz FP, Hill MC, Barzi M, Leyton CK *et al* (2015) Development and rescue of human familial hypercholesterolaemia in a xenograft mouse model. *Nat Commun* 6: 7339

Bjornsson E, Gunnarsdottir K, Halldorsson GH, Sigurdsson A, Arnadottir GA, Jonsson H, Olafsdottir EF, Niehus S, Kehr B, Sveinbjornsson G *et al* (2021) Lifelong Reduction in LDL (Low-Density Lipoprotein) Cholesterol due to a Gain-of-Function Mutation in LDLR. *Circ Genom Precis Med* 14: e003029

Blair HA (2022) Valoctocogene Roxaparvovec: First Approval. *Drugs* 82: 1505-1510

Blom DJ, Harada-Shiba M, Rubba P, Gaudet D, Kastelein JJP, Charng MJ, Pordy R, Donahue S, Ali S, Dong Y *et al* (2020) Efficacy and Safety of Alirocumab in Adults With Homozygous Familial Hypercholesterolemia: The ODYSSEY HoFH Trial. *J Am Coll Cardiol* 76: 131-142

Bril WS, van Helden PM, Hausl C, Zuurveld MG, Ahmad RU, Hollestelle MJ, Reitsma PH, Fijnvandraat K, van Lier RA, Schwarz HP *et al* (2006) Tolerance to factor VIII in a transgenic mouse expressing human factor VIII cDNA carrying an Arg(593) to Cys substitution. *Thromb Haemost* 95: 341-347

Brown BD, Sitia G, Annoni A, Hauben E, Sergi LS, Zingale A, Roncarolo MG, Guidotti LG, Naldini L (2007) In vivo administration of lentiviral vectors triggers a type I interferon response that restricts hepatocyte gene transfer and promotes vector clearance. *Blood* 109: 2797-2805

Brown BD, Venneri MA, Zingale A, Sergi Sergi L, Naldini L (2006) Endogenous microRNA regulation suppresses transgene expression in hematopoietic lineages and enables stable gene transfer. *Nat Med* 12: 585-591

Brown MS, Goldstein JL (1974) Familial hypercholesterolemia: defective binding of lipoproteins to cultured fibroblasts associated with impaired regulation of 3-hydroxy-3-methylglutaryl coenzyme A reductase activity. *Proc Natl Acad Sci U S A* 71: 788-792

Browning JD, Horton JD (2010) Fasting reduces plasma proprotein convertase, subtilisin/kexin type 9 and cholesterol biosynthesis in humans. *J Lipid Res* 51: 3359-3363

Cannon CP, Braunwald E, McCabe CH, Rader DJ, Rouleau JL, Belder R, Joyal SV, Hill KA, Pfeffer MA, Skene AM *et al* (2004) Intensive versus moderate lipid lowering with statins after acute coronary syndromes. *N Engl J Med* 350: 1495-1504

Cantore A, Ranzani M, Bartholomae CC, Volpin M, Valle PD, Sanvito F, Sergi LS, Gallina P, Benedicenti F, Bellinger D *et al* (2015) Liver-directed lentiviral gene therapy in a dog model of hemophilia B. *Sci Transl Med* 7: 277ra228

Canuel M, Sun X, Asselin MC, Paramithiotis E, Prat A, Seidah NG (2013) Proprotein convertase subtilisin/kexin type 9 (PCSK9) can mediate degradation of the low density lipoprotein receptor-related protein 1 (LRP-1). *PLoS One* 8: e64145

Carrasquilla GD, Christiansen MR, Kilpelainen TO (2021) The Genetic Basis of Hypertriglyceridemia. *Curr Atheroscler Rep* 23: 39

Cavazzana M, Bushman FD, Miccio A, Andre-Schmutz I, Six E (2019) Gene therapy targeting haematopoietic stem cells for inherited diseases: progress and challenges. *Nat Rev Drug Discov* 18: 447-462

Cesana D, Calabria A, Rudilosso L, Gallina P, Benedicenti F, Spinozzi G, Schiroli G, Magnani A, Acquati S, Fumagalli F *et al* (2021) Retrieval of vector integration sites from cell-free DNA. *Nat Med* 27: 1458-1470

Chan JC, Piper DE, Cao Q, Liu D, King C, Wang W, Tang J, Liu Q, Higbee J, Xia Z *et al* (2009) A proprotein convertase subtilisin/kexin type 9 neutralizing antibody reduces serum cholesterol in mice and nonhuman primates. *Proc Natl Acad Sci U S A* 106: 9820-9825

Chen SH, Habib G, Yang CY, Gu ZW, Lee BR, Weng SA, Silberman SR, Cai SJ, Deslypere JP, Rosseneu M *et al* (1987) Apolipoprotein B-48 is the product of a messenger RNA with an organ-specific in-frame stop codon. *Science* 238: 363-366

Choi SY, Komaromy MC, Chen J, Fong LG, Cooper AD (1994) Acceleration of uptake of LDL but not chylomicrons or chylomicron remnants by cells that secrete apoE and hepatic lipase. *J Lipid Res* 35: 848-859

Cholesterol Treatment Trialists C (2022) Effect of statin therapy on muscle symptoms: an individual participant data meta-analysis of large-scale, randomised, double-blind trials. *Lancet* 400: 832-845

Chowdhury JR, Grossman M, Gupta S, Chowdhury NR, Baker JR, Jr., Wilson JM (1991) Long-term improvement of hypercholesterolemia after ex vivo gene therapy in LDLR-deficient rabbits. *Science* 254: 1802-1805

Cohen J, Pertsemlidis A, Kotowski IK, Graham R, Garcia CK, Hobbs HH (2005) Low LDL cholesterol in individuals of African descent resulting from frequent nonsense mutations in PCSK9. *Nat Genet* 37: 161-165

Cohen JC, Boerwinkle E, Mosley TH, Jr., Hobbs HH (2006) Sequence variations in PCSK9, low LDL, and protection against coronary heart disease. *N Engl J Med* 354: 1264-1272

Cooper AD (1997) Hepatic uptake of chylomicron remnants. *J Lipid Res* 38: 2173-2192

Cristofori P, Crivellente F, Campagnola M, Pasini AF, Garbin U, Rigoni A, Tosetti M, Turton J, Faustinelli I, Cominacini L (2004) Reduced progression of atherosclerosis in apolipoprotein E-deficient mice treated with lacidipine is associated with a decreased susceptibility of low-density lipoprotein to oxidation. *Int J Exp Pathol* 85: 105-114

Cuchel M, Bruckert E, Ginsberg HN, Raal FJ, Santos RD, Hegele RA, Kuivenhoven JA, Nordestgaard BG, Descamps OS, Steinhagen-Thiessen E *et al* (2014) Homozygous familial hypercholesterolaemia: new insights and guidance for clinicians to improve detection and clinical management. A position paper from the Consensus Panel on Familial Hypercholesterolaemia of the European Atherosclerosis Society. *Eur Heart J* 35: 2146-2157

Cuchel M, Meagher EA, du Toit Theron H, Blom DJ, Marais AD, Hegele RA, Averna MR, Sirtori CR, Shah PK, Gaudet D *et al* (2013) Efficacy and safety of a microsomal triglyceride transfer protein inhibitor in patients with homozygous familial hypercholesterolaemia: a single-arm, open-label, phase 3 study. *Lancet* 381: 40-46

Dalwadi DA, Calabria A, Tiyaboonchai A, Posey J, Naugler WE, Montini E, Grompe M (2021) AAV integration in human hepatocytes. *Mol Ther* 29: 2898-2909

David RM, Doherty AT (2017) Viral Vectors: The Road to Reducing Genotoxicity. *Toxicol Sci* 155: 315-325

Davis HR, Jr., Hoos LM, Tetzloff G, Maguire M, Zhu LJ, Graziano MP, Altmann SW (2007) Deficiency of Niemann-Pick C1 Like 1 prevents atherosclerosis in ApoE-/- mice. *Arterioscler Thromb Vasc Biol* 27: 841-849

DePolo NJ, Reed JD, Sheridan PL, Townsend K, Sauter SL, Jolly DJ, Dubensky TW, Jr. (2000) VSV-G pseudotyped lentiviral vector particles produced in human cells are inactivated by human serum. *Mol Ther* 2: 218-222

Dewey FE, Gusarova V, Dunbar RL, O'Dushlaine C, Schurmann C, Gottesman O, McCarthy S, Van Hout CV, Bruse S, Dansky HM *et al* (2017) Genetic and Pharmacologic Inactivation of ANGPTL3 and Cardiovascular Disease. *N Engl J Med* 377: 211-221

Doudna JA (2020) The promise and challenge of therapeutic genome editing. *Nature* 578: 229-236

Duan D (2018) Systemic AAV Micro-dystrophin Gene Therapy for Duchenne Muscular Dystrophy. *Mol Ther* 26: 2337-2356

Duisit G, Saleun S, Douthe S, Barsoum J, Chadeuf G, Moullier P (1999) Baculovirus vector requires electrostatic interactions including heparan sulfate for efficient gene transfer in mammalian cells. *J Gene Med* 1: 93-102

Dull T, Zufferey R, Kelly M, Mandel RJ, Nguyen M, Trono D, Naldini L (1998) A third-generation lentivirus vector with a conditional packaging system. *J Virol* 72: 8463-8471

Dunbar CE, High KA, Joung JK, Kohn DB, Ozawa K, Sadelain M (2018) Gene therapy comes of age. *Science* 359

Elovson J, Chatterton JE, Bell GT, Schumaker VN, Reuben MA, Puppione DL, Reeve JR, Jr., Young NL (1988) Plasma very low density lipoproteins contain a single molecule of apolipoprotein B. *J Lipid Res* 29: 1461-1473

Esposito F, Lyubenova H, Tornabene P, Auricchio S, Iuliano A, Nusco E, Merlin S, Olgasi C, Manni G, Gargaro M *et al* (2022) Liver gene therapy with intein-mediated F8 trans-splicing corrects mouse haemophilia A. *EMBO Mol Med* 14: e15199

Feng Y, Li Q, Ou G, Yang M, Du L (2021) Bile acid sequestrants: a review of mechanism and design. *J Pharm Pharmacol* 73: 855-861

Filice G, Cereda PM, Varnier OE (1988) Infection of rabbits with human immunodeficiency virus. *Nature* 335: 366-369

Finkelshtein D, Werman A, Novick D, Barak S, Rubinstein M (2013) LDL receptor and its family members serve as the cellular receptors for vesicular stomatitis virus. *Proc Natl Acad Sci U S A* 110: 7306-7311

Fitzgerald K, Frank-Kamenetsky M, Shulga-Morskaya S, Liebow A, Bettencourt BR, Sutherland JE, Hutabarat RM, Clausen VA, Karsten V, Cehelsky J *et al* (2014) Effect of an RNA interference drug on the synthesis of proprotein convertase subtilisin/kexin type 9 (PCSK9) and the concentration of serum LDL cholesterol in healthy volunteers: a randomised, single-blind, placebo-controlled, phase 1 trial. *Lancet* 383: 60-68

Fitzgerald K, White S, Borodovsky A, Bettencourt BR, Strahs A, Clausen V, Wijngaard P, Horton JD, Taubel J, Brooks A *et al* (2017) A Highly Durable RNAi Therapeutic Inhibitor of PCSK9. *N Engl J Med* 376: 41-51

Follenzi A, Ailles LE, Bakovic S, Geuna M, Naldini L (2000) Gene transfer by lentiviral vectors is limited by nuclear translocation and rescued by HIV-1 pol sequences. *Nat Genet* 25: 217-222

Follenzi A, Battaglia M, Lombardo A, Annoni A, Roncarolo MG, Naldini L (2004) Targeting lentiviral vector expression to hepatocytes limits transgene-specific immune response and establishes long-term expression of human antihemophilic factor IX in mice. *Blood* 103: 3700-3709

Frank-Kamenetsky M, Grefhorst A, Anderson NN, Racie TS, Bramlage B, Akinc A, Butler D, Charisse K, Dorkin R, Fan Y *et al* (2008) Therapeutic RNAi targeting PCSK9 acutely lowers plasma cholesterol in rodents and LDL cholesterol in nonhuman primates. *Proc Natl Acad Sci U S A* 105: 11915-11920

Friedmann T, Roblin R (1972) Gene therapy for human genetic disease? *Science* 175: 949-955

Furberg CD, Pitt B (2001) Withdrawal of cerivastatin from the world market. *Curr Control Trials Cardiovasc Med* 2: 205-207

Getz GS, Reardon CA (2006) Diet and murine atherosclerosis. *Arterioscler Thromb Vasc Biol* 26: 242-249

Goldstein I, Hager GL (2015) Transcriptional and Chromatin Regulation during Fasting - The Genomic Era. *Trends Endocrinol Metab* 26: 699-710

Graham MJ, Lee RG, Brandt TA, Tai LJ, Fu W, Peralta R, Yu R, Hurh E, Paz E, McEvoy BW *et al* (2017) Cardiovascular and Metabolic Effects of ANGPTL3 Antisense Oligonucleotides. *N Engl J Med* 377: 222-232

Greig JA, Limberis MP, Bell P, Chen SJ, Calcedo R, Rader DJ, Wilson JM (2017a) Non-Clinical Study Examining AAV8.TBG.hLDLR Vector-Associated Toxicity in Chow-Fed Wild-Type and LDLR(+/-) Rhesus Macaques. *Hum Gene Ther Clin Dev* 28: 39-50

Greig JA, Limberis MP, Bell P, Chen SJ, Calcedo R, Rader DJ, Wilson JM (2017b) Nonclinical Pharmacology/Toxicology Study of AAV8.TBG.mLDLR and AAV8.TBG.hLDLR in a Mouse Model of Homozygous Familial Hypercholesterolemia. *Hum Gene Ther Clin Dev* 28: 28-38

Grossman M, Rader DJ, Muller DW, Kolansky DM, Kozarsky K, Clark BJ, 3rd, Stein EA, Lupien PJ, Brewer HB, Jr., Raper SE *et al* (1995) A pilot study of ex vivo gene therapy for homozygous familial hypercholesterolaemia. *Nat Med* 1: 1148-1154

Grossman M, Raper SE, Wilson JM (1992) Transplantation of genetically modified autologous hepatocytes into nonhuman primates: feasibility and short-term toxicity. *Hum Gene Ther* 3: 501-510

Gu HM, Adijiang A, Mah M, Zhang DW (2013) Characterization of the role of EGF-A of low density lipoprotein receptor in PCSK9 binding. *J Lipid Res* 54: 3345-3357

Halpern KB, Shenhav R, Matcovitch-Natan O, Toth B, Lemze D, Golan M, Massasa EE, Baydatch S, Landen S, Moor AE *et al* (2017) Single-cell spatial reconstruction reveals global division of labour in the mammalian liver. *Nature* 542: 352-356

He L, Pu W, Liu X, Zhang Z, Han M, Li Y, Huang X, Han X, Li Y, Liu K *et al* (2021) Proliferation tracing reveals regional hepatocyte generation in liver homeostasis and repair. *Science* 371

Heinecke JW (2012) The not-so-simple HDL story: A new era for quantifying HDL and cardiovascular risk? *Nat Med* 18: 1346-1347

Henderson CJ, Otto DM, Carrie D, Magnuson MA, McLaren AW, Rosewell I, Wolf CR (2003) Inactivation of the hepatic cytochrome P450 system by conditional deletion of hepatic cytochrome P450 reductase. *J Biol Chem* 278: 13480-13486

Hirai M, Kadowaki N, Kitawaki T, Fujita H, Takaori-Kondo A, Fukui R, Miyake K, Maeda T, Kamihira S, Miyachi Y *et al* (2011) Bortezomib suppresses function and survival of plasmacytoid dendritic cells by targeting intracellular trafficking of Toll-like receptors and endoplasmic reticulum homeostasis. *Blood* 117: 500-509

Hobbs HH, Russell DW, Brown MS, Goldstein JL (1990) The LDL receptor locus in familial hypercholesterolemia: mutational analysis of a membrane protein. *Annu Rev Genet* 24: 133-170

Hoekstra M, Korporaal SJ, Li Z, Zhao Y, Van Eck M, Van Berkel TJ (2010) Plasma lipoproteins are required for both basal and stress-induced adrenal glucocorticoid synthesis and protection against endotoxemia in mice. *Am J Physiol Endocrinol Metab* 299: E1038-1043

Homer VM, Marais AD, Charlton F, Laurie AD, Hurndell N, Scott R, Mangili F, Sullivan DR, Barter PJ, Rye KA *et al* (2008) Identification and characterization of two non-secreted PCSK9 mutants associated with familial hypercholesterolemia in cohorts from New Zealand and South Africa. *Atherosclerosis* 196: 659-666

Horton JD, Bashmakov Y, Shimomura I, Shimano H (1998) Regulation of sterol regulatory element binding proteins in livers of fasted and refed mice. *Proc Natl Acad Sci U S A* 95: 5987-5992

Horton JD, Goldstein JL, Brown MS (2002) SREBPs: activators of the complete program of cholesterol and fatty acid synthesis in the liver. *J Clin Invest* 109: 1125-1131

Hosel M, Huber A, Bohlen S, Lucifora J, Ronzitti G, Puzzo F, Boisgerault F, Hacker UT, Kwanten WJ, Kloting N *et al* (2017) Autophagy determines efficiency of liver-directed gene therapy with adeno-associated viral vectors. *Hepatology* 66: 252-265

Hovingh GK, Rader DJ, Hegele RA (2015) HDL re-examined. *Curr Opin Lipidol* 26: 127-132

Hu J, Zhang Z, Shen WJ, Azhar S (2010) Cellular cholesterol delivery, intracellular processing and utilization for biosynthesis of steroid hormones. *Nutr Metab (Lond)* 7: 47

Huang JK, Lee HC (2022) Emerging Evidence of Pathological Roles of Very-Low-Density Lipoprotein (VLDL). *Int J Mol Sci* 23

Huang TP, Newby GA, Liu DR (2021) Precision genome editing using cytosine and adenine base editors in mammalian cells. *Nat Protoc* 16: 1089-1128

Innerarity TL, Weisgraber KH, Arnold KS, Mahley RW, Krauss RM, Vega GL, Grundy SM (1987) Familial defective apolipoprotein B-100: low density lipoproteins with abnormal receptor binding. *Proc Natl Acad Sci U S A* 84: 6919-6923

Ishibashi S, Brown MS, Goldstein JL, Gerard RD, Hammer RE, Herz J (1993) Hypercholesterolemia in low density lipoprotein receptor knockout mice and its reversal by adenovirus-mediated gene delivery. *J Clin Invest* 92: 883-893

Ishigaki Y, Kawagishi N, Hasegawa Y, Sawada S, Katagiri H, Satomi S, Oikawa S (2019) Liver Transplantation for Homozygous Familial Hypercholesterolemia. *J Atheroscler Thromb* 26: 121-127

Islam SMT, Osa-Andrews B, Jones PM, Muthukumar AR, Hashim I, Cao J (2022) Methods of Low-Density Lipoprotein-Cholesterol Measurement: Analytical and Clinical Applications. *EJIFCC* 33: 282-294

Kaiser J (2022) A gentler way to tweak genes: epigenome editing. *Science* 376: 1034-1035

Kang Y, Xie L, Tran DT, Stein CS, Hickey M, Davidson BL, McCray PB, Jr. (2005) Persistent expression of factor VIII in vivo following nonprimate lentiviral gene transfer. *Blood* 106: 1552-1558

Kankkonen HM, Vahakangas E, Marr RA, Pakkanen T, Laurema A, Leppanen P, Jalkanen J, Verma IM, Yla-Herttuala S (2004) Long-term lowering of plasma cholesterol levels in LDL-receptor-deficient WHHL rabbits by gene therapy. *Mol Ther* 9: 548-556

Kapelanski-Lamoureux A, Chen Z, Gao ZH, Deng R, Lazaris A, Lebeaupin C, Giles L, Malhotra J, Yong J, Zou C *et al* (2022) Ectopic clotting factor VIII expression and

misfolding in hepatocytes as a cause for hepatocellular carcinoma. *Mol Ther* 30: 3542-3551

Kasiewicz LN, Biswas S, Beach A, Ren H, Dutta C, Mazzola AM, Rohde E, Chadwick A, Cheng C, Musunuru K *et al* (2021) Lipid nanoparticles incorporating a GalNAc ligand enable in vivo liver ANGPTL3 editing in wild-type and somatic LDLR knockout non-human primates. *bioRxiv*: 2021.2011.2008.467731

Kassim SH, Li H, Bell P, Somanathan S, Lagor W, Jacobs F, Billheimer J, Wilson JM, Rader DJ (2013) Adeno-associated virus serotype 8 gene therapy leads to significant lowering of plasma cholesterol levels in humanized mouse models of homozygous and heterozygous familial hypercholesterolemia. *Hum Gene Ther* 24: 19-26

Kathiresan S, Melander O, Guiducci C, Surti A, Burtt NP, Rieder MJ, Cooper GM, Roos C, Voight BF, Havulinna AS *et al* (2008) Six new loci associated with blood low-density lipoprotein cholesterol, high-density lipoprotein cholesterol or triglycerides in humans. *Nat Genet* 40: 189-197

Keam SJ (2022) Eladocagene Exuparvovec: First Approval. *Drugs* 82: 1427-1432

Khera A, Lee R, Rohde E, Jayaram H, Kathiresan S, Bellinger A (2022) An in vivo CRISPR base editing therapy to inactivate the ANGPTL3 gene: nomination of a development candidate for VERVE-201. *European Heart Journal* 43

Kingsman SM, Mitrophanous K, Olsen JC (2005) Potential oncogene activity of the woodchuck hepatitis post-transcriptional regulatory element (WPRE). *Gene Ther* 12: 3-4

Koishi R, Ando Y, Ono M, Shimamura M, Yasumo H, Fujiwara T, Horikoshi H, Furukawa H (2002) Angptl3 regulates lipid metabolism in mice. *Nat Genet* 30: 151-157

Lagace TA, Curtis DE, Garuti R, McNutt MC, Park SW, Prather HB, Anderson NN, Ho YK, Hammer RE, Horton JD (2006) Secreted PCSK9 decreases the number of LDL receptors in hepatocytes and in livers of parabiotic mice. *J Clin Invest* 116: 2995-3005

Leborgne C, Barbon E, Alexander JM, Hanby H, Delignat S, Cohen DM, Collaud F, Muraleetharan S, Lupo D, Silverberg J *et al* (2020) IgG-cleaving endopeptidase enables in vivo gene therapy in the presence of anti-AAV neutralizing antibodies. *Nat Med* 26: 1096-1101

Lee J, Hegele RA (2014) Abetalipoproteinemia and homozygous hypobetalipoproteinemia: a framework for diagnosis and management. *J Inherit Metab Dis* 37: 333-339

Lee RG, Mazzola AM, Braun MC, Platt C, Vafai SB, Kathiresan S, Rohde E, Bellinger AM, Khera AV (2022) Efficacy and Safety of an Investigational Single-course CRISPR Base Editing Therapy Targeting PCSK9 in Non-human Primate and Mouse Models. *Circulation*

Leebeek FWG, Miesbach W (2021) Gene therapy for hemophilia: a review on clinical benefit, limitations, and remaining issues. *Blood* 138: 923-931

Li Z, Zhao P, Zhang Y, Wang J, Wang C, Liu Y, Yang G, Yuan L (2021) Exosome-based Ldlr gene therapy for familial hypercholesterolemia in a mouse model. *Theranostics* 11: 2953-2965

Libby P (2021a) The changing landscape of atherosclerosis. *Nature* 592: 524-533

Libby P (2021b) Inflammation during the life cycle of the atherosclerotic plaque. *Cardiovasc Res* 117: 2525-2536

Libby P, Buring JE, Badimon L, Hansson GK, Deanfield J, Bittencourt MS, Tokgozoglu L, Lewis EF (2019) Atherosclerosis. *Nat Rev Dis Primers* 5: 56

Lisowski L, Dane AP, Chu K, Zhang Y, Cunningham SC, Wilson EM, Nygaard S, Grompe M, Alexander IE, Kay MA (2014) Selection and evaluation of clinically relevant AAV variants in a xenograft liver model. *Nature* 506: 382-386

Loncharich MF, Anderson CW (2022) Interferon Inhibition for Lupus with Anifrolumab: Critical Appraisal of the Evidence Leading to FDA Approval. *ACR Open Rheumatol* 4: 486-491

Makino H, Koezuka R, Tamanaha T, Ogura M, Matsuki K, Hosoda K, Harada-Shiba M (2019) Familial Hypercholesterolemia and Lipoprotein Apheresis. *J Atheroscler Thromb* 26: 679-687

Maxwell KN, Breslow JL (2004) Adenoviral-mediated expression of Pcsk9 in mice results in a low-density lipoprotein receptor knockout phenotype. *Proc Natl Acad Sci U S A* 101: 7100-7105

McIntosh J, Lenting PJ, Rosales C, Lee D, Rabbanian S, Raj D, Patel N, Tuddenham EG, Christophe OD, McVey JH *et al* (2013) Therapeutic levels of FVIII following a single peripheral vein administration of rAAV vector encoding a novel human factor VIII variant. *Blood* 121: 3335-3344

Mehta A, Shapiro MD (2022) Apolipoproteins in vascular biology and atherosclerotic disease. *Nat Rev Cardiol* 19: 168-179

Meliani A, Boisgerault F, Hardet R, Marmier S, Collaud F, Ronzitti G, Leborgne C, Costa Verdera H, Simon Sola M, Charles S *et al* (2018) Antigen-selective modulation of AAV immunogenicity with tolerogenic rapamycin nanoparticles enables successful vector re-administration. *Nat Commun* 9: 4098

Mendes VM, Coelho M, Tome AR, Cunha RA, Manadas B (2019) Validation of an LC-MS/MS Method for the Quantification of Caffeine and Theobromine Using Non-Matched Matrix Calibration Curve. *Molecules* 24

Merlin S, Fama R, Borroni E, Zanolini D, Bruscaggin V, Zucchelli S, Follenzi A (2019) FVIII expression by its native promoter sustains long-term correction avoiding immune response in hemophilic mice. *Blood Adv* 3: 825-838

Milani M, Annoni A, Bartolaccini S, Biffi M, Russo F, Di Tomaso T, Raimondi A, Lengler J, Holmes MC, Scheiflinger F *et al* (2017) Genome editing for scalable production of alloantigen-free lentiviral vectors for in vivo gene therapy. *EMBO Mol Med* 9: 1558-1573

Milani M, Annoni A, Moalli F, Liu T, Cesana D, Calabria A, Bartolaccini S, Biffi M, Russo F, Visigalli I *et al* (2019) Phagocytosis-shielded lentiviral vectors improve liver gene therapy in nonhuman primates. *Sci Transl Med* 11

Milani M, Canepari C, Liu T, Biffi M, Russo F, Plati T, Curto R, Patarroyo-White S, Drager D, Visigalli I *et al* (2022) Liver-directed lentiviral gene therapy corrects hemophilia A mice and achieves normal-range factor VIII activity in non-human primates. *Nature Communications* 13: 2454

Mombaerts P, Iacomini J, Johnson RS, Herrup K, Tonegawa S, Papaioannou VE (1992) RAG-1-deficient mice have no mature B and T lymphocytes. *Cell* 68: 869-877

Moulay G, Scherman D, Kichler A (2010) Fasting increases the in vivo gene delivery of AAV vectors. *Clin Transl Sci* 3: 333-336

Mullick AE, Fu W, Graham MJ, Lee RG, Witchell D, Bell TA, Whipple CP, Crooke RM (2011) Antisense oligonucleotide reduction of apoB-ameliorated atherosclerosis in LDL receptor-deficient mice. *J Lipid Res* 52: 885-896

Musunuru K (2022) Moving toward genome-editing therapies for cardiovascular diseases. *J Clin Invest* 132

Musunuru K, Chadwick AC, Mizoguchi T, Garcia SP, DeNizio JE, Reiss CW, Wang K, Iyer S, Dutta C, Clendaniel V *et al* (2021) In vivo CRISPR base editing of PCSK9 durably lowers cholesterol in primates. *Nature* 593: 429-434

Musunuru K, Pirruccello JP, Do R, Peloso GM, Guiducci C, Sougnez C, Garimella KV, Fisher S, Abreu J, Barry AJ *et al* (2010) Exome sequencing, ANGPTL3 mutations, and familial combined hypolipidemia. *N Engl J Med* 363: 2220-2227

Myocardial Infarction Genetics Consortium I, Stitziel NO, Won HH, Morrison AC, Peloso GM, Do R, Lange LA, Fontanillas P, Gupta N, Duga S *et al* (2014) Inactivating mutations in NPC1L1 and protection from coronary heart disease. *N Engl J Med* 371: 2072-2082

Nakajima K, Nakano T, Tokita Y, Nagamine T, Inazu A, Kobayashi J, Mabuchi H, Stanhope KL, Havel PJ, Okazaki M *et al* (2011) Postprandial lipoprotein metabolism: VLDL vs chylomicrons. *Clin Chim Acta* 412: 1306-1318

Nathwani AC (2019) Gene therapy for hemophilia. *Hematology Am Soc Hematol Educ Program* 2019: 1-8

Nehlig A (2018) Interindividual Differences in Caffeine Metabolism and Factors Driving Caffeine Consumption. *Pharmacol Rev* 70: 384-411

Nguyen GN, Everett JK, Kafle S, Roche AM, Raymond HE, Leiby J, Wood C, Assenmacher CA, Merricks EP, Long CT *et al* (2021) A long-term study of AAV gene therapy in dogs with hemophilia A identifies clonal expansions of transduced liver cells. *Nat Biotechnol* 39: 47-55

Nicholls SJ, Ditmarsch M, Kastelein JJ, Rigby SP, Kling D, Curcio DL, Alp NJ, Davidson MH (2022) Lipid lowering effects of the CETP inhibitor obicetrapib in combination with high-intensity statins: a randomized phase 2 trial. *Nat Med* 28: 1672-1678

Nicolas CT, VanLith CJ, Hickey RD, Du Z, Hillin LG, Guthman RM, Cao WJ, Haugo B, Lillegard A, Roy D *et al* (2022) In vivo lentiviral vector gene therapy to cure hereditary tyrosinemia type 1 and prevent development of precancerous and cancerous lesions. *Nat Commun* 13: 5012

Nilsson SK, Heeren J, Olivecrona G, Merkel M (2011) Apolipoprotein A-V; a potent triglyceride reducer. *Atherosclerosis* 219: 15-21

Nissen SE, Nicholls SJ, Sipahi I, Libby P, Raichlen JS, Ballantyne CM, Davignon J, Erbel R, Fruchart JC, Tardif JC *et al* (2006) Effect of very high-intensity statin therapy on regression of coronary atherosclerosis: the ASTEROID trial. *JAMA* 295: 1556-1565

Nordestgaard BG, Chapman MJ, Humphries SE, Ginsberg HN, Masana L, Descamps OS, Wiklund O, Hegele RA, Raal FJ, Defesche JC *et al* (2013) Familial hypercholesterolaemia is underdiagnosed and undertreated in the general population:

guidance for clinicians to prevent coronary heart disease: consensus statement of the European Atherosclerosis Society. *Eur Heart J* 34: 3478-3490a

Oldenborg PA, Gresham HD, Lindberg FP (2001) CD47-signal regulatory protein alpha (SIRPalpha) regulates Fcgamma and complement receptor-mediated phagocytosis. *J Exp Med* 193: 855-862

Pedersen TR, Kjekshus J, Berg K, Haghfelt T, Faergeman O, Faergeman G, Pyorala K, Miettinen T, Wilhelmsen L, Olsson AG *et al* (2004) Randomised trial of cholesterol lowering in 4444 patients with coronary heart disease: the Scandinavian Simvastatin Survival Study (4S). 1994. *Atheroscler Suppl* 5: 81-87

Pejic RN (2014) Familial hypercholesterolemia. *Ochsner J* 14: 669-672

Pieri V, Gallotti AL, Drago D, Cominelli M, Pagano I, Conti V, Valtorta S, Coliva A, Lago S, Michelatti D *et al* (2023) Aberrant L-Fucose Accumulation and Increased Core Fucosylation Are Metabolic Liabilities in Mesenchymal Glioblastoma. *Cancer Res* 83: 195-218

Pisciotta L, Favari E, Magnolo L, Simonelli S, Adorni MP, Sallo R, Fancello T, Zavaroni I, Ardigo D, Bernini F *et al* (2012) Characterization of three kindreds with familial combined hypolipidemia caused by loss-of-function mutations of ANGPTL3. *Circ Cardiovasc Genet* 5: 42-50

Poirier S, Mayer G, Benjannet S, Bergeron E, Marcinkiewicz J, Nassoury N, Mayer H, Nimpf J, Prat A, Seidah NG (2008) The proprotein convertase PCSK9 induces the degradation of low density lipoprotein receptor (LDLR) and its closest family members VLDLR and ApoER2. *J Biol Chem* 283: 2363-2372

Poletti V, Mavilio F (2021) Designing Lentiviral Vectors for Gene Therapy of Genetic Diseases. *Viruses* 13

Poothong J, Pottekat A, Siirin M, Campos AR, Paton AW, Paton JC, Lagunas-Acosta J, Chen Z, Swift M, Volkmann N *et al* (2020) Factor VIII exhibits chaperone-dependent and glucose-regulated reversible amyloid formation in the endoplasmic reticulum. *Blood* 135: 1899-1911

Powell LM, Wallis SC, Pease RJ, Edwards YH, Knott TJ, Scott J (1987) A novel form of tissue-specific RNA processing produces apolipoprotein-B48 in intestine. *Cell* 50: 831-840

Raal FJ, Giugliano RP, Sabatine MS, Koren MJ, Langslet G, Bays H, Blom D, Eriksson M, Dent R, Wasserman SM *et al* (2014) Reduction in lipoprotein(a) with PCSK9 monoclonal

antibody evolocumab (AMG 145): a pooled analysis of more than 1,300 patients in 4 phase II trials. *J Am Coll Cardiol* 63: 1278-1288

Raal FJ, Santos RD, Blom DJ, Marais AD, Charng MJ, Cromwell WC, Lachmann RH, Gaudet D, Tan JL, Chasan-Taber S *et al* (2010) Mipomersen, an apolipoprotein B synthesis inhibitor, for lowering of LDL cholesterol concentrations in patients with homozygous familial hypercholesterolaemia: a randomised, double-blind, placebo-controlled trial. *Lancet* 375: 998-1006

Racanelli V, Rehermann B (2006) The liver as an immunological organ. *Hepatology* 43: S54-62

Rader DJ, Hovingh GK (2014) HDL and cardiovascular disease. *Lancet* 384: 618-625

Rader DJ, Tall AR (2012) The not-so-simple HDL story: Is it time to revise the HDL cholesterol hypothesis? *Nat Med* 18: 1344-1346

Raedler L (2015) Velcade (Bortezomib) Receives 2 New FDA Indications: For Retreatment of Patients with Multiple Myeloma and for First-Line Treatment of Patients with Mantle-Cell Lymphoma. *Am Health Drug Benefits* 8: 135-140

Ranzani M, Cesana D, Bartholomae CC, Sanvito F, Pala M, Benedicenti F, Gallina P, Sergi LS, Merella S, Bulfone A *et al* (2013) Lentiviral vector-based insertional mutagenesis identifies genes associated with liver cancer. *Nat Methods* 10: 155-161

Raper A, Kolansky DM, Sachais BS, Meagher EA, Baer AL, Cuchel M (2015) Long-term clinical results of microsomal triglyceride transfer protein inhibitor use in a patient with homozygous familial hypercholesterolemia. *J Clin Lipidol* 9: 107-112

Rashid S, Curtis DE, Garuti R, Anderson NN, Bashmakov Y, Ho YK, Hammer RE, Moon YA, Horton JD (2005) Decreased plasma cholesterol and hypersensitivity to statins in mice lacking Pcsk9. *Proc Natl Acad Sci U S A* 102: 5374-5379

Ray KK, Landmesser U, Leiter LA, Kallend D, Dufour R, Karakas M, Hall T, Troquay RP, Turner T, Visseren FL *et al* (2017) Inclisiran in Patients at High Cardiovascular Risk with Elevated LDL Cholesterol. *N Engl J Med* 376: 1430-1440

Reardon CA, Blachowicz L, White T, Cabana V, Wang Y, Lukens J, Bluestone J, Getz GS (2001) Effect of immune deficiency on lipoproteins and atherosclerosis in male apolipoprotein E-deficient mice. *Arterioscler Thromb Vasc Biol* 21: 1011-1016

Robinson JG, Farnier M, Krempf M, Bergeron J, Luc G, Averna M, Stroes ES, Langslet G, Raal FJ, El Shahawy M *et al* (2015) Efficacy and safety of alirocumab in reducing lipids and cardiovascular events. *N Engl J Med* 372: 1489-1499

Ronzitti G, Gross DA, Mingozzi F (2020) Human Immune Responses to Adeno-Associated Virus (AAV) Vectors. *Front Immunol* 11: 670

Rothgangl T, Dennis MK, Lin PJC, Oka R, Witzigmann D, Villiger L, Qi W, Hruzova M, Kissling L, Lenggenhager D *et al* (2021) In vivo adenine base editing of PCSK9 in macaques reduces LDL cholesterol levels. *Nat Biotechnol* 39: 949-957

Sabatine MS, Giugliano RP, Keech AC, Honarpour N, Wiviott SD, Murphy SA, Kuder JF, Wang H, Liu T, Wasserman SM *et al* (2017) Evolocumab and Clinical Outcomes in Patients with Cardiovascular Disease. *N Engl J Med* 376: 1713-1722

Santoni de Sio FR, Cascio P, Zingale A, Gasparini M, Naldini L (2006) Proteasome activity restricts lentiviral gene transfer into hematopoietic stem cells and is down-regulated by cytokines that enhance transduction. *Blood* 107: 4257-4265

Santoni de Sio FR, Gritti A, Cascio P, Neri M, Sampaolesi M, Galli C, Luban J, Naldini L (2008) Lentiviral vector gene transfer is limited by the proteasome at postentry steps in various types of stem cells. *Stem Cells* 26: 2142-2152

Santos RD, Stein EA, Hovingh GK, Blom DJ, Soran H, Watts GF, Lopez JAG, Bray S, Kurtz CE, Hamer AW *et al* (2020) Long-Term Evolocumab in Patients With Familial Hypercholesterolemia. *J Am Coll Cardiol* 75: 565-574

Schauber CA, Tuerk MJ, Pacheco CD, Escarpe PA, Veres G (2004) Lentiviral vectors pseudotyped with baculovirus gp64 efficiently transduce mouse cells in vivo and show tropism restriction against hematopoietic cell types in vitro. *Gene Ther* 11: 266-275

Schneider WJ, Beisiegel U, Goldstein JL, Brown MS (1982) Purification of the low density lipoprotein receptor, an acidic glycoprotein of 164,000 molecular weight. *J Biol Chem* 257: 2664-2673

Shepherd J, Cobbe SM, Ford I, Isles CG, Lorimer AR, MacFarlane PW, McKillop JH, Packard CJ (1995) Prevention of coronary heart disease with pravastatin in men with hypercholesterolemia. West of Scotland Coronary Prevention Study Group. *N Engl J Med* 333: 1301-1307

Shimizugawa T, Ono M, Shimamura M, Yoshida K, Ando Y, Koishi R, Ueda K, Inaba T, Minekura H, Kohama T *et al* (2002) ANGPTL3 decreases very low density lipoprotein triglyceride clearance by inhibition of lipoprotein lipase. *J Biol Chem* 277: 33742-33748

Simioni P, Tormene D, Tognin G, Gavasso S, Bulato C, Iacobelli NP, Finn JD, Spiezia L, Radu C, Arruda VR (2009) X-linked thrombophilia with a mutant factor IX (factor IX Padua). *N Engl J Med* 361: 1671-1675

Sniderman AD, Qi Y, Ma CI, Wang RH, Naples M, Baker C, Zhang J, Adeli K, Kiss RS (2013) Hepatic cholesterol homeostasis: is the low-density lipoprotein pathway a regulatory or a shunt pathway? *Arterioscler Thromb Vasc Biol* 33: 2481-2490

Sniderman AD, Thanassoulis G, Glavinovic T, Navar AM, Pencina M, Catapano A, Ference BA (2019) Apolipoprotein B Particles and Cardiovascular Disease: A Narrative Review. *JAMA Cardiol* 4: 1287-1295

Starzl TE, Bilheimer DW, Bahnson HT, Shaw BW, Jr., Hardesty RL, Griffith BP, Iwatsuki S, Zitelli BJ, Gartner JC, Jr., Malatack JJ *et al* (1984) Heart-liver transplantation in a patient with familial hypercholesterolaemia. *Lancet* 1: 1382-1383

Stein EA, Gipe D, Bergeron J, Gaudet D, Weiss R, Dufour R, Wu R, Pordy R (2012) Effect of a monoclonal antibody to PCSK9, REGN727/SAR236553, to reduce low-density lipoprotein cholesterol in patients with heterozygous familial hypercholesterolaemia on stable statin dose with or without ezetimibe therapy: a phase 2 randomised controlled trial. *Lancet* 380: 29-36

Sundaram M, Yao Z (2010) Recent progress in understanding protein and lipid factors affecting hepatic VLDL assembly and secretion. *Nutr Metab (Lond)* 7: 35

Swift LL, Jovanovska A, Kakkad B, Ong DE (2005) Microsomal triglyceride transfer protein expression in mouse intestine. *Histochem Cell Biol* 123: 475-482

Swift LL, Zhu MY, Kakkad B, Jovanovska A, Neely MD, Valyi-Nagy K, Roberts RL, Ong DE, Jerome WG (2003) Subcellular localization of microsomal triglyceride transfer protein. *J Lipid Res* 44: 1841-1849

Tada H, Kawashiri MA, Ohtani R, Noguchi T, Nakanishi C, Konno T, Hayashi K, Nohara A, Inazu A, Kobayashi J *et al* (2011) A novel type of familial hypercholesterolemia: double heterozygous mutations in LDL receptor and LDL receptor adaptor protein 1 gene. *Atherosclerosis* 219: 663-666

Tall AR, Rader DJ (2018) Trials and Tribulations of CETP Inhibitors. *Circ Res* 122: 106-112

Trapani L, Segatto M, Pallottini V (2012) Regulation and deregulation of cholesterol homeostasis: The liver as a metabolic "power station". *World J Hepatol* 4: 184-190

Tromp TR, Hartgers ML, Hovingh GK, Vallejo-Vaz AJ, Ray KK, Soran H, Freiberger T, Bertolini S, Harada-Shiba M, Blom DJ *et al* (2022) Worldwide experience of homozygous familial hypercholesterolaemia: retrospective cohort study. *Lancet* 399: 719-728

Tucci F, Galimberti S, Naldini L, Valsecchi MG, Aiuti A (2022) A systematic review and meta-analysis of gene therapy with hematopoietic stem and progenitor cells for monogenic disorders. *Nat Commun* 13: 1315

van de Sluis B, Wijers M, Herz J (2017) News on the molecular regulation and function of hepatic low-density lipoprotein receptor and LDLR-related protein 1. *Curr Opin Lipidol* 28: 241-247

Van Heek M, France CF, Compton DS, McLeod RL, Yumibe NP, Alton KB, Sybertz EJ, Davis HR, Jr. (1997) In vivo metabolism-based discovery of a potent cholesterol absorption inhibitor, SCH58235, in the rat and rhesus monkey through the identification of the active metabolites of SCH48461. *J Pharmacol Exp Ther* 283: 157-163

Vigna E, Naldini L (2000) Lentiviral vectors: excellent tools for experimental gene transfer and promising candidates for gene therapy. *J Gene Med* 2: 308-316

Voight BF, Peloso GM, Orho-Melander M, Frikke-Schmidt R, Barbalic M, Jensen MK, Hindy G, Holm H, Ding EL, Johnson T *et al* (2012) Plasma HDL cholesterol and risk of myocardial infarction: a mendelian randomisation study. *Lancet* 380: 572-580

von Drygalski A, Gomez E, Giermasz A, Castaman G, Key NS, Lattimore SS, Leebeek FWG, Miesbach WA, Recht M, Gut RZ *et al* (2022) Stable and durable factor IX levels in hemophilia B patients over 3 years post etranacogene dezaparvovec gene therapy. *Blood Adv*

Vonada A, Tiyaboonchai A, Nygaard S, Posey J, Peters AM, Winn SR, Cantore A, Naldini L, Harding CO, Grompe M (2021) Therapeutic liver repopulation by transient acetaminophen selection of gene-modified hepatocytes. *Sci Transl Med* 13

Wang D, Tai PWL, Gao G (2019) Adeno-associated virus vector as a platform for gene therapy delivery. *Nat Rev Drug Discov* 18: 358-378

Wang L, Muthuramu I, Somanathan S, Zhang H, Bell P, He Z, Yu H, Zhu Y, Tretiakova AP, Wilson JM (2021) Developing a second-generation clinical candidate AAV vector for gene therapy of familial hypercholesterolemia. *Mol Ther Methods Clin Dev* 22: 1-10

Wang L, Smith J, Breton C, Clark P, Zhang J, Ying L, Che Y, Lape J, Bell P, Calcedo R *et al* (2018) Meganuclease targeting of PCSK9 in macaque liver leads to stable reduction in serum cholesterol. *Nat Biotechnol* 36: 717-725

Wang Y, Gusarova V, Banfi S, Gromada J, Cohen JC, Hobbs HH (2015) Inactivation of ANGPTL3 reduces hepatic VLDL-triglyceride secretion. *J Lipid Res* 56: 1296-1307

Wolska A, Dunbar RL, Freeman LA, Ueda M, Amar MJ, Sviridov DO, Remaley AT (2017) Apolipoprotein C-II: New findings related to genetics, biochemistry, and role in triglyceride metabolism. *Atherosclerosis* 267: 49-60

Wu L, Soundarapandian MM, Castoreno AB, Millar JS, Rader DJ (2020) LDL-Cholesterol Reduction by ANGPTL3 Inhibition in Mice Is Dependent on Endothelial Lipase. *Circ Res* 127: 1112-1114

Wu M, Dong B, Cao A, Li H, Liu J (2012) Delineation of molecular pathways that regulate hepatic PCSK9 and LDL receptor expression during fasting in normolipidemic hamsters. *Atherosclerosis* 224: 401-410

Xiao C, Stahel P, Lewis GF (2019) Regulation of Chylomicron Secretion: Focus on Post-Assembly Mechanisms. *Cell Mol Gastroenterol Hepatol* 7: 487-501

Yamamoto H, Yamanashi Y, Takada T, Mu S, Tanaka Y, Komine T, Suzuki H (2019) Hepatic Expression of Niemann-Pick C1-Like 1, a Cholesterol Reabsorber from Bile, Exacerbates Western Diet-Induced Atherosclerosis in LDL Receptor Mutant Mice. *Mol Pharmacol* 96: 47-55

Yamamoto T, Bishop RW, Brown MS, Goldstein JL, Russell DW (1986) Deletion in cysteine-rich region of LDL receptor impedes transport to cell surface in WHHL rabbit. *Science* 232: 1230-1237

Yoon E, Babar A, Choudhary M, Kutner M, Pyrsopoulos N (2016) Acetaminophen-Induced Hepatotoxicity: a Comprehensive Update. *J Clin Transl Hepatol* 4: 131-142

Yu L, Hammer RE, Li-Hawkins J, Von Bergmann K, Lutjohann D, Cohen JC, Hobbs HH (2002a) Disruption of Abcg5 and Abcg8 in mice reveals their crucial role in biliary cholesterol secretion. *Proc Natl Acad Sci U S A* 99: 16237-16242

Yu L, Li-Hawkins J, Hammer RE, Berge KE, Horton JD, Cohen JC, Hobbs HH (2002b) Overexpression of ABCG5 and ABCG8 promotes biliary cholesterol secretion and reduces fractional absorption of dietary cholesterol. *J Clin Invest* 110: 671-680

Zanta-Boussif MA, Charrier S, Brice-Ouzet A, Martin S, Opolon P, Thrasher AJ, Hope TJ, Galy A (2009) Validation of a mutated PRE sequence allowing high and sustained transgene expression while abrogating WHV-X protein synthesis: application to the gene therapy of WAS. *Gene Ther* 16: 605-619

Zhang L, Yan F, Zhang S, Lei D, Charles MA, Cavigiolio G, Oda M, Krauss RM, Weisgraber KH, Rye KA *et al* (2012) Structural basis of transfer between lipoproteins by cholesteryl ester transfer protein. *Nat Chem Biol* 8: 342-349

Zhang R (2016) The ANGPTL3-4-8 model, a molecular mechanism for triglyceride trafficking. *Open Biol* 6: 150272

Zhao H, Li Y, He L, Pu W, Yu W, Li Y, Wu YT, Xu C, Wei Y, Ding Q *et al* (2020) In Vivo AAV-CRISPR/Cas9-Mediated Gene Editing Ameliorates Atherosclerosis in Familial Hypercholesterolemia. *Circulation* 141: 67-79

Zufferey R, Donello JE, Trono D, Hope TJ (1999) Woodchuck hepatitis virus posttranscriptional regulatory element enhances expression of transgenes delivered by retroviral vectors. *J Virol* 73: 2886-2892

Zufferey R, Dull T, Mandel RJ, Bukovsky A, Quiroz D, Naldini L, Trono D (1998) Self-inactivating lentivirus vector for safe and efficient in vivo gene delivery. *J Virol* 72: 9873-9880

